

UNIVERSIDADE DE SÃO PAULO – USP
ESCOLA POLITÉCNICA
PROGRAMA DE PÓS-GRADUAÇÃO EM ENGENHARIA ELÉTRICA

Rodrigo Jacinto do Vale

**Evaluation of lithium-ion battery aging in the operation of
hybrid ship power systems**

São Paulo

2021

Rodrigo Jacinto do Vale

**Evaluation of lithium-ion battery aging in the operation of
hybrid ship power systems**

Versão corrigida

Dissertação de mestrado apresentada à
Escola Politécnica da Universidade de São
Paulo para obtenção do título de Mestre em
Ciências.

Área de concentração: Sistemas Elétricos
de Potência

Orientador: Prof. Dr. Maurício Barbosa de
Camargo Salles

São Paulo

2021

Autorizo a reprodução e divulgação total ou parcial deste trabalho, por qualquer meio convencional ou eletrônico, para fins de estudo e pesquisa, desde que citada a fonte.

Este exemplar foi revisado e corrigido em relação à versão original, sob responsabilidade única do autor e com a anuência de seu orientador.

São Paulo, _____ de _____ de _____

Assinatura do autor: _____

Assinatura do orientador: _____

Catalogação-na-publicação

do Vale, Rodrigo Jacinto

Evaluation of lithium-ion battery aging in the operation of hybrid ship power systems / R. J. do Vale -- versão corr. -- São Paulo, 2021.

154 p.

Dissertação (Mestrado) - Escola Politécnica da Universidade de São Paulo. Departamento de Engenharia de Energia e Automação Elétricas.

1.Baterias de íon-lítio 2.Degradação da bateria 3.Embarcações híbridas
4.Consumo de combustível 5.Emissões de CO₂ I.Universidade de São Paulo.
Escola Politécnica. Departamento de Engenharia de Energia e Automação
Elétricas II.t.

Dissertação de autoria de Rodrigo Jacinto do Vale, sob o título **Evaluation of lithium-ion battery aging in the operation of hybrid ship power systems**, apresentada à Escola Politécnica da Universidade de São Paulo, para obtenção do título de Mestre em Ciências pelo Programa de Pós-graduação em Engenharia Elétrica, na área de concentração Sistemas de Potência, aprovada em 11 de Dezembro de 2020 pela comissão julgadora constituída pelos doutores:

Prof. Dr. Mauricio Barbosa de Camargo Salles

Instituição: Universidade de São Paulo – USP

Presidente

Prof. Dr. Gerhard Ett

Instituição: Centro Universitário da FEI

Prof. Dr. José Carlos de Melo Vieira Júnior

Instituição: EESC – USP

This work is dedicated to my parents Maria das Graças and Cicero.

To my siblings Carolina, Gabriela, Mariana, Daniela, Nathalia, and Fernando.

My goddaughter Isabella and niece Beatriz.

Acknowledgements

To the Polytechnic School at the University of São Paulo.

To the Research Centre for Gas Innovation (RCGI - FAPESP/Shell) for the support to all members of 45 projects through several training sessions which allow me improved new skills and performance.

To the Foundation for the Support of the University of São Paulo (FUSP) for the financial support to this work and for the Master Scholarship.

To the Numerical Offshore Tank (TPN - USP) for the laboratory support for adequately running to this work.

To the Supervisor Professor Dr. Mauricio Barbosa de Camargo Salles (LGrid - USP) for the great support, for the comments precise and suggestions that enormously contributed to this Master's Thesis.

To the Advisor Professor Dr. Claudio M. P. Sampaio for the support in Project 4 (RCGI) and for enormously contributed to this Master's Thesis, mainly for diesel-electric propulsion on vessels.

To my dear colleagues divided among TPN – USP, LGrid – USP, and LMAG – USP laboratories such as Alejandro Gutierrez, Alex Huang, Bruno Mendes, Cesar Peralta, Cristiana Pirpiris, Felipe Marino, Fernanda Hille, Giovani Vieira, Gloria Milena Vargas, Humberto Sasaki, Lucas Carmo, Luís Lourenço, and Rodrigo Schiller.

“Student is not a container you have to fill but a torch you have to light up”

(Albert Einstein).

Resumo

VALE, Rodrigo Jacinto do. **Avaliação da degradação da bateria de lithium-ion na operação de embarcações híbridas.** 2021. 154 f. Dissertação (Mestrado em Ciências) – Escola Politécnica, Universidade de São Paulo, São Paulo, 2021.

As emissões de gases de efeito estufa crescerão nas próximas décadas e estima-se que até 2050, as emissões de CO_2 subirão dos atuais 1 bilhão para 1.6 bilhões de toneladas por ano. Os navios são responsáveis por cerca de 2.6% das emissões globais de CO_2 . É fundamental o estudo e a implementação de sistemas híbridos em diversos setores. Os navios híbridos estão se tornando mais frequentes no mundo e diversas restrições internacionais estão sendo estabelecidas por agentes de regulação. A IMO – International Maritime Organization – por exemplo, impõe restrições rígidas de emissões através de normas para o setor de navegação. Neste contexto, esta dissertação aborda a simulação de baterias de Lítio Fosfato de Ferro (Lithium-Iron Phosphate – LiFePO₄ – *LFP*) e de Lítio Óxido Níquel Manganês Cobalto (Lithium Nickel Cobalt Manganese Oxide – LiNiCoMnO₂ – *NMC*) com aplicação em embarcações do tipo *PSV* – Platform Supply Vessel. As simulações foram executadas utilizando o software denominado HOMER, onde dois modelos de baterias foram utilizados para analisar quatro casos de desempenho técnico e outros quatro casos focados nos aspectos econômicos das baterias ao longo da vida útil. Alguns parâmetros como a capacidade de potência e de energia, profundidade de descarga, a degradação da bateria, os custos dos componentes do sistema do navio são avaliados em relação ao potencial de redução do consumo de combustível, emissões de CO_2 , número de ciclos, vida útil e parâmetros econômicos como despesas de capital – *CAPEX*, despesas operacionais – *OPEX*, *payback* e Valor Presente Líquido – *VPL*. O potencial de redução de emissões de CO_2 mais significativo é de cerca de 11% ao ano. Em geral, o modelo de bateria que desconsidera o processo de envelhecimento tem um desempenho melhor do que o modelo que inclui a degradação. Além disso, a bateria operando a 70 % *DoD* é uma opção mais vantajosa do que utilizando 80 % *DoD*. Os resultados desse trabalho demonstram que o desempenho tecnico-econômico da bateria *NMC* é ligeiramente superior ao sistema dimensionado com a célula *LFP*. Isso se deve ao menor custo e maior número de ciclos apresentada pela primeira. O cálculo do *payback* indica que o retorno de investimento de uma bateria operando conectada à rede nas operações portuárias pode atingir 6 anos e quando a mesma bateria opera sempre desconectada da rede, seu tempo de retorno de investimento subirá para 9 anos. Por fim, através de uma metodologia que integra todos os casos analisados, recomenda-se uma bateria que atenda parte do perfil operacional do *PSV* com uma capacidade de 600 kWh (1000 kW) considerando ambas tecnologias de baterias, um C-rate entre 0.40 e 0.60C para a célula *LFP* e C-rate no intervalo de 0.60 e 0.80C para a célula *NMC* (bateria de 1000 kWh).

Palavras-chaves: Baterias de íon-lítio; Embarcações Híbridas; Processos de Degradação da Bateria; Consumo de Combustível; Emissões de CO_2 .

Abstract

VALE, Rodrigo Jacinto do. **Evaluation of Lithium-ion Battery Aging in the Operation of Hybrid Ship Power Systems.** 2021. 154 p. Dissertation (Master of Science) – Polytechnic School, University of São Paulo, São Paulo, 2021.

The Greenhouse Gas (*GHG*) Emissions will grow in the next decades and it is estimated by 2050 that the *CO₂* emissions will be about 1600 million tons per year. Currently, this estimation is below 1000 million tons per year and *CO₂* emissions from ships all over the world are approximately 2.6% of global emissions. It is essential to study and implement hybrid systems in several sectors. Hybrid Ship Power Systems have been becoming more frequent in the world and international regulations are establishing restrictions to the shipping sector due to rapidly increasing these emissions. In terms of regulatory, the IMO - International Maritime Organization – imposes stiffer regulations to the naval industry for the reduction of greenhouse gas emissions and pollutants. This Master's Thesis approaches the batteries of Lithium-Iron Phosphate (LiFePO₄ – *LFP*) and Lithium Nickel Cobalt Manganese Oxide (LiNiCoMnO₂ – *NMC*) that are analyzed in Maritime application for typical Platform Supply Vessel – *PSV*. Simulations are run through HOMER Energy software. This work proposes two battery models that are analyzed although four simulation cases to technical performance and other four simulations cases related to the economic model. Battery model simplified, advanced and the same ones with economic model integrated are compared. Some characteristics such as power/energy capacities, C-rate, depth-of-discharge (*DoD*), cycle aging, and equipment costs are evaluated concerning the potential reduction of fuel consumption, *CO₂* emissions, fuel costs savings, equivalent full cycles (*EFC*), battery expected life, furthermore economic parameters as Capital Expenditures (*CAPEX*), Operational Expenditures (*OPEX*), *payback* and Net Present Value (*NPV*). The most significant potential *CO₂* emissions reduction among the analyzed cases is approximately 11% of the total emissions. In general, the battery model that disregards the aging process has a better performance than the degradation model, and a battery operating at 70% *DoD* is a preferable option. The results demonstrate that the Li-ion *NMC* battery system presents the techno-economic performance slightly higher than *LFP* cell due to the superior number of cycles and lower cost. The *payback* indicates that a battery connected in the grid during port operation is more attractive than the stand-alone mode operation, resulting in the *payback* time of 6 and 9 years to the same capacity, respectively. Finally, considering the integrated solution for all cases simulated, the battery operation on the *PSV* is recommended for the battery capacity at 600 kWh (1000 kW) to both cell technologies. However, the C-rate is limited between 0.40 and 0.60C for *LFP* cell and the interval at 0.40 and 0.80C for *NMC* cell (considering the energy capacity at 1000 kWh).

Keywords: Lithium-ion Battery; Hybrid Vessels; Battery Aging Processes; Fuel Consumption; *CO₂* Emissions.

List of Figures

Figure 1 – Evolution of Ship Power Systems. (a) Conventional power system. (b) Integrated AC power system. (c) Integrated DC power system.	27
Figure 2 – Stages of historical development of the Ship Electrical Power Systems from 1830 to 2020. During WWI was first vessels with turbo-electric propulsion, and WWII served as the base to the development of T2-tanker with turbo-electric propulsion.	28
Figure 3 – Criteria adopted for dimensioning Lithium-ion batteries for Platform Supply Vessel.	31
Figure 4 – Flowchart of the proposed method on this Master’s Thesis considering Optimization software.	31
Figure 5 – Battery Management System.	37
Figure 6 – Parts of a Battery System and its inclusion into a 20 and 40-foot container. .	38
Figure 7 – Battery operating as Spinning reserve.	40
Figure 8 – Battery operating as Peak-shaving.	40
Figure 9 – Battery operating as Strategic-loading for a range from 20% to 90% <i>SoC</i> . The battery energy capacity of 1000 kWh can be operated with different C-rates.	41
Figure 10 – Aging mechanisms that influence the battery cell performance.	42
Figure 11 – Capacity fade testing for different battery technology that uses Lithium-ions as a key component of its electrochemistry (80% and 70% remaining capacity as a battery’s <i>EoL</i> condition).	43
Figure 12 – Cycles to Failure vs. Depth-of-discharge curve for <i>LFP</i> and <i>NMC</i> battery cells (Wöhler-Curves). (a) Original curve (b) Curve detailed for range at 70 - 100% <i>DoD</i>	45
Figure 13 – Degradation mechanisms represented by the model of a Lithium-ion battery cell.	46
Figure 14 – Battery models approach used for market analysis. This Master’s Thesis address the single objective function in the optimization model.	49
Figure 15 – Battery configuration.	50
Figure 16 – Kinetic battery model.	51

Figure 17 – Indication of main Balmat Platform Supply Vessel (<i>PSV</i>) dimensions. Beam B; Depth D; Draft T; Length overall L_{OA} ; Length between perpendiculars L_{pp}	56
Figure 18 – Single Diagram for a Typical Platform Supply Vessel.	58
Figure 19 – Operational profile for a typical <i>PSV</i> (Total power demand).	59
Figure 20 – Fuel Consumption curves for Main Gen-sets and Auxiliary Gen-sets. (a) <i>SFOC</i> - Specific Fuel Oil Consumption for Main and Auxiliary Marine Engine. (b) Fuel Consumption curve for Main Diesel Engine. (c) Fuel Consumption for Auxiliary Diesel Engine. Efficiency curves. (d) Main Diesel Marine Engine. (e) Auxiliary Diesel Marine Engine.	62
Figure 21 – CO_2 emission reduction potential in vessels considering 5 main categories of individual measures.	65
Figure 22 – Investment cost estimate for Ship's Equipment considering Gen-sets, <i>PCS</i> , <i>BS</i> , and <i>PCSEq</i>	71
Figure 23 – Battery cell costs for Ship Power System. Cost of investment and installation. .	71
Figure 24 – Battery Cost Curve. Cost of Investment and replacement for <i>LFP</i> and <i>NMC</i> cells.	73
Figure 25 – Flowchart of the proposed method (detailed) on this Master's Thesis considering Optimization software.	78
Figure 26 – Flowchart of the entire methodology, simulation process, and data analysis. .	81
Figure 27 – Reduction of CO_2 for Hybrid <i>PSV</i> Power System with battery included. Sensitivity analysis from 200 to 2000 kWh for battery cell technologies analysed. (a) <i>LFP</i> (ΔE capacity). (b) <i>NMC</i> (ΔE capacity). The Nominal C-rate (axis X) represents the fixed battery power capacity of 1000 kW.	83
Figure 28 – Battery Expected life (years) for the battery included in the Hybrid <i>PSV</i> Power System. Sensitivity analysis from 200 to 2000 kWh for battery cell technologies analysed. (a) <i>LFP</i> (ΔE capacity). (b) <i>NMC</i> (ΔE capacity). The Nominal C-rate (axis X) represents the fixed battery power capacity of 1000 kW.	85
Figure 29 – Fuel Savings (Millions of Liters) of Battery-powered Hybrid <i>PSV</i> Power Systems. Sensitivity analysis from 200 to 2000 kWh for battery cell technologies analysed. (a) <i>LFP</i> (ΔE capacity). (b) <i>NMC</i> (ΔE capacity). The Nominal C-rate (axis X) represents the fixed battery power capacity of 1000 kW.	85

Figure 30 – Reduction of Fuel Costs (in US\$) for Hybrid PSV Power Systems with battery included. Sensitivity analysis from 200 to 2000 kWh for battery cell technologies analysed. (a) <i>LFP</i> (ΔE capacity). (b) <i>NMC</i> (ΔE capacity). The Nominal C-rate (axis X) represents the fixed battery power capacity of 1000 kW.	86
Figure 31 – Reduction of Fuel Costs (in US\$) for Hybrid PSV Power Systems with battery included. Evaluation was based on Oil price scenarios from 2019 to 2049. <i>HDP</i> - High Diesel Price, <i>RDP</i> - Reference Diesel Price, and <i>LDP</i> - Low Diesel Price. Sensitivity analysis from 200 to 2000 kWh for battery cell technologies analysed. (a) <i>LFP</i> (ΔE capacity). (b) <i>NMC</i> (ΔE capacity). The Nominal C-rate (axis X) represents the fixed battery power capacity of 1000 kW.	86
Figure 32 – <i>EFC</i> - Equivalent Full Cycles for each battery capacity studied. Sensitivity analysis from 200 to 2000 kWh for battery cell technologies analysed. (a) <i>LFP</i> (ΔE capacity). (b) <i>NMC</i> (ΔE capacity). The Nominal C-rate (axis X) represents the fixed battery power capacity of 1000 kW.	87
Figure 33 – Evaluation of <i>CAPEX</i> and <i>OPEX</i> for Hybrid PSV Power System. <i>CAPEX</i> . (a) <i>LFP</i> (ΔE capacity). Sensitivity analysis from 200 to 2000 kWh for battery cell technologies analysed. (b) <i>NMC</i> (ΔE capacity). <i>OPEX</i> . (c) <i>LFP</i> (ΔE capacity). (d) <i>NMC</i> (ΔE capacity). The Nominal C-rate (axis X) represents the fixed battery power capacity of 1000 kW.	88
Figure 34 – Evaluation of <i>NPV</i> for Hybrid PSV system. Sensitivity analysis from 200 to 2000 kWh for battery cell technologies analysed. (a) <i>LFP</i> (ΔE capacity). (b) <i>NMC</i> (ΔE capacity). The Nominal C-rate (axis X) represents the fixed battery power capacity of 1000 kW.	89
Figure 35 – Theoretical <i>payback</i> calculation parameters for PSV powered by battery. Sensitivity analysis from 200 to 2000 kWh for battery cell technologies analysed. (a) <i>LFP</i> (ΔE capacity). (b) <i>NMC</i> (ΔE capacity). The Nominal C-rate (axis X) represents the fixed battery power capacity of 1000 kW. . . .	90
Figure 36 – Reduction of <i>CO₂</i> to Hybrid PSV Power System with battery included. Sensitivity analysis from 200 to 2000 kW for battery cell technologies analysed. (a) <i>LFP</i> (ΔP capacity). (b) <i>NMC</i> (ΔP capacity). The Nominal C-rate (axis X) represents the fixed battery energy capacity of 1000 kWh.	90

Figure 37 – Battery Expected life (years) to Hybrid PSV Power System with battery included. Sensitivity analysis from 200 to 2000 kW for battery cell technologies analysed. (a) <i>LFP</i> (ΔP capacity). (b) <i>NMC</i> (ΔP capacity). The Nominal C-rate (axis X) represents the fixed battery energy capacity of 1000 kWh.	91
Figure 38 – Fuel Savings (Millions of Liters) of Battery-powered Hybrid PSV Power Systems. Sensitivity analysis from 200 to 2000 kW for battery cell technologies analysed. (a) <i>LFP</i> (ΔP capacity). (b) <i>NMC</i> (ΔP capacity). The Nominal C-rate (axis X) represents the fixed battery energy capacity of 1000 kWh.	92
Figure 39 – Reduction of Fuel Costs (in US\$) to Hybrid PSV Power Systems with battery included. Sensitivity analysis from 200 to 2000 kW for battery cell technologies analysed. (a) <i>LFP</i> (ΔP capacity). (b) <i>NMC</i> (ΔP capacity). The Nominal C-rate (axis X) represents the fixed battery energy capacity of 1000 kWh.	92
Figure 40 – Reduction of Fuel Costs (in US\$) to Hybrid PSV Power Systems with battery included. Evaluation was based on Oil price scenarios from 2019 to 2049. <i>HDP</i> - High Diesel Price, <i>RDP</i> - Reference Diesel Price, and <i>LDP</i> - Low Diesel Price. Sensitivity analysis from 200 to 2000 kW for battery cell technologies analysed. (a) <i>LFP</i> (ΔP capacity). (b) <i>NMC</i> (ΔP capacity). The Nominal C-rate (axis X) represents the fixed battery energy capacity of 1000 kWh.	93
Figure 41 – <i>EFC</i> - Equivalent Full Cycles for each battery capacity studied. Sensitivity analysis from 200 to 2000 kW for battery cell technologies analysed. (a) <i>LFP</i> (ΔE capacity). (b) <i>NMC</i> (ΔE capacity). The Nominal C-rate (axis X) represents the fixed battery energy capacity of 1000 kWh.	94
Figure 42 – Evaluation of <i>CAPEX</i> and <i>OPEX</i> for Hybrid PSV Power System. <i>CAPEX</i> . Sensitivity analysis from 200 to 2000 kW for battery cell technologies analysed. (a) <i>LFP</i> (ΔP capacity). (b) <i>NMC</i> (ΔP capacity). <i>OPEX</i> . (c) <i>LFP</i> (ΔP capacity). (d) <i>NMC</i> (ΔP capacity). The Nominal C-rate (axis X) represents the fixed battery energy capacity of 1000 kWh.	95
Figure 43 – Evaluation of <i>NPV</i> for Hybrid PSV system. Sensitivity analysis from 200 to 2000 kW for battery cell technologies analysed. (a) <i>LFP</i> (ΔP capacity). (b) <i>NMC</i> (ΔP capacity). The Nominal C-rate (axis X) represents the fixed battery energy capacity of 1000 kWh.	96

Figure 44 – Theoretical <i>payback</i> calculation parameters for <i>PSV</i> powered by battery. Sensitivity analysis from 200 to 2000 kW for battery cell technologies analysed. (a) <i>LFP</i> (ΔP capacity). (b) <i>NMC</i> (ΔP capacity). The Nominal C-rate (axis X) represents the fixed battery energy capacity of 1000 kWh.	96
Figure 45 – Reduction of CO_2 to Hybrid <i>PSV</i> Power System with battery included. Sensitivity analysis from 200 to 2000 kWh for battery cell technologies analysed. (a) <i>LFP</i> (ΔE capacity). (b) <i>NMC</i> (ΔE capacity). The Nominal C-rate (axis X) represents the fixed battery power capacity of 1000 kW.	97
Figure 46 – Battery Expected life (years) to Hybrid <i>PSV</i> Power System with battery included. Sensitivity analysis from 200 to 2000 kWh for battery cell technologies analysed. (a) <i>LFP</i> (ΔE capacity). (b) <i>NMC</i> (ΔE capacity). The Nominal C-rate (axis X) represents the fixed battery power capacity of 1000 kW. . . .	98
Figure 47 – Fuel Savings (Millions of Liters) of Battery-powered Hybrid <i>PSV</i> Power Systems. Sensitivity analysis from 200 to 2000 kWh for battery cell technologies analysed. (a) <i>LFP</i> (ΔE capacity). (b) <i>NMC</i> (ΔE capacity). The Nominal C-rate (axis X) represents the fixed battery power capacity of 1000 kW. . . .	99
Figure 48 – Reduction of Fuel Costs (in US\$) to Hybrid <i>PSV</i> Power Systems with battery included. Sensitivity analysis from 200 to 2000 kWh for battery cell technologies analysed. (a) <i>LFP</i> (ΔE capacity). (b) <i>NMC</i> (ΔE capacity). The Nominal C-rate (axis X) represents the fixed battery power capacity of 1000 kW. . . .	100
Figure 49 – Reduction of Fuel Costs (in US\$) to Hybrid <i>PSV</i> Power Systems with battery included. Evaluation was based on Oil price scenarios from 2019 to 2049. <i>HDP</i> - High Diesel Price, <i>RDP</i> - Reference Diesel Price, and <i>LDP</i> - Low Diesel Price. Sensitivity analysis from 200 to 2000 kWh for battery cell technologies analysed. (a) <i>LFP</i> (ΔE capacity). (b) <i>NMC</i> (ΔE capacity). The Nominal C-rate (axis X) represents the fixed battery power capacity of 1000 kW.	101
Figure 50 – <i>EFC</i> - Equivalent Full Cycles for each battery capacity studied. Sensitivity analysis from 200 to 2000 kWh for battery cell technologies analysed. (a) <i>LFP</i> (ΔE capacity). (b) <i>NMC</i> (ΔE capacity). The Nominal C-rate (axis X) represents the fixed battery power capacity of 1000 kW.	101

Figure 51 – Evaluation of <i>CAPEX</i> and <i>OPEX</i> for Hybrid <i>PSV</i> Power System. <i>CAPEX</i> . (a) <i>LFP</i> (ΔE capacity). (b) <i>NMC</i> (ΔE capacity). <i>OPEX</i> . (c) <i>LFP</i> (ΔE capacity). (d) <i>NMC</i> (ΔE capacity). The Nominal C-rate (axis X) represents the fixed battery power capacity of 1000 kW.	102
Figure 52 – Evaluation of <i>NPV</i> for Hybrid <i>PSV</i> system. Sensitivity analysis from 200 to 2000 kWh for battery cell technologies analysed. (a) <i>LFP</i> (ΔE capacity). (b) <i>NMC</i> (ΔE capacity). The Nominal C-rate (axis X) represents the fixed battery power capacity of 1000 kW.	103
Figure 53 – Theoretical <i>payback</i> calculation parameters for <i>PSV</i> powered by battery. Sensitivity analysis from 200 to 2000 kWh for battery cell technologies analysed. (a) <i>LFP</i> (ΔE capacity). (b) <i>NMC</i> (ΔE capacity). The Nominal C-rate (axis X) represents the fixed battery power capacity of 1000 kW. . . .	104
Figure 54 – Reduction of <i>CO₂</i> to Hybrid <i>PSV</i> Power System with battery included. Sensitivity analysis from 200 to 2000 kW for battery cell technologies analysed. (a) <i>LFP</i> (ΔP capacity). (b) <i>NMC</i> (ΔP capacity). The Nominal C-rate (axis X) represents the fixed battery energy capacity of 1000 kWh.	105
Figure 55 – Battery Expected life (years) to Hybrid <i>PSV</i> Power System with battery included. Sensitivity analysis from 200 to 2000 kW for battery cell technologies analysed. (a) <i>LFP</i> (ΔP capacity). (b) <i>NMC</i> (ΔP capacity). The Nominal C-rate (axis X) represents the fixed battery energy capacity of 1000 kWh. . .	106
Figure 56 – Fuel Savings (Millions of Liters) of Battery-powered Hybrid <i>PSV</i> Power Systems. Sensitivity analysis from 200 to 2000 kW for battery cell technologies analysed. (a) <i>LFP</i> (ΔP capacity). (b) <i>NMC</i> (ΔP capacity). The Nominal C-rate (axis X) represents the fixed battery energy capacity of 1000 kWh. . .	106
Figure 57 – Reduction of Fuel Costs (in US\$) to Hybrid <i>PSV</i> Power Systems with battery included. Sensitivity analysis from 200 to 2000 kW for battery cell technologies analysed. (a) <i>LFP</i> (ΔP capacity). (b) <i>NMC</i> (ΔP capacity). The Nominal C-rate (axis X) represents the fixed battery energy capacity of 1000 kWh. . .	107

Figure 58 – Reduction of Fuel Costs (in US\$) to Hybrid PSV Power Systems with battery included. Evaluation was based on Oil price scenarios from 2019 to 2049. <i>HDP</i> - High Diesel Price, <i>RDP</i> - Reference Diesel Price, and <i>LDP</i> - Low Diesel Price. Sensitivity analysis from 200 to 2000 kW for battery cell technologies analysed. (a) <i>LFP</i> (ΔP capacity). (b) <i>NMC</i> (ΔP capacity). The Nominal C-rate (axis X) represents the fixed battery energy capacity of 1000 kWh.	108
Figure 59 – <i>EFC</i> - Equivalent Full Cycles for each battery capacity studied. Sensitivity analysis from 200 to 2000 kW for battery cell technologies analysed. (a) <i>LFP</i> (ΔP capacity). (b) <i>NMC</i> (ΔP capacity). The Nominal C-rate (axis X) represents the fixed battery energy capacity of 1000 kWh.	109
Figure 60 – Evaluation of <i>CAPEX</i> and <i>OPEX</i> for Hybrid PSV Power System. <i>CAPEX</i> . (a) <i>LFP</i> (ΔP capacity). (b) <i>NMC</i> (ΔP capacity). <i>OPEX</i> . (c) <i>LFP</i> (ΔP capacity). (d) <i>NMC</i> (ΔP capacity). The Nominal C-rate (axis X) represents the fixed battery energy capacity of 1000 kWh.	110
Figure 61 – Evaluation of <i>NPV</i> for Hybrid PSV system. Sensitivity analysis from 200 to 2000 kW for battery cell technologies analysed. (a) <i>LFP</i> (ΔP capacity). (b) <i>NMC</i> (ΔP capacity). The Nominal C-rate (axis X) represents the fixed battery energy capacity of 1000 kWh.	111
Figure 62 – Theoretical <i>payback</i> calculation parameters for PSV powered by battery. Sensitivity analysis from 200 to 2000 kW for battery cell technologies analysed. (a) <i>LFP</i> (ΔP capacity). (b) <i>NMC</i> (ΔP capacity). The Nominal C-rate (axis X) represents the fixed battery energy capacity of 1000 kWh.	112
Figure 63 – Integrated solution for the battery models performance and economic viability. Part 1 – Range recommended for battery energy capacity variation from 200 to 2000 kWh (Sensitivity analysis). Nominal C-rate represents the fixed battery power capacity of 1000 kW. Part 2 – Similar to the Sensitivity analysis of battery power capacity variation.	114
Figure 64 – Recommendation – Range selected integrating all cases simulated. The Nominal C-rate represents the fixed battery power capacity at 1000 kW or fixed battery energy capacity at 1000 kWh, depending on the sensitivity analysis selected.	115

Figure 65 – Battery models performance – Range recommended for battery energy capacity variation from 200 to 2000 kWh (Sensitivity analysis). The Nominal C-rate represents the fixed battery power capacity of 1000 kW. Indicators evaluated for the battery models. Reduction of CO_2 emission, expected life, reduction of fuel consumption, and EFC	132
Figure 66 – Economic performance – Range recommended for battery energy capacity variation from 200 to 2000 kWh (Sensitivity analysis). The Nominal C-rate represents the fixed battery power capacity of 1000 kW. Indicators evaluated for the battery operating at 70% and 80% DoD . Reduction of fuel costs, $CAPEX$, $OPEX$, and NPV	133
Figure 67 – Battery models performance – Range recommended for battery power capacity variation from 200 to 2000 kW (Sensitivity analysis). The Nominal C-rate represents the fixed battery energy capacity of 1000 kWh. Indicators evaluated for the battery models. Reduction of CO_2 emission, expected life, reduction of fuel consumption, and EFC	134
Figure 68 – Economic performance – Range recommended for battery power capacity variation from 200 to 2000 kW (Sensitivity analysis). The Nominal C-rate represents the fixed battery energy capacity of 1000 kWh. Indicators evaluated for the battery operating at 70% and 80% DoD . Reduction of fuel costs, $CAPEX$, $OPEX$, and NPV	135
Figure 69 – Example of Round-trip Energy Efficiency for a battery connected to Switchboard.	139

List of Tables

Table 1 – Assumptions and specifications adopted for dimensioning Lithium-ion battery systems applied on Hybrid <i>PSV</i> Power System.	54
Table 2 – <i>PSV</i> 1500, 3000 and 4500 dimensions and their Marine Diesel Oil consumption.	57
Table 3 – Marine Diesel Oil consumption per <i>PSV</i> according to each operation mode.	57
Table 4 – Manufacturer’s Marine Diesel Generator-sets Specification Sheet.	63
Table 5 – Reduction of CO_2 emissions and fuel consumption for several vessels presented in the literature. Optimization strategy, battery capacities, Gen-sets capacity, and Payback for Hybrid Vessel simulated.	67
Table 6 – Description of the cases simulated in this Master’s Thesis.	80
Table 7 – The results of Base Case simulation (Homer software) for CO_2 emissions, fuel consumption, and economic analyses of a Typical <i>PSV</i> Power Systems.	82
Table 8 – Types of battery cells, packing, manufacturers, historical, applications and their main chemical/constructive characteristics.	143
Table 9 – Parameters for main Li-ion batteries cells: Lifetime, <i>EFC</i> , Nominal/minimum voltage, Full dis(charge), C-rate(dis-charge), Cont. Power Cap. and round-trip efficiency.	144
Table 10 – Parameters for main Li-ion batteries cells: maximum and minimum temperature, specific energy density, volumetric energy density, self-discharge efficiency, and comments.	145
Table 11 – Cost of investment, installation, O&M and Total Cost Fixed for Li-ion battery cells.	147
Table 12 – Investment, replacement, O&M costs and lifetime for Generator-sets, control system and converter.	148
Table 13 – Theoretical <i>payback</i> calculation parameters for <i>PSV</i> powered by battery.	150

List of abbreviations and acronyms

<i>AIS</i>	Automatic Identification System
<i>BMS</i>	Battery Management System
<i>BS</i>	Balance of System
<i>CAPEX</i>	Capital Expenditures
<i>CC</i>	Cycle Charging Strategy Controller (HOMER software)
<i>DNV-GL</i>	Det Norske Veritas (Classification Society)
<i>DP</i>	Dynamic Positioning
<i>DWT</i>	Deadweight tonnage or tons of deadweight
<i>ECA</i>	Emission Control Area
<i>EEDI</i>	Energy Efficiency Design Index
<i>EEXI</i>	Efficiency Design Index for Existing Ships
<i>EFC</i>	Equivalent Full Cycles
<i>EPC</i>	Engineer-Procure-Construct
<i>HDP</i>	High Diesel Price
<i>HOMER</i>	Hybrid Optimization of Multiple Electric Renewables
<i>HS</i>	Hybrid System
<i>HV</i>	Hybrid Vessel

<i>IRR</i>	Internal Rate of Return
<i>LDP</i>	Low Diesel Price
<i>MKBM</i>	Modified Kinetic Battery Model
<i>NMC</i>	Lithium Nickel Manganese Cobalt Oxide
<i>NPV</i>	Net Present Value
<i>NREL</i>	National Renewable Energy Laboratory
<i>O&M</i>	Operation and Maintenance
<i>OPEX</i>	Operational Expenditures
<i>PCS</i>	Power Control System
<i>PCSEq</i>	Power Conversion System Equipment
<i>PSV</i>	Platform Supply Vessel
<i>RDP</i>	Reference Diesel Price
<i>RTEE</i>	Round-trip Energy Efficiency
<i>SA</i>	Sensitivity Analysis
<i>SBM</i>	Simplified Battery Model
<i>SEEMP</i>	Ship Energy Efficiency Management Plan
<i>SEI</i>	Solid Electrolyte Interphase
<i>SFOC</i>	Specific Fuel Oil Consumption

List of symbols

$t_{payback}$	<i>Payback period in [years]</i>
A_{pb}	Battery initial investment cost [<i>US\$</i>]
B_{pb}	Fuel price [<i>US\$/liter</i>]
C_{pb}	Diesel consumption rate [<i>liter/hour</i>]
D_{pb}	Time operation of Hybrid <i>PSV</i> Power System [<i>days</i>]
E_{pb}	Vessel operation hours of stand-alone mode [<i>hour/day</i>]
F_{pb}	Stand-connected mode [<i>hour/day</i>]
G_{pb}	Shore connection electricity cost [<i>US\$/kWh</i>]
H_{pb}	Power rating of battery system in [<i>kW</i>]
I_{pb}	Total efficiency of battery system
J_{pb}	Carbon credit in [<i>US\$/ton</i>]
K_{pb}	Avoided emission of carbon dioxide given in [<i>ton/years</i>]
$F(P_{Gen-set})$	Fuel consumption as a function of load
a	Coefficient of the second-order polynomial function
b	Coefficient of the second-order polynomial function
F_0	Coefficients of the second-order polynomial function
$P_{Gen-set}$	Loading of the Gen-sets as a percentage of the electrical power output in [%]

$P_{Gen-set}$	Loading of the Gen-sets as a percentage of the electrical power output in [kW]
$\eta_{Gen-set}$	Gen-set efficiency in [%]
\dot{m}_{fuel}	Mass flow rate of the Diesel fuel in [kg/h]
LHV_{fuel}	Lower Heating Value in [MJ/kg]
ρ_{fuel}	Fuel density in [kg/liter]
lb	1 Pound is a measure of Weight used in Standard system and equivalent to 0.119826427 gallon (gal)
$U.S.gal$	Gallon is a measure of Volume used in Cooking system. US gallon is equal to 3.785411784 liters
V_{tank}^{Ship}	Total fuel tank capacity in [liter]
$P_{Gen-set}^{total}$	Total power ship
$t_{autonomous}$	Autonomous operation time
$kWh - throughput_{lifetime}$	Energy throughput during battery lifetime

Contents

1	Introduction	25
1.1	<i>Objectives</i>	32
1.2	<i>Limitations</i>	32
1.3	<i>Structure of the Master's Thesis</i>	33
2	Battery Modeling	34
2.1	<i>Battery technology</i>	34
2.2	<i>Lithium-ion battery cell technologies applied in Ship Power System</i>	35
2.3	<i>Modules, packs, BMS and container</i>	36
2.3.1	Battery Space, Fire Safety, and Cooling Systems	38
2.4	<i>Operation modes for Lithium-ion Batteries applied on Hybrid Ship</i>	39
2.5	<i>Battery aging</i>	41
2.5.1	Cycle aging and Calendar aging mechanisms	42
2.5.2	Counting the number of cycles	45
2.5.3	Degradation phenomena in the positive-negative electrodes and electrolyte	46
2.6	<i>Battery models</i>	48
2.7	<i>Assumptions adopted for battery system specification applied to the PSV Power System</i>	54
2.8	<i>Synthesis</i>	55
3	Hybrid Platform Supply Vessel Test System	56
3.1	<i>PSV Operating Characteristic</i>	56
3.2	<i>Diesel-electric systems</i>	57
3.3	<i>Typical operational profile of PSV Power System</i>	59
3.4	<i>Diesel generator-sets</i>	60
3.4.1	Generator-sets characteristics and specifications	60
3.5	<i>Dispatch modeling</i>	63
3.6	<i>Emissions reduction potential in Hybrid Vessels and State of the Art</i>	64
3.7	<i>Synthesis</i>	68
4	Cost Analysis Methodology for Battery Aging	69

4.1	<i>Components costs</i>	69
4.1.1	Generator-sets, power converter, and <i>O&M</i> costs	70
4.1.2	Battery costs	72
4.2	<i>Economic metrics for Lithium-ion batteries performance evaluation</i>	73
4.2.1	Net Present Value (<i>NPV</i>)	73
4.2.2	<i>CAPEX</i> and <i>OPEX</i>	74
4.2.3	Internal Rate of Return	75
4.2.4	<i>Payback</i> and <i>Discounted Payback</i>	75
4.2.5	Levelized Cost of Energy (<i>LCOE</i>)	76
4.3	<i>Objective function</i>	76
4.4	<i>Sensitivity analysis</i>	77
4.5	<i>Synthesis</i>	79
5	Results and Discussion	80
5.1	<i>Base case</i>	82
5.2	<i>Sensitivity analysis for Simplified battery model</i>	83
5.2.1	Pollutant emission estimation (Energy variation)	83
5.2.2	Battery expected life (Energy variation)	84
5.2.3	Reduction of fuel consumption (Energy variation)	85
5.2.4	Fuel costs savings (Energy variation)	86
5.2.5	Equivalent Full Cycle (Energy variation)	87
5.2.6	Economic analysis (Energy variation) – Hybrid PSV Power System	88
5.2.7	Pollutant emission estimation (Power variation)	90
5.2.8	Battery expected life (Power variation)	91
5.2.9	Reduction of fuel consumption (Power variation)	91
5.2.10	Fuel costs savings (Power variation)	92
5.2.11	Equivalent Full Cycle (Power variation)	93
5.2.12	Economic analysis (Power variation) – Hybrid PSV Power System	94
5.3	<i>Impact of battery energy capacity variation</i>	97
5.3.1	Pollutant emission estimation	97
5.3.2	Battery expected life	98
5.3.3	Reduction of fuel consumption	99
5.3.4	Fuel costs savings	99

5.3.5	Equivalent Full Cycle	101
5.3.6	Economic analysis – Hybrid PSV Power System	102
5.4	<i>Impact of battery C-rate variation</i>	104
5.4.1	Pollutant emission estimation	104
5.4.2	Battery expected life	105
5.4.3	Reduction of fuel consumption	106
5.4.4	Fuel costs savings	107
5.4.5	Equivalent Full Cycle	108
5.4.6	Economic analysis – Hybrid PSV Power System	109
5.5	<i>Recommendations for battery operation in the hybrid PSV power system</i> .	112
5.6	<i>Synthesis</i>	116
6	Final Remarks	118
6.1	<i>List of Publications</i>	121
BIBLIOGRAPHY		122
A	Recommendations for battery operation – performance of indicators	131
B	Glossary	136
C	Types of battery cells and their characteristics	142
D	Investment, replacement and O&M costs	146
E	Theoretical payback calculation parameters.	149
Index	151

Chapter 1

Introduction

The Greenhouse Gas (*GHG*) Emissions will grow in the next decades and it is estimated by 2050 that the CO_2 emissions will be about 1600 million tons per year. Currently, this estimation is below 1000 million tons per year. It is essential to study and implement the hybridization of several types of Ships. Hybrid Ship Power Systems have been becoming more frequent in the world and international regulations are establishing restrictions to the shipping sector due to rapidly increasing these emissions [1].

The transportation sector accounts for 25% of the total energy consumed in the world. Maritime transport sector accounts for 30% of CO_2 emissions to the transport sector and 3% to 4% of CO_2 emissions from all human activities sectors [1]. According to [2], specifically, CO_2 emissions from ships all over the world are approximately 2.6% of global emissions. Thus, the reduction of pollutant emissions to maritime transport is an important goal considered by the naval industry.

In terms of regulatory aspects, the International Maritime Organization (*IMO*) imposes stiffer regulations to the naval industry for the reduction of *GHG* emissions and pollutants, mainly NO_x , CO_2 , SO_2 , sulfur dioxide, carbon oxide and ozone particles [1]. Besides, new legislation forces ship owners to design vessels with lower emission considering new Emissions Control Areas - *ECA* [3].

There are only two mandatory requirements addressing *GHG* emissions related to seaborne transportation: the Energy Efficiency Design Index (*EEDI*) and Ship Energy Efficiency Management Plan (*SEEMP*). The former is destined for newbuilds with a mandating up to 30% improvement in design performance and also measures of the amount of CO_2 emissions that a cargo ship produces per mile and per tonne of goods; and the latter though it contains

no mandatory performance requirements, is directed for all ships in operation [4]. During International Convention for the Prevention of Pollution from Ships (MARPOL) [5], in 2008, were discussed the Enhanced *SEEMP*, and the application of the *EEDI* retroactively to all existing vessels using the parameter denominated Energy Efficiency Design Index for Existing Ships (*EEXI*). For other ship types, the same measures are being assessed [6]. According to the Third *IMO* Greenhouse Gas Study 2014 [7], the greenhouse gases (CO_2 , CH_4 , N_2O , HFC, among others) that are produced by ships will increase between 50-250%, considering energy developments and future economic growth.

After January 2016, came into force the *IMO* Tier 3 for Diesel engines with a power output of more than 130 kW that established a reduction of NOx emission limits to 2.0 g/kWh and 3.4 g/kWh for ships that operate in Emissions Control Areas (*ECA*), [3, 6, 7]. Furthermore, the novel climate agreement denominated Paris Protocol was recently established by the European Commission with a long-term goal of reducing global emissions up to 60% until 2050 [2].

The energy sector has been extremely impacted by the COVID-19 pandemic, resulting in decreasing energy demand and price reductions of electricity, gas, and oil [8]. These effects are directly related to reductions of emissions and the production of valuable minerals for the delivery of equipment to power plants with energy storage technologies, renewable energy, or smart grids [8, 9]. Global tracking data extracted by the Automatic Identification System (*AIS*) from January to May 2020 compared with the same period in 2019 demonstrates a significant impact on seaborne trade. This impact resulted in a decrease of around 6% in transport capacity in deadweight tonnage-miles (DWT-miles) for Container ship and a similar tendency for Cargo vessels. Conversely, the Oil tanker vessels have presented growth around 3% in DWT-miles in the same period [4].

As reported by [4], the total demand for seaborne transportation will have decreased by about 8% in 2020. For a short-term horizon is observed an abrupt reduction of carbon emission; while the mid-term horizon (years) focus on stimulating economic recovery and a sustaining of the clean energy transition in new scenarios of Environmental politics and Macroeconomics; and long-term horizon (decades) should be focused on create polities that integrate lessons learned during the crisis [8, 9]. Until 2023, the *IMO* intends to implement the first tranche of additional *GHG* regulations [4].

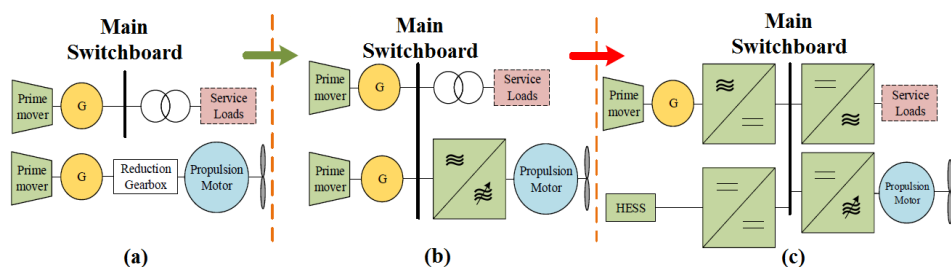
The marine sector is of great importance in order to save fuel and reduce emissions. The operational profile of vessels is diversified: for instance, a typical *PSV* can run several tasks, such as port operation; high transit; Dynamic Positioning (*DP*); low transit; and stand-

by operation [6, 10, 11]. As a consequence of the multiplicity of operational activities, the propulsion systems have to perform well on several criteria [6], such as fuel consumption; emissions; propulsion availability; maneuverability; maintenance cost due to engine thermal, and mechanical loading; purchase cost; and others. This commitment to adaptability and efficiency to operational profiles of ships has driven to a diversity of propulsion systems architectures, which can be categorized as follows: AC or DC electrical distribution; Mechanical propulsion (usually Diesel); electrical propulsion or a hybrid combination of both; and Power generation with generator-sets (combustion engines); energy storage (mainly batteries); fuel cells or a hybrid combination.

Diesel-electric propulsion has been implementing in the marine industry mainly due to the fast development of power electronics, the improved power density of electric generators, and higher efficiency when is compared with the mechanical propulsion system. Some advantages of Diesel-electric propulsion are related to the possibility to optimize the loading of Diesel Gen-sets, and consequently, provide the reduction of fuel consumption; the higher reliability due to Gen-set redundancy; and flexibility in the location of Gen-sets (Main and Auxiliary), switchboards, and thruster devices. These characteristics indicate that major users of the electric propulsion system are ship in which the load profile presents changing operational conditions and equipped with electrical actuators such as *PSV* case [12].

A few decades ago, the shipboard microgrids have been evolving due to the integration of AC and DC system, development of power electronics interface based on renewable power sources/storage systems, and this complexity of vessel microgrid presents a philosophy comparable to the terrestrial one. Moreover, the main switchboard is not a radial structure where generation and load are connected separately such as the conventional system [2]. Figure 1 illustrates the evolution of Ship Power Systems.

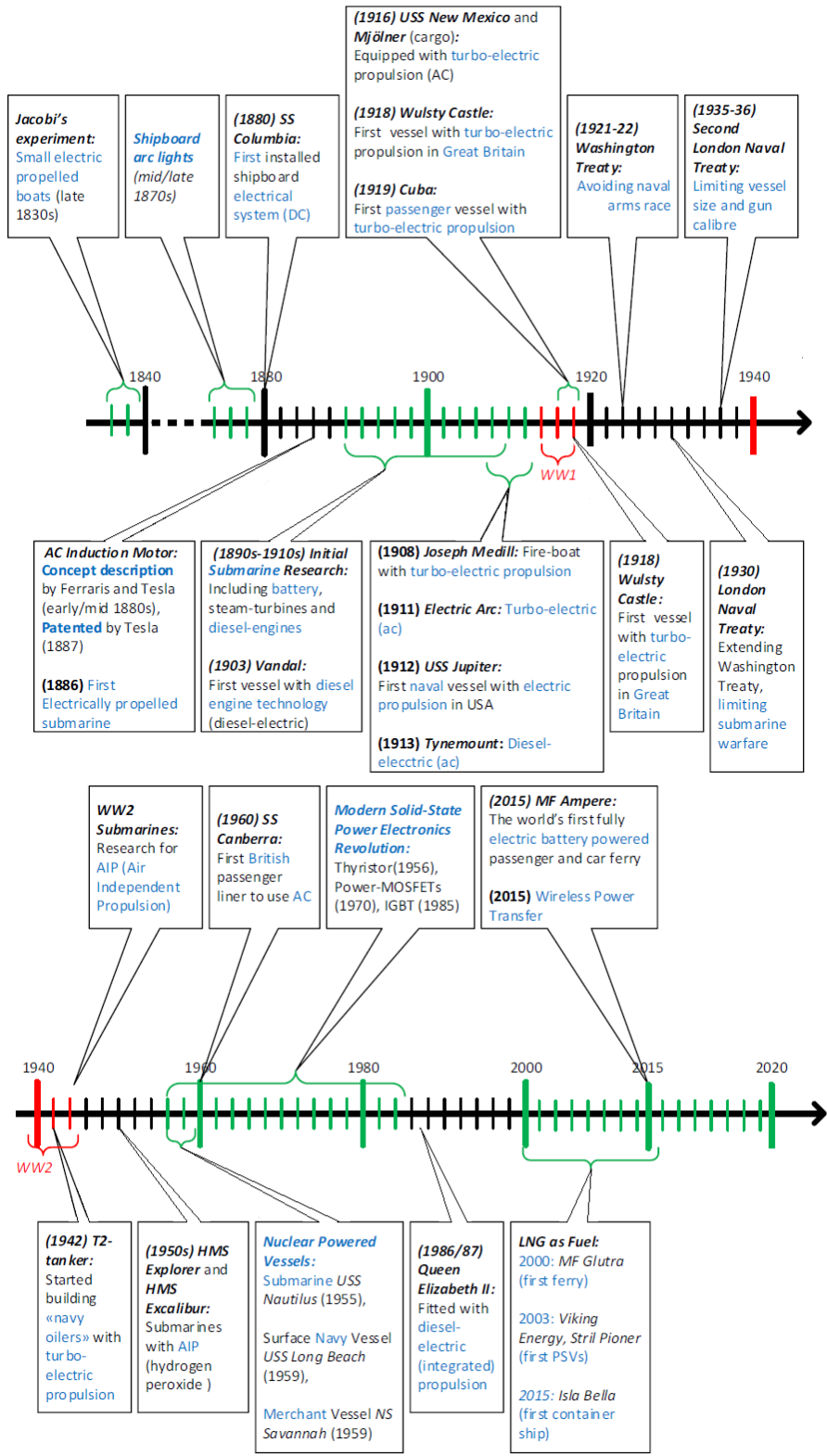
Figure 1 – Evolution of Ship Power Systems. (a) Conventional power system. (b) Integrated AC power system. (c) Integrated DC power system.



Source: Adapted from [2].

Figure 2 illustrates Stages of Historical development of the Marine Vessel Electrical Power Systems from 1830 to 2020.

Figure 2 – Stages of historical development of the Ship Electrical Power Systems from 1830 to 2020. During WWI was first vessels with turbo-electric propulsion, and WWII served as the base to the development of T2-tanker with turbo-electric propulsion.



Source: Adapted from [13].

Currently, due to the vessels designed and their great variability in the operation modes and power generation systems, it is not clear in which segment of shipping sector that hybrid vessels would contribute to reduce fuel consumption and emissions. Thus, it is hard to evaluate the benefits and profitability of the ship without performing a detailed analysis of the techno-economic impacts of installing a Li-ion battery on a vessel that have a certain type of mission. Hybrid vessel (*HV*), in this context, is a ship that has a energy storage system and these devices provide part of demanded power of loads. Several alternative terms can be used to define hybrid vessels, such as some focused on the propulsion system, especially for comparison between the conventional propulsion system – where the Diesel engine is connected directly to the propulsion system – and hybrid propulsion system with Diesel-electric generation. In the context of this work, a hybrid system means the inclusion of batteries operating in parallel with the main generation [3].

The use of renewable energy [14] and batteries in existing *PSV* vessels can provide benefits as reduction of CO_2 emissions and reduction of operational costs, mainly for offshore ships operating under fluctuating conditions because of peak loads at short period of time [15]; satisfy the power demand for peak load; enhance power systems reliability and power quality; and improve energy efficiency of Ship Power System.

By comparing the conventional and hybrid system propulsion, the latter can include new components to provide a reduction of emissions, such as energy storage systems [6]. The difference between the storage system and any other components is that it can deliver and absorb energy, behaving as a generator and as a load [16]. However, when included a battery system to the Diesel conventional system, it gives flexibility to the power production to supply the demand in several operational modes, such as strategic loading; spinning reserve; peak-shaving; enhanced dynamic performance; and zero-emissions operation [16, 17]. Besides, batteries can compensate for power demanded fluctuations, allowing the Gen-sets to run at higher efficiency operations points; Gen-sets can operate more at medium to high power with lower Specific Fuel Oil Consumption (*SFOC*) and lower emissions when a battery is included; battery can be connected instantly and can supply any peak power demand by DP operation; and DP operation can be aborted safely when all Gen-sets should stop and not start again [15]. However, the survey limited in optimization of batteries deployment and intelligent use of DC architectures has shown that smart control strategies can deliver reductions of 10–35% in fuel consumption and emissions [6].

Some examples of Hybrid Vessel (*HV*) are:

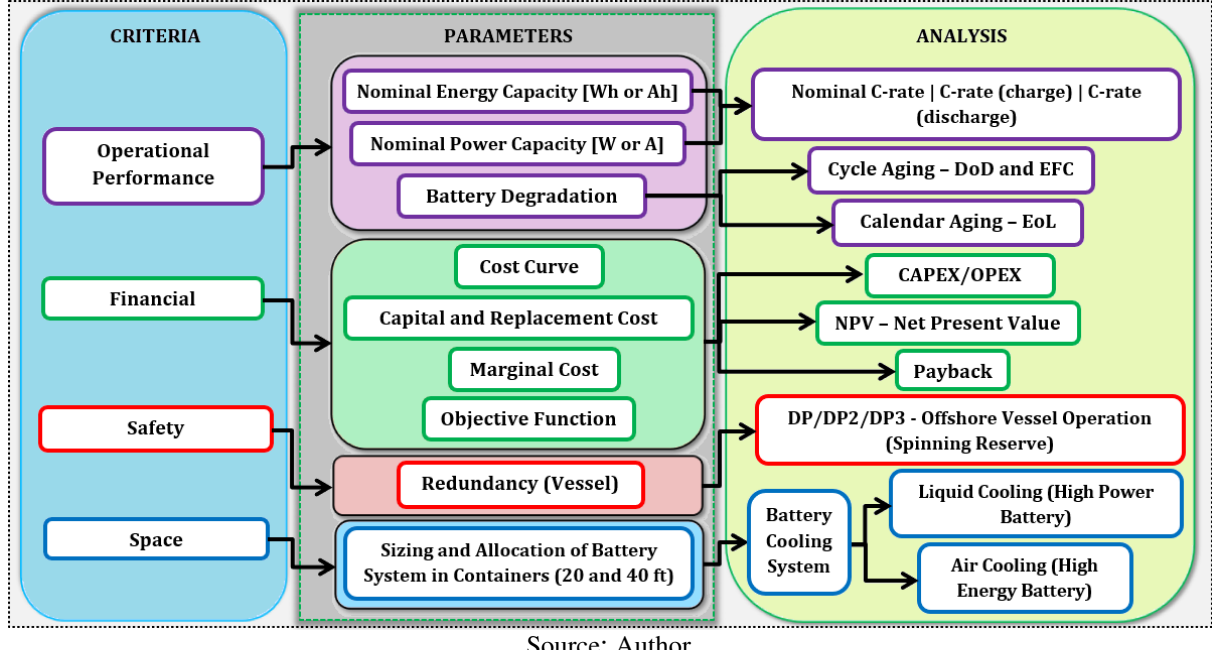
- Nemo H2 project, the vessel developed in Amsterdam in 2009 that operates with a PEMFC fuel cell system of 60-79 kW and 70 kWh battery capacity [1, 18].
- Hybrid TUG RT Adrian was the first European hybrid TUG developed in 2011 and this vessel combine the battery system and Diesel Gen-sets, being able to operate for low power modes (all-electric or diesel-electric mode), in the mid power range (conventional mode) and in full power (combined mode), when the diesel propulsion engines and electrical motors are used simultaneously. This system is called "Xeropoint Schematic Propulsion Systems" [1].
- In 2009, Viking Lady – owned by Eidesvik Offshore ASA – was the first merchant vessel to use fuel cell (about 320 kW). In 2016, a battery of 450 kWh was installed making the first hybrid PSV. This vessel is equipped with four dual-fuel engines that can run on natural gas. Fellowship Project consortium was initiated by Det Norske Veritas (DNV-GL, classification society), Wärtsilä, and MTU Onsite Energy GmbH [3, 19].
- Viking Princess, the first-ever hybrid offshore vessel where a battery system of 533 kWh capacities (90 battery modules) replaced the Gen-set. Originally, this vessel fitted with 4 engines running on LNG (2x W6L20DF and 2x W6L34DF) [20].

The technical parameters for Lithium-ion batteries which can be assessed are [21]: Energy Capacity [kWh], Power Capacity [kW], C-rate [1/hour], Round-trip Efficiency [%], Expected Life [year], Cycle Life, Depth-of-discharge - *DoD*, State-of-charge - *SoC*, Lifetime Throughput [kWh], End of Life - *EoL*, and Internal Resistance. These previous parameters definition can be verified in Glossary (B) present in this work.

The battery dimensioning process for *PSVs* can include criteria as: (1) operational performance (Strategic loading, peak shaving, etc); (2) financial criteria which can use costs model to compare different cases; (3) safety criteria that are totally related to DP redundancy aspect during vessel operation for battery operating as Spinning reserve; and (4) space criteria when is considered the dimension limits by a container, usually 20 or 40 foot [22–24]. This Master's thesis is focused on the first two criteria. The main criteria which may be used for dimensioning Lithium-ion batteries for *PSV* are shown in Figure 3.

The originality of this Master's Thesis includes the consideration of different technologies of battery cells (*LFP* and *NMC*), a sensitivity analysis over parameters of the battery degradation process considering cycle aging and calendar aging modelling for *PSV* Power System and

Figure 3 – Criteria adopted for dimensioning Lithium-ion batteries for Platform Supply Vessel.



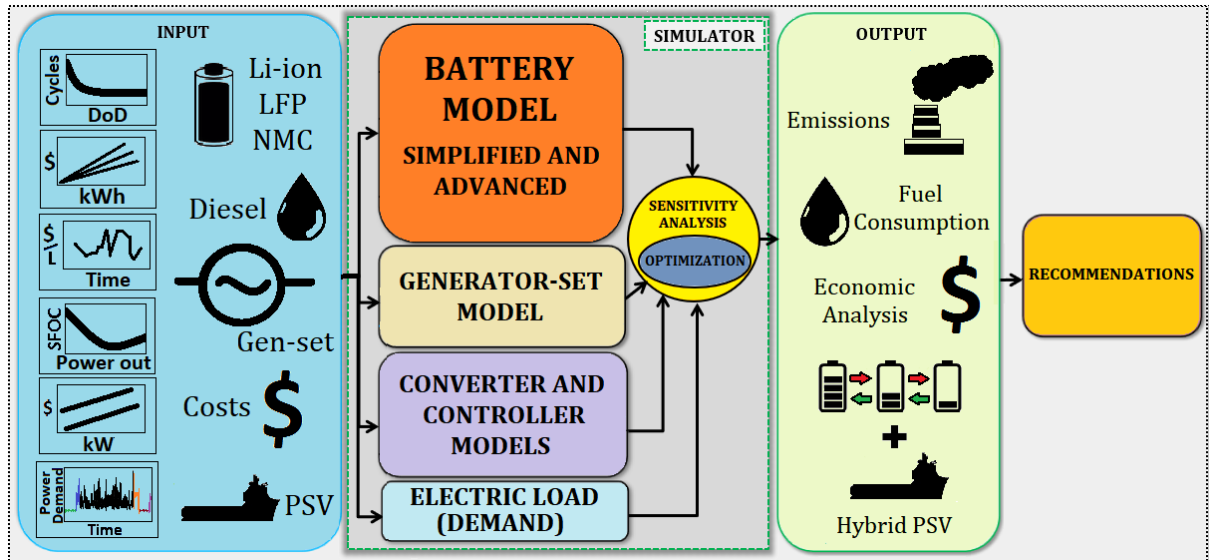
Source: Author.

analyzing the impact of Lithium-ion batteries with regard to the reduction of CO_2 emissions, fuel consumption, fuel-saving, fuel cost, and economical aspects.

These aspects are worth considering since there are multiple battery technologies with different round-trip efficiencies and several ship power system architectures. In addition, requirements for each part of the mission are different, which implies that the use of batteries and auxiliary generators could also differ for each part.

The general methodology used in this work can be visualized in Figure 4.

Figure 4 – Flowchart of the proposed method on this Master's Thesis considering Optimization software.



Source: Author.

Homer Energy software is used to simulate several cases that include a substantial quantity of data obtained through the literature review about hybrid systems, dimensioning Li-ion batteries, generator-sets, vessel operational profile, and economic parameters for hybrid vessels. These data are entered into the HOMER (Input). The energy storage models are separated into two types: simplified and advanced. Together with the other system component models, the simulator runs the simulation with several combinations, obtaining a list of simulated cases. The best results can be selected and analyzed according to the survey proposed. Thus, these studies can create recommendations related to battery operation on Hybrid Power Systems.

1.1 Objectives

The main goal of this Master's Thesis is to analyze and quantify the main techno-economic impacts of installing Lithium-ion batteries on the Platform Supply Vessel (*PSV*). The specific goals are listed following:

1. Evaluation of optimal size battery to attend part of the demand - Operational profile - for a typical *PSV* Power System.
2. Evaluation of battery size considering technical performance and the degradation processes of battery cells (*EFC* and expected life).
3. Evaluation of battery size considering the reduction of CO_2 emissions, fuel consumption, fuel-saving of battery-powered *PSV*.
4. Evaluation of battery size considering techno-economic performance through the comparison between the Conventional Diesel vessel and Hybrid vessel.

1.2 Limitations

In this Master's Thesis, HOMER software used to simulate the cases presents some limitations mainly related to the optimization process, that is not described in its User Guide and literature [25]. Some works [26–30] describe the objective function considered by software, the limited ability to component parameterize, the dynamic characteristics that are not incorporated to HOMER's tools that, consequently, it is not allow simulating devices transients that are necessary to give the realism as conditions fluctuate during operations specific of vessel mission. The modeling for each component is precisely detailed, including items about controllers, dispatch,

and order of dispatch priority. Based on this, peak-shaving analysis or other operational modes for batteries that operate to short-time duration are not considered adequate scopes of this Master's dissertation.

1.3 Structure of the Master's Thesis

The Master's thesis has been structured into six chapters: Chapter 2 detail the battery modelling. Chapter 3 illustrates the Platform Supply Vessel test system and emissions reduction potential in Hybrid Ships. Chapter 4 presents the cost analysis methodology for the battery system and other system components. The economic metrics, the objective function for optimization model, and the sensitivity analysis are presented. Chapter 5 shows the results and discussion of battery performance in *PSV* Power Systems considering the techno-economic evaluation of cases simulated. The Chapter is divided into four main parts that describe the Base Case (Vessel without batteries included), the impact of battery energy capacity variation, power capacity (or battery C-rate) variation, and some recommendations based on the best results. Chapter 6 presents the conclusions.

Chapter 2

Battery Modeling

2.1 *Battery technology*

This chapter shows an introduction to the terminology used to compare, classify, and describe batteries for the Hybrid Ship Power System. Several variables describe battery operating conditions and they can be defined in terms of nominal and maximum characteristics certificated by the manufacturer. Some battery parameters are defined throughout this Chapter, but the Annex B (Glossary) presents other definitions mentioned in the text.

Lithium-ion battery capacity has increased by nearly 25% in the last 3 years and more than doubled in comparison 10 years ago. In the same period, the Li-ion battery costs have decreased by a factor of ten [31]. This rapid technological evolution comes uncertainty about batteries' performance in new or different applications, as the Marine sector. There are discrepancies in the form as suppliers describe battery performance: how constitutes a high-performing battery, and what battery cell technology should be selected, these facts can result in confusion among batteries buyers [31, 32].

Lithium-ion batteries are typically classified into a cell form factor, which characterizes three different formats: Prismatic, Pouch, or Cylindrical; this design issue discussed at this point because of the degradation of *SOC* battery range depends on the type of battery cells as well as their format. Prismatic cells have a polymer or aluminum in their fixed terminals, efficient packing, but are expensive with risks of swelling. Pouch cells present themselves in varying sizes but are polymer pouch vacuum-sealed around the battery electrochemical materials, that have risks of swelling, and need compression. Moreover, cylindrical cells are manufactured in 21700, 26650, and 18650 standard formats, they have a stable design and are pressure-resistant, but show poor packing efficiency and cooling difficulties [33, 34].

2.2 *Lithium-ion battery cell technologies applied in Ship Power System*

The main Lithium-ion battery cells chemistries used to many application are Lithium Manganese Oxide (*LMO* – LiMn₂O₄) and Lithium Cobalt Oxide (*LCO* – LiCoO₂), Lithium Nickel Cobalt Aluminum Oxide (*NCA* – LiNi_xCo_yAl_{1-x-y}O₂), Lithium Titanate (*LTO* – Li₂TiO₃ or Li₄Ti₅O₁₂), Lithium Iron Phosphate (*LFP* - LiFePO₄), and Lithium Nickel Manganese Cobalt Oxide (*NMC* or *NCM* – LiNiMnCoO₂).

LMO cell technology has great potential for high loads applications due to high-current discharging capabilities, higher thermal stability, and better safety. It relies on manganese, which is five times more economical than cobalt. Conversely, a low calendar and cycle life (only 700 cycles), lower energy performance [35, 36] can be considered disadvantages important for marine battery applications. Normally, *LMO* and *NMC* are combined to provide a balance between performance and cost of cells [36].

LCO cells use a cobalt oxide cathode and a graphite carbon anode. Its applications are more popularly choice for smartphones, and laptops due to the high specific energy. Some disadvantages of *LCO* cells are their limited specific power capacities, short lifespan, the drawback of Lithium diffusion, overheating caused by low thermal stability [35, 36]. These problems do not accredit this cell technology for marine applications due to its risk of fire.

NCA can be used in Electric Powertrains and industrial applications, but its low lifespan of up to 500 cycles is a limit for ship ones. Nevertheless, this cell has a high energy density of 200 - 260Wh/kg. This battery has been applying on the Mobility market – for instance in Tesla Motors EVs – and its cathode with 5% Aluminium doping has been permitted a growing performance and a higher economical effective than cobalt [35, 36].

Tests performed in DNV-GL's labs [31, 32, 37] show the *LTO*, *LFP*, and *NMC* cells performance under a range of conditions, providing an independent ranking and evaluation. These batteries are considered the three principal Lithium-ion cell chemistries applied in maritime batteries.

LTO cells have titanate in the anode instead of graphite frequently used in other battery cell technology. Besides, its cathode can present other electrode chemistry, offering stable Lithium-ion chemistry. This cell allows high power density, fast charging, or very large equivalent full cycles (*EFC*), including excellent safety characteristics, and long lifespan [38–40]. *LTO* cell does not form a Solid Electrolyte Interface (*SEI*) film or Lithium plating when is fast charging

or charged in low temperature [35]. A negative aspect is the fact of *LTO* cell presents a lower energy density and higher average cost [39,41]. This battery technology trends to decrease cost and grow its market share mainly in high-power applications related to frequency regulation [42].

LFP cells may be used in applications that need good thermal stability features with a type of chemistry considered one of the safest among main Lithium-ion batteries [38, 39]. It has also the ability to withstand very high temperatures above 300°C [40]. This cell presents a low cost for a high power density, full power at 100% *DoD* can be delivered because its discharge voltage is very constant. Elevated self-discharge levels and low energy capacity are limiting factors to *LFP* cell application [39]. *LFP* can also be advantaged in applications that need high C-rates and endurance such as starter battery [35].

NMC (or *NCM*) technology is the market leader in the maritime sector and its relative composition and quantities sized can be tweaked to produce different values, demonstrating balanced performance and flexibility characteristics in terms of energy/power density, safety, cycle life, and cost [38, 39]. This cell is available with different composition of cobalt, nickel, and manganese. The safety of *NMC* is lower than *LFP* electrodes, but it can demonstrate the high advantage of the cathode blends including several properties present in other elements [40]. The reduced cost is obtained because the partial replacement of cobalt with nickel is cheaper [35].

Based on these tests, the simulation presented in this work will be in consonance with the specifications of *NMC* and *LFP* cells. All battery cells previously cited and their main parameters and characteristics can be seen in Annex C (Tables 8, 9, and 10), and Annex D (Table 11).

2.3 Modules, packs, BMS and container

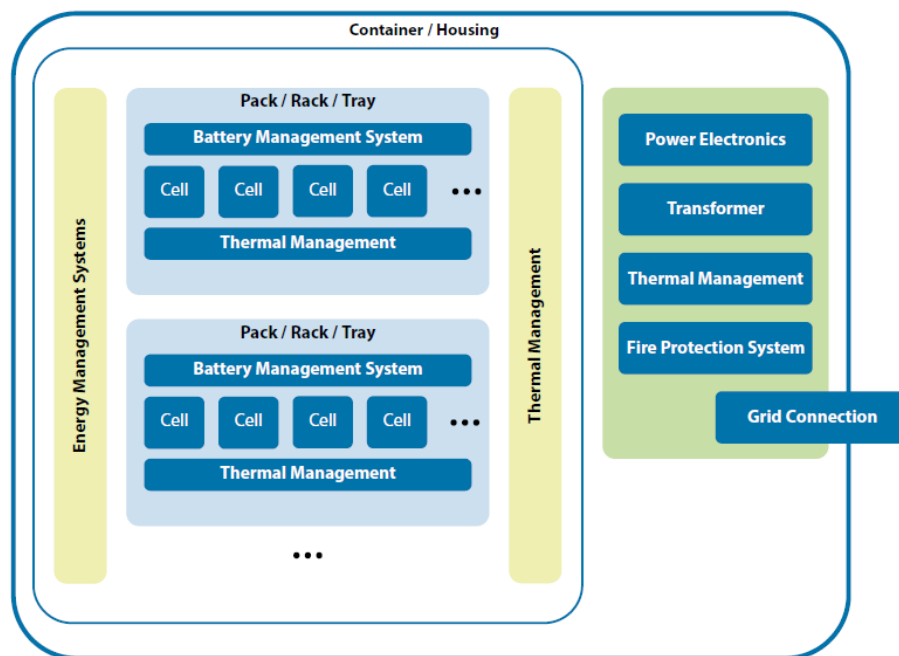
As reported by the *IEC 62620 Standard (2014)* [43] – Secondary Cells And Batteries Containing Alkaline Or Other Non-Acid Electrolytes – there are specific requirements for Lithium-ion cells used in industrial applications. This *IEC* Standard also defines that the battery system can be divided into smaller units and the smaller one can be tested as the representative storage system. The smallest unit is a battery cell, but it is not ready for use in the application because it is not powered with its terminal arrangement and electronic control device. The smaller unit considered by the standard is a battery module that is a group of cells connected in a series and parallel configuration. Besides, the battery pack is composed of one or more modules connected together a monitoring circuit that provides information to a battery system.

Each module is physically located in the Battery Space (or Compartment) that is integrated into several trays known as Rack [36].

When it is necessary to cut off the battery system in case of over-current, over-discharge, under-voltage, over-voltage, overcharge, voltage unbalance, or overheating, a *BMS* - Battery Management System - is driven. In the part of *BMS* is located a “balancing circuit” that has a function of forcing all cells within a module to have identical voltages. In the case of the absence of a balancing circuit, a failure of one or more battery cells may result in under-charged or overcharged [43, 44]. Besides, *BMS* can also monitor the battery string current, and over-temperature conditions. This system should be continuously powered and in case of the event of failure, an audible and visual alarm should be displayed [44]. Another similar device onboard a vessel is denominated *PMS* – Power Management System – and it can share the load among different power Generator-sets and battery or shed load when generated power is insufficient [43].

Figure 5 illustrates a *BMS* integrated into a container.

Figure 5 – Battery Management System.

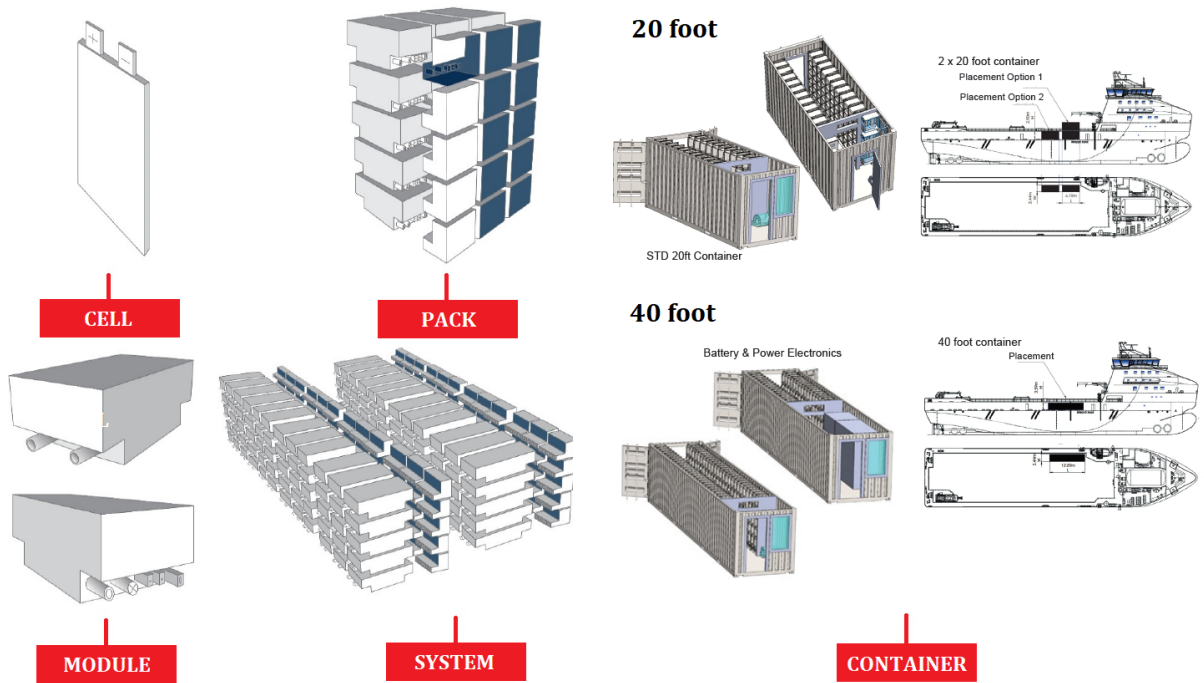


Source: Adapted from [36].

There are two container sizes usually employed to accommodate a battery pack and applied in a *PSV* vessel: 20ft (6.058m x 2.438m x 2.591m) or 40ft (12.192m x 2.438m x 2.591m) container. These containers include a Lithium-ion energy storage system specifically designed and built for marine applications where lightweight and high charge/discharge power are fundamental pre-requisites. Both container sizes induce space (area/volume) constraints for

the battery pack sizing where, besides the battery pack (power converter systems, electrical installations, cooling systems, etc.) requirements there is also the need to provide access for maintenance of the system [23, 45]. Figure 6 illustrates the composition of a battery system and its inclusion in a container.

Figure 6 – Parts of a Battery System and its inclusion into a 20 and 40-foot container.



Source: Adapted from [43, 45].

2.3.1 Battery Space, Fire Safety, and Cooling Systems

Battery spaces should be installed with appropriate means to vent mechanically gases ventilated gases from the battery to the open deck, where such gases will not cause an explosion, fire, or a toxic hazard to nearby operators. For flammable gas detection, a device should give an alarm and automatically disconnect the battery system to the concentration of gas reaches 30% Lower Explosive Limit (*LEL*). Battery system risk should involve an evaluation of the chemical composition of the Lithium-ion battery cell used and this assessment should indicate if the flammable gas is released in normal operation. In this case, the ventilation system has to be interlocked together with the battery chargers, preventing any battery charge during gas release. For the Lithium-ion batteries that present high risk of explosion, the battery space has to be classified as a hazardous area, as IEC 60079-10-1 guidance [43, 44, 46].

A PSV Power System is a Dynamic Positioning (*DP*) vessel. For this type of operation mode, its battery can be operated to supply power to thrusters during fault ride through on *DP2/DP3* in a closed bus, satisfying redundancy criteria [43,44].

2.4 Operation modes for Lithium-ion Batteries applied on Hybrid Ship

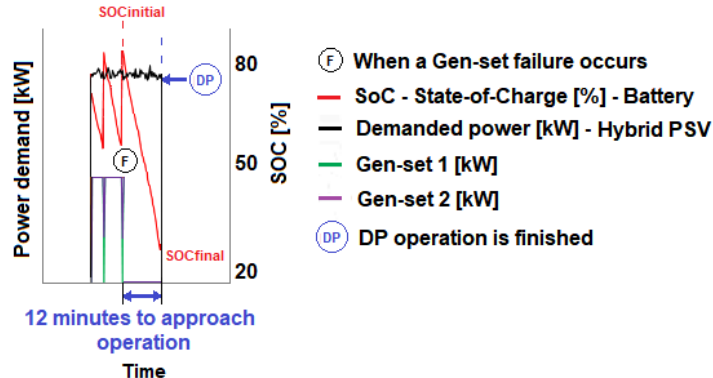
Batteries can be classified basically in two types of electrochemical forms: primary and secondary batteries. The former converts chemical energy into electrical energy and its electrochemical reaction is non-reversible when it is fully discharged and the latter is a battery that can be recharged because its electrochemical reaction is reversible [47–49]. The rechargeable battery is usually used in ships for emergency power for control circuits, essential power demand, and starting power for Main Gen-sets. Also, this battery can be applied for programs to reduce emissions, promoting more efficient energy use [47]. The term hybrid vessel presents several meanings. However, it can be represented by an energy storage device as part of the total power generation. This definition is similar to batteries used in hybrid vehicles and will be appropriate for this work [3].

Some criteria used to justify the application of batteries for hybrid vessels are:

- **Facilitate energy harvesting** – For a case that renewable sources included on a vessel, the battery is necessary for efficient onboard harvesting, for example, from solar energy [3].
- **Harbor mode** – If the battery system installation is sufficiently sized, it can administer all power demand in the harbor, and thus there is no need to operate the Gen-sets, eliminating local emissions [3]. This operation mode is also called Zero Emissions Operation and it is interesting as a requirement to reduce gas emission next to highly populated areas [3, 17].
- **Power redundancy** – Also known as Spinning reserve mode, the battery can provide power and, therefore, fewer engines are used while satisfying rules for redundancy [3, 50]. The battery is capable of providing power instantly to the system, and consequently, the number of Gen-sets running hours is reduced, growing the time required until its maintenance is necessary. Besides, the load percentage of a Gen-set can increase while the other one is disconnected, resulting in reducing fuel consumption and CO₂ emissions [17]. Specifically, redundancy is related to the time necessary to approach operations on the high sea during Dynamic Positioning (*DP*) operations on *PSVs* [50]. For instance, Figure 7 illustrates that a battery can support 12 minutes from instant F that shuts down the Gen-

sets immediately. The manoeuvre should be aborted if adequate and follow the safety requirements to do so until the *DP* operation be finished (instant *DP* instant).

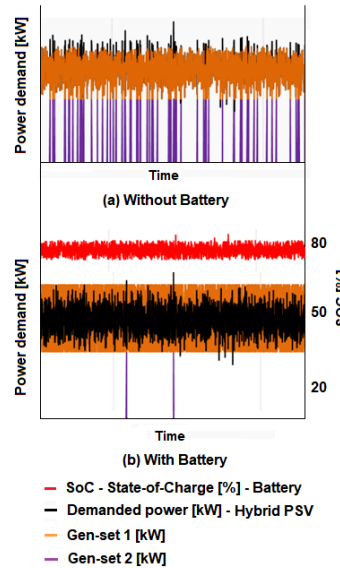
Figure 7 – Battery operating as Spinning reserve.



Source: Author.

- **Peak-shaving** – Also called transient mode, meaning that a battery can handle the transient demand providing power to attenuate the peak. Figure 8 (b) shows that the Gen-sets peak does so by battery action. Peak-shaving provides a reduction in fuel consumption since this transient rate is higher than the stationary state fuel consumption [3, 17].

Figure 8 – Battery operating as Peak-shaving.



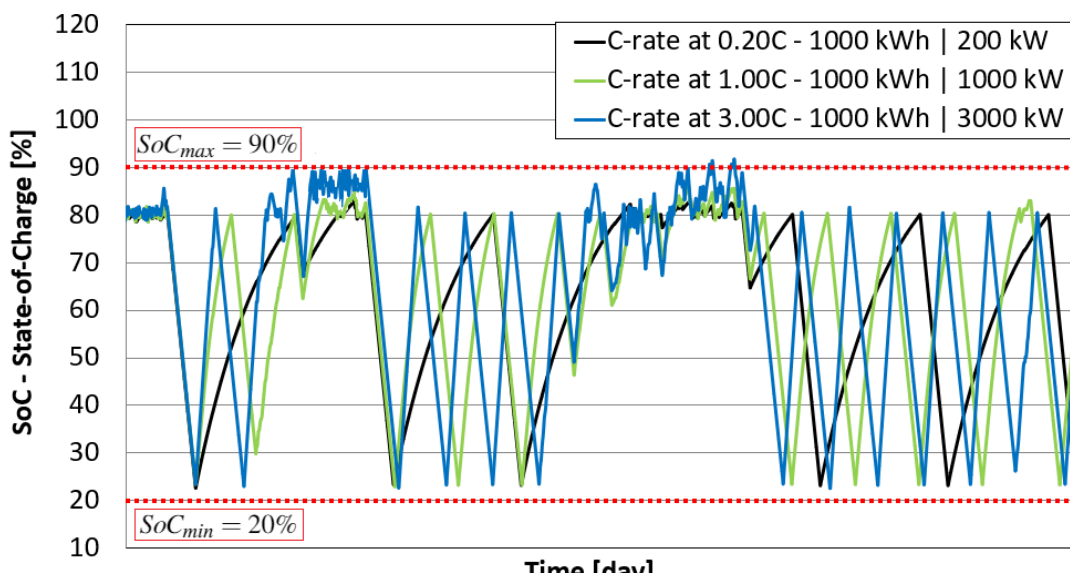
Source: Author.

Recently, a line of research has started to integrate the optimization of batteries for peak-shaving and frequency regulation. The batteries present a response time near seconds required by fast frequency control [51]. The peak-shaving evaluation needs data measurements near-instantaneous response time. However, the vessel's operational profile data are

usually divided by time steps and it is measured in minutes [52–54], as will be described in the next Chapter. Thus, peak-shaving is not included in the scope of this work.

- **Strategic loading** – When diesel and gas engines operate in a conventional vessel, emissions are far worse for low loads than high loads (as mentioned in the previous chapter). For the hybrid vessel, the battery can be used to allow the Gen-sets to operate closer to the optimal load point. By discharging and charging the battery, the operation can be strategically optimized with the main goal being the minimization of the average fuel consumption and its emissions. Battery should be charged until the maximum State-of-charge set-point (SoC_{max}) and be discharged until the minimum state-of-charge set-point (SoC_{min}), behaving as an effect of hysteresis in relation to SoC . Figure 9 exemplifies this behavior for three different battery capacities (or different C-rates), where the $SoC_{min} = 20\%$ and $SoC_{max} = 90\%$.

Figure 9 – Battery operating as Strategic-loading for a range from 20% to 90% SoC . The battery energy capacity of 1000 kWh can be operated with different C-rates.



Source: Author.

For all cases simulated in this work were considered the Strategic-loading as the battery operation mode.

2.5 Battery aging

This section shows a summary of the aging mechanisms for Li-ion batteries. These phenomena can be classified as cycle aging and calendar aging. The variables that describe

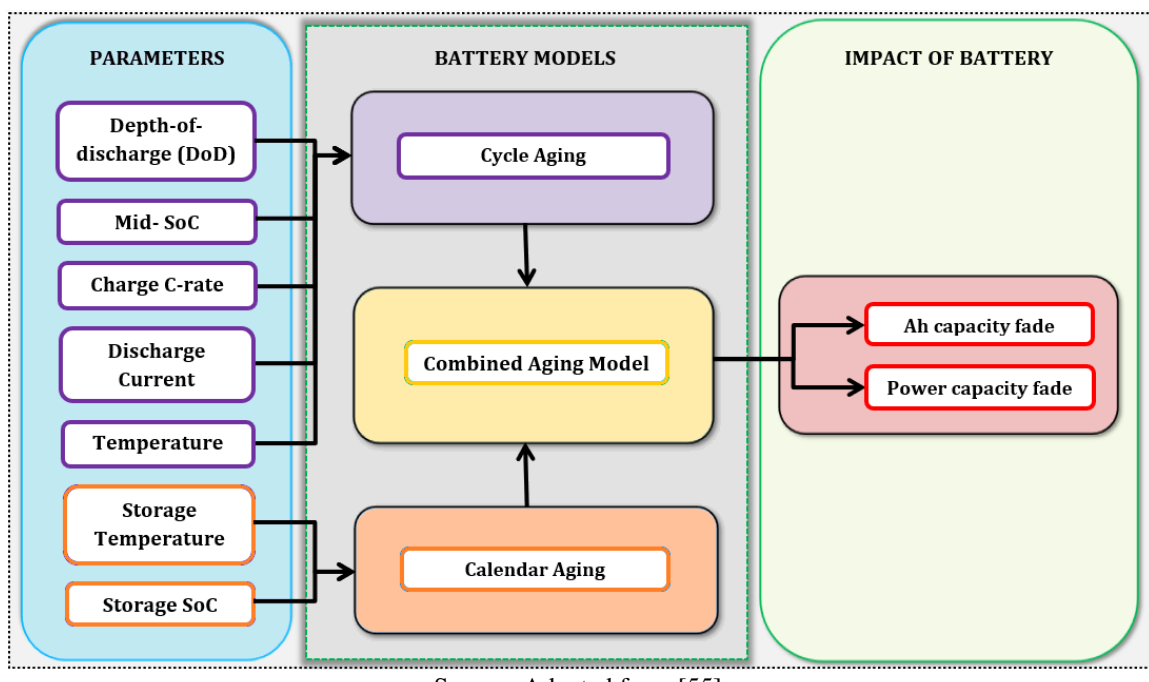
battery operating conditions are Depth-of-Discharge (*DoD*), Middle State-of-Charge (*SoC*), C-rate (or current amplitude), discharge current and temperature, which these parameters are related to cycle aging. Conversely, the calendar aging occurs to cell storage and it is usually modeled as a function of storage *SoC*, and storage temperature.

2.5.1 Cycle aging and Calendar aging mechanisms

Degradation processes occur during operation, denominated cycling aging, and during stationary time periods, called calendar aging, when the current flowing through cells is zero (or when C-rate is zero). These both independent factors are modeled separately for degradation analyses [55]. Depth-of-discharge *DoD*, middle - *SoC*, charge C-rate, discharge current and temperature are parameters that can be modelled for cycle aging evaluation because they are associated with a number of cycles limited by lifetime throughput. However, only storage temperature and storage *SoC* are used to modelling calendar aging [31, 55].

Regardless of a battery is being operated or not, there are chemical and physical changes in the electrode and electrolyte. Capacity fade is related to the decrease of power capability by the increase in the internal resistance or impedance of the unit cell. Besides, this parameter means the loss in the discharge capacity over time [56]. They can be classified as schematized in the Figure 10.

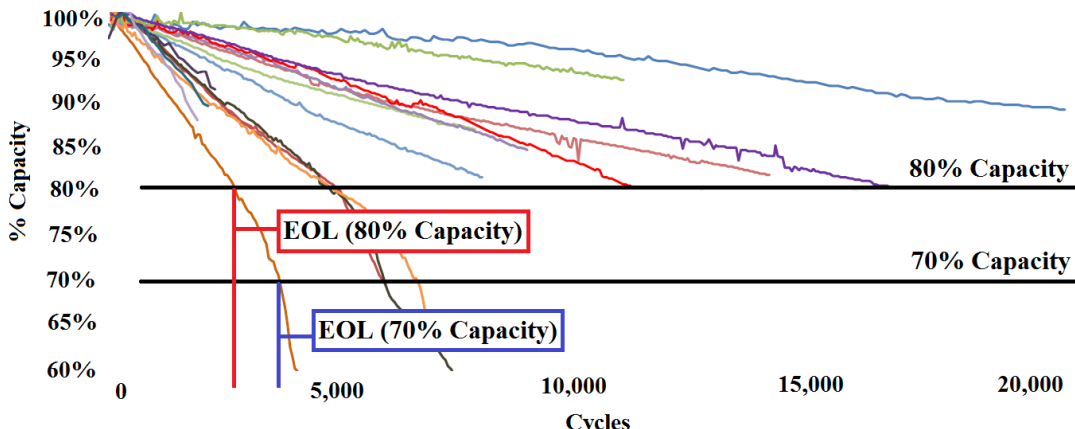
Figure 10 – Aging mechanisms that influence the battery cell performance.



Source: Adapted from [55].

Figure 11 illustrates the capacity fade testing for different Li-ion battery cells manufacturers [31] considering 80% and 70% remaining capacity as a battery's End of Life (*EoL*) condition. Note that depending on the battery curve, the manufacturer may provide a different number of cycles in keeping with the battery depth-of-discharge. When a battery operates at 70% *DoD*, it presents higher *EoL* in comparison 80% *DoD*. *EoL* definition can be seen in Glossary (page 137).

Figure 11 – Capacity fade testing for different battery technology that uses Lithium-ions as a key component of its electrochemistry (80% and 70% remaining capacity as a battery's *EoL* condition).



Source: Adapted from [31].

During the development of Lithium-ion batteries for Electric vehicles and other applications, 10 years of life created, battery achieving 3,000 cycles, and one cycle per day, are requirement which a battery is reasonably considered as a "good" battery. The industry sector traditionally assigns 80% remaining capacity as battery End of Life (*EoL*). However, depending on battery technology – *NMC*, *LFP*, *LTO*, among others [57] – it can achieve a different quantity of equivalent full cycles (*EFC*) for this percentage [31, 56].

The Depth-of-Discharge *DoD* can be defined in different ways in the literature. According to [58], there are five different *DoD* definitions that are listed below:

1. *DoD* can be defined as the inverse of State-of-Charge (*SoC*) that is an expression of the present battery capacity as a percentage of maximum capacity [59, 60]. *SoC* is calculated following the Equation 1 [56]:

$$SoC(t) = SoC(t_0) - \frac{1}{C_{max}} \int_{t_0}^t I(t) dt \quad (1)$$

For instance, if a battery operate with a *SoC* of 20%, its *DoD* is 80%. The second term of Equation (1) is defined as *DoD* [55]. This relationship is represented by following Equation (2) associated with Equation (3), resulting in the Equation (4):

$$DoD(t) = \frac{1}{C_{max}} \int_{t_0}^t I(t) dt \quad (2)$$

and

$$SoC(t) = \frac{C_{max} - \int_{t_0}^t I(t) dt}{C_{max}} \quad (3)$$

$$SoC = 1 - DoD \quad (4)$$

Thus, *DoD* in function of *SoC* is determined by:

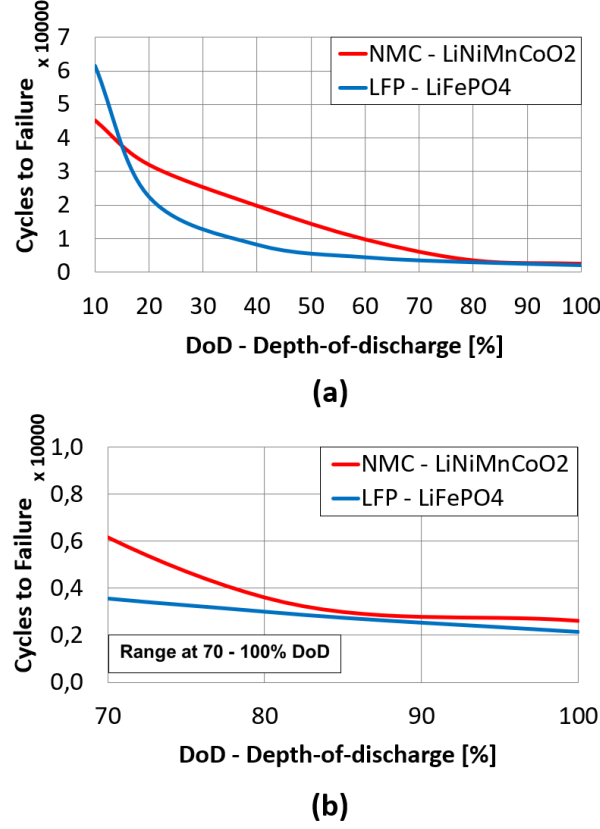
$$DoD = 1 - SoC \quad (5)$$

where $SoC(t_0)$ is the initial *SoC* expressed in percentage; C_{max} is the maximum battery capacity in *ampere – hour* and $SoC(t)$ express the present condition of battery.

2. The ratio of the *Ah* (or *Wh*) discharge from the battery nominal capacity at a given rate to the rated capacity. In other words, if a battery cell capacity at 140 *Wh* is discharged from a battery cell a rated capacity at 200 *Wh*, its *DoD* is defined as 30%.
3. The variation of *DoD* measure considering the last charge is expressed as a percentage. It happens, for example, when a battery changes its *SoC* from 80% to 20%, presenting the 60% *DoD*. However, when occurs the inverse situation, a battery changes its *SoC* from 20% to 80%, it is *DoD* is 0%.
4. The range between SoC_{max} and SoC_{min} during the charging process is the same for the discharging process, meaning that from 80% *DoD* to 20% *DoD* and back results in 60% *DoD*. This item is the opposite of the previous one.
5. If a battery cell starting at 60% *SoC* to 100% - charging completely - and after that, discharging completely to 0%, charging back to 60%, this full cycle represents at 100% *DoD*.

Figure 12 shows cycles to failure as function of *DoD* to *LFP* and *NMC* Li-ion battery cells (Wöhler-Curve for batteries).

Figure 12 – Cycles to Failure vs. Depth-of-discharge curve for *LFP* and *NMC* battery cells (Wöhler-Curves). (a) Original curve (b) Curve detailed for range at 70 - 100% *DoD*.



Source: Adapted from [61, 62].

2.5.2 Counting the number of cycles

The number of cycles [63] for Simplified Battery Model is calculated by Equation 6:

$$N_{cycles}^{NoAging} = \frac{E_{battery}}{2 \cdot (E_{SoC_{max}} - E_{SoC_{min}})} \quad (6)$$

where $N_{cycles}^{NoAging}$ is the number of cycles disregarding degradation process, $E_{battery}$ [kWh] is the total cycled energy through the battery, and $E_{SoC_{min}}$ and $E_{SoC_{max}}$ are Battery capacity defined a specific range *SoC*.

For the Advanced Battery Model the number of cycles ("cycle degradation") is estimated by following Equation 7 [25]:

$$\frac{1}{N_{cycles}^{Aging}} = \alpha \cdot DoD^{\beta} \quad (7)$$

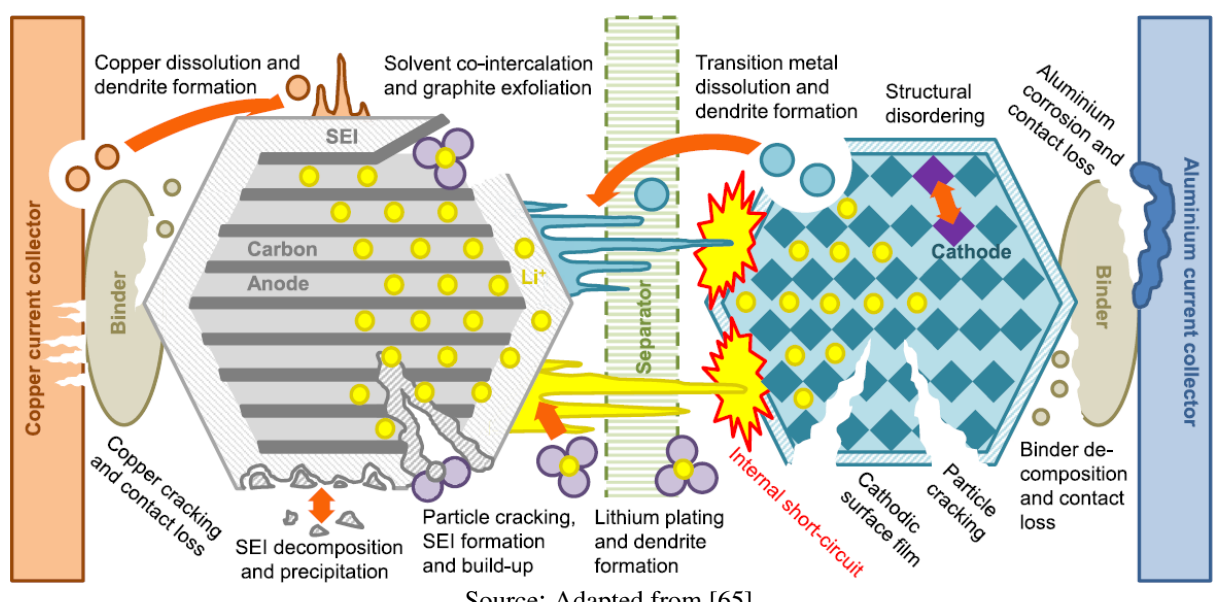
where N_{cycles}^{Aging} is the number of cycles to failure given by cycle curve to the specific battery cell, DoD [%] is Depth-of-discharge (a fractional number between 0 and 1), α and β are fitted

constants. These constants are fitted to the data you enter in the cycles versus *DoD*. The constant α is scaled so that the degradation variable goes from zero to capacity degradation limit defined by a user as is illustrated in Figure 11. The inverse of α presents a physical significance related to the nominal cycles to failure at 100% *DoD* times the capacity degradation limit chosen. However, β equal to 1.0 indicate a constant number of kWh-throughput to *EoL*. The constant β is 0 for a set number of cycles to failure, without dependence on *DoD*.

2.5.3 Degradation phenomena in the positive-negative electrodes and electrolyte

The aging mechanisms are a non-stop process that occurs in the positive and the negative electrodes as well as in a battery electrolyte. Mechanical or/and chemical phenomena can be justified by the loss of active Lithium and loss of active material in the electrodes. The intensity of degradation depends on the operation mode of the battery, environmental conditions, and storage level [56]. Most batteries use Graphite as a negative electrode and its properties are the reason for batteries degradation. In the contact between the graphite surface and electrolyte is created a layer denominated Solid Electrolyte Interphase (SEI), frequently formed in anode material [56, 64]. Figure 13 illustrates a schematic of a typical Lithium-ion battery cell with the metal-oxide cathode and graphite anode, including the SEI layer formed.

Figure 13 – Degradation mechanisms represented by the model of a Lithium-ion battery cell.



This schematic shows the Copper (Cu) and Aluminum (Al) as the current collectors at electrodes and the active components and function principle of Li-ion battery depends on the

intercalation of Li-ions (Li^+) with metal oxide type cathode and graphite anode transported via an organic liquid electrolyte [66]. An intercalation cathode is a solid network which can store or remove ions reversibly. Intercalation compounds can be divided into crystal structures, such as tavorite, layered, olivine, and spinel [57]. Generally, state-of-art technologies employed for stationary storage systems are based on Carbon-Graphite anode together with Metal-Oxide (MOX)-type cathode as *LFP* (Li-Iron-Phosphate), *NMC* (Nickel-Manganese-Cobalt), *LTO* (Li-Titanate-Oxide), and *NCA* (Nickel-Manganese-Cobalt) [66].

Different parts of batteries can interact in complex ways and, as a consequence, it difficult to analyses cause and effect. For instance, the negative electrode is aged due to the physical and chemical properties of graphite. However, the positive electrode presents a minor impact on the overall unit cell degradation. Other causes of battery aging are mechanical stress associated with phase transitions and volume changes during cycling [67]. Figure 13 illustrates a schematic of a typical Lithium-ion battery cell with the metal-oxide cathode and graphite anode, including the *SEI* layer formed.

Note that the *SEI* layer is formed mainly on the Graphite anode side during the first cycles of the cell. Therefore, not only the *SEI* sheet protects the anode from direct contact with the electrolyte, but also results in a loss of active Lithium [56, 66].

In general, there are two aging mechanisms category as those related to the active species (e.g. Li^+) and those that increase the internal resistance, not changing the active species of the cell. The former is associated with Lithium consuming parasitic reactions that result in an accumulation of the *SEI* layer at the negative electrode (particle cracking, *SEI* formation and build-up), and irreversible Lithium metal plating [67]. The graphite can be isolated due to the formation of the *SEI* (graphite exfoliation) and, consequently, it prevents further decomposition of the electrolyte [56].

In addition, the *SEI* layer presents parts of decomposition products formed from electrolytes at the graphite anode. Therefore, these products influence the initial performance and long-term capacity of the unit cells. The *SEI* formation mechanism is considerably affected by a concentration of electrolyte salt, temperature, and reduction of current rate [64].

There are different ways to form the *SEI* layer, depending on the structure of graphite/carbon surface and composition. These aspects are dictated by pore size, particle size, basal-to-edge-plane ratio, surface chemical composition, and degree of crystallinity. The contact area of small particles is greater than large ones considering the same weight [64].

Recently, studies have been dedicated to improving to *SEI* layer architectures using new additives [68], current density and charge-discharge reaction kinetics due to modification of anode surface; achieving charge-discharge cycles that highlight *SEI* layer formation, and avoiding lithium inventory loss using alternative electrolytes [64]. According to [60, 69], the *SEI* layer grows rapidly its thickness for the first few cycles. When the anode is kept at high reducing potentials, the growth rate of the *SEI* layer thickness is high in a unit cell cycled with a higher temperature. In this case, a long cycle is obtained with transport limitations of particles. Additional internal resistance is created by the growth layer thickness.

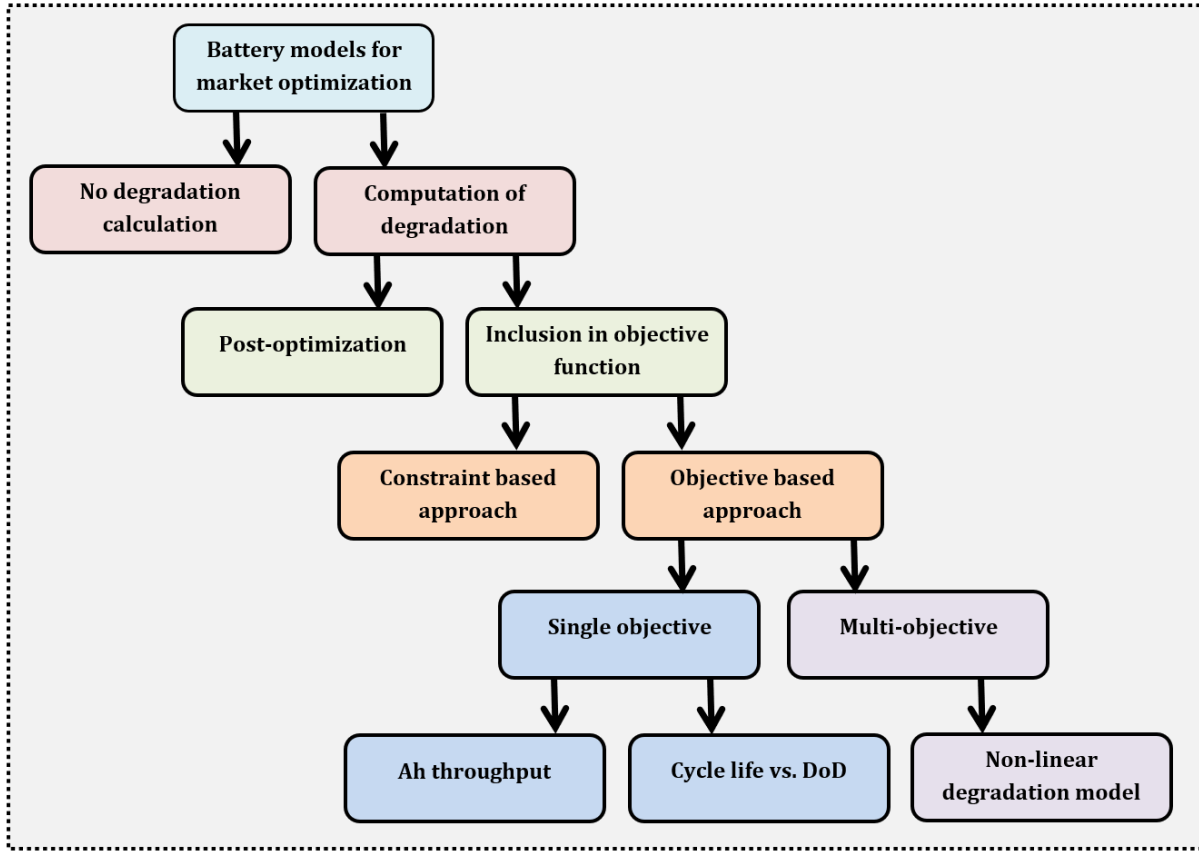
2.6 *Battery models*

The battery model can be divided between models that include the degradation calculation and those do not compute the aging processes as schematized in Figure 14. When the degradation is considered in the optimization, it can involve the inclusion in the objective function (as HOMER software case) or a Post-optimization. The objective function can be simulated considering the constraint-based or objective based [56, 70]. The constraint-based approach allows the determination of battery Ah throughput and the cycle life vs. *DoD* may be used for a single objective function. The HOMER software solves the problem to minimize the total cost by the single objective function that sometimes involves capital and operational costs or marginal cost of operation [25, 56, 71–73]. The objective function is described in the Chapter 4.

Hybrid Optimization of Multiple Electric Renewables - HOMER - is a microgrid design tool that applies to several sectors in the energy industry. Initially developed by *NREL* (National Renewable Energy Laboratory), this simulator presents the micropower optimization model which can be evaluating designs for off-grid and grid-connected power systems on a range of applications. Besides, HOMER can be applied for techno-economic sizing of micro-power hybrid systems such as batteries, being adequately used for analysis in the marine sector [25, 26]. For instance, when is simulated marine design, some components or equipment can be included and control systems must be configured (see Figure 4). A list of decisions can be created during simulations and the results present possible cases for user evaluation.

There are two major ways to model batteries on the HOMER software: electrochemical models and equivalent-circuit models [3]. The battery models can be divided by a Simplified Battery Model (*SBM*) and Advanced one, denominated Modified Kinetic Battery Model

Figure 14 – Battery models approach used for market analysis. This Master’s Thesis address the single objective function in the optimization model.



Source: Adapted from [56].

(MKBM) [25, 28]. The former presents the possibility of dimensioning a battery by its nominal capacity, C-rate, Round-trip efficiency, nominal voltage, maximum (dis)charge current, the number of batteries, minimum *SoC*, *DoD*, and cost curves while the latter presents the same data input being included by thermal curves and degradation limit for *DoD* curves. Thus, the HOMER software can include integration between electrochemical and equivalent-circuit models.

In the HOMER software, some procedures should be adopted previously of data inclusion. The design for a suitable sizing of battery systems should be following these steps [47]:

- Select the type of battery (electrochemistry) that can be used to attend the overall requirements.
- The number of series cells should be determined to meet the voltage requirements.
- Determine the battery Ah capacity discharge required to the power demand of the vessel.
- Determine the maximum allowable Depth-of-discharge (*DoD*) for the required number of C/D Ratio life.

- The battery Ah capacity is determined by dividing the Ah discharge needed to power demand by the allowable *DoD*.
- Determine the charge and discharge rates and necessary controls to protect against over-charging and over-discharging.
- In this step, determine the temperature rise and the thermal cooling requirement, which can be an air cooling or a liquid cooling. These types of cooling systems can be used to determine the maximum charge and discharge currents and, consequently, the maximum charge C-rate e discharge C-rate.
- Finally, can be determined the ventilation need of the battery room.

The battery systems can be sized by N_{serie} cells connected in a string in series; $N_{parallel}$ cells connected in a string in parallel; V_{cell} represents the nominal voltage in each cell; Ah_{cell} is cell capacity in ampere-hour; and A_{cell} is cell capacity in ampere. The battery capacities [74] are given by Equations 8 and 9:

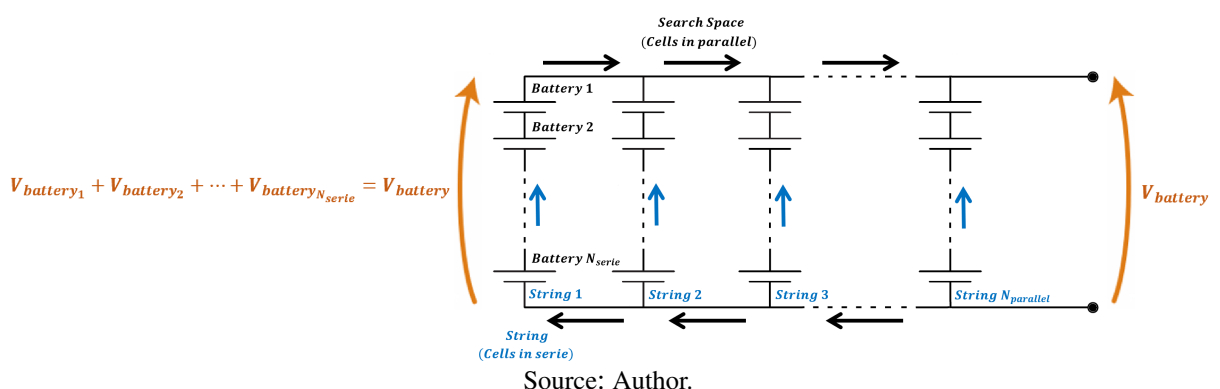
$$C_{energy}^{battery} = N_{serie} \cdot N_{parallel} \cdot V_{cell} \cdot Ah_{cell} \quad [\text{watt-hours}] \quad (8)$$

and equivalently,

$$C_{power}^{battery} = N_{serie} \cdot N_{parallel} \cdot V_{cell} \cdot A_{cell} \quad [\text{watt}] \quad (9)$$

Figure 15 illustrates a battery configuration where a string is defined as the number of series cells and the search space is the number of parallel cells. These parameters are necessary as input data to the HOMER software.

Figure 15 – Battery configuration.

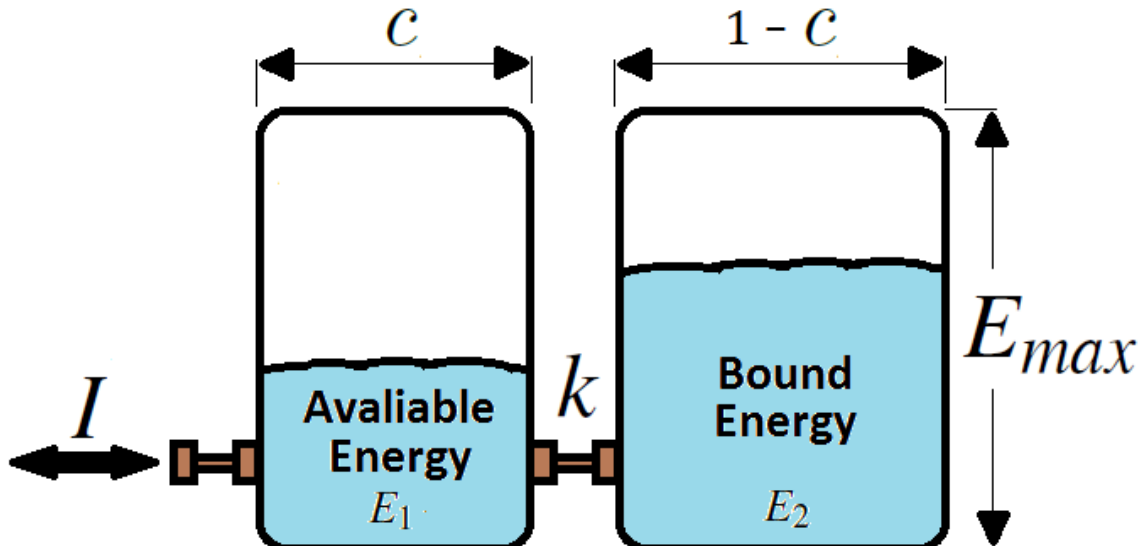


It is important mention that V_{cell} is considered constant when the battery is sized by Equation 8 and Equation 9. However, there are two ways to describe the battery voltage: cut-off

voltage (or end voltage) and charge voltage. The former means the voltage when the discharge may be considered complete and the latter represents a voltage when a battery is charged to full capacity [59, 60].

Simplified model, also known as the Kinetic Battery Model, is based on the concepts of electrochemical kinetics, where it can be estimated the energy absorbed by or withdrawn from the battery bank each time step. This storage bank is modeled as a two tank system. According to Figure 16 the "available energy" and "bound energy" are represented by the first tank and the second tank, respectively. Available energy is readily available for conversion to electricity. The energy that is chemically bound is related to "bound energy" and it is not immediately available for withdrawal [28].

Figure 16 – Kinetic battery model.



Source: Adapted from [28].

In [25, 28], the two tanks can be described by three parameters such as the maximum (or theoretical) storage capacity (E_{max}), capacity ratio (c) that is a ratio of the size of the available energy tank to the size of the two tanks - and the rate constant (k) is a measure of how quickly the "bound energy" is converted "available energy" or vice-versa (related to the conductance between two tanks). The sum of the available and bound energy is defined as the maximum amount of energy stored by the battery system, represented by Expression (10):

$$E_{max} = E_1 + E_2 \quad (10)$$

where E_1 is the available energy and E_2 is the bound energy. The battery model can be described by differential Equations 11 and 12:

$$\frac{dE_1}{dt} = -I - k \cdot (h_1 - h_2) \quad (11)$$

$$\frac{dE_2}{dt} = k \cdot (h_1 - h_2) \quad (12)$$

Head in each tank is given by the volume divided by the area:

$$h_1 = \frac{E_1}{c} \quad (13)$$

$$h_2 = \frac{E_2}{1 - c} \quad (14)$$

For mathematical simplicity, a new rate constant δ is defined as:

$$\delta = \frac{k}{c \cdot (1 - c)} \quad (15)$$

Thus, the new differential equations are determined by Expressions 16 and 17 :

$$\frac{dE_1}{dt} = -I - \delta \cdot (1 - c) \cdot E_1 + \delta \cdot c \cdot E_2 \quad (16)$$

$$\frac{dE_2}{dt} = \delta \cdot (1 - c) \cdot E_1 - \delta \cdot c \cdot E_2 \quad (17)$$

As detailed in [28], the solution of differential equations applied to the two tanks model can show the maximum amount of power that the battery can discharge over a specific time step Δt . The discharge power is given by the following Equation (18):

$$P_{\text{discharge}}^{\max} = \frac{-c \cdot \delta \cdot E_{\max} + \delta \cdot E_1^{\text{initial}} \cdot e^{-\delta \Delta t} + c \cdot \delta \cdot E_{\max} \cdot (1 - e^{-\delta \Delta t})}{1 - e^{-\delta \Delta t} + c \cdot (\delta \Delta t - 1 + e^{-\delta \Delta t})} \quad (18)$$

Similarly, the charge power is given by the Equation (19):

$$P_{\text{charge}}^{\max} = \frac{\delta \cdot E_1^{\text{initial}} \cdot e^{-\delta \Delta t} + c \cdot \delta \cdot E_{\max} \cdot (1 - e^{-\delta \Delta t})}{1 - e^{-\delta \Delta t} + c \cdot (\delta \Delta t - 1 + e^{-\delta \Delta t})} \quad (19)$$

The amount of available and bound energy at the end of the time step can be determined by two Equations 20 and 21:

$$E_1^{final} = E_1^{initial} \cdot e^{-\delta\Delta t} + \frac{(E_{max} \cdot \delta \cdot c - P) \cdot (1 - e^{-\delta\Delta t})}{\delta} + \frac{P \cdot c \cdot (\delta \cdot \Delta t - 1 + e^{-\delta\Delta t})}{\delta} \quad (20)$$

$$E_2^{final} = E_2^{initial} \cdot e^{-\delta\Delta t} + E_{max} \cdot (1 - c) \cdot (1 - e^{-\delta\Delta t}) + \frac{P \cdot (1 - c) \cdot (\delta \cdot \Delta t - 1 + e^{-\delta\Delta t})}{\delta} \quad (21)$$

where $E_1^{initial}$ is the available energy; $E_2^{initial}$ is the bound energy; both at the beginning of each time step; E_1^{final} is the available energy; E_2^{final} is the bound energy; both at the end of the time step; P is the power into (positive) or out of (negative) the battery bank; and Δt is the length of the time step.

2.7 Assumptions adopted for battery system specification applied to the PSV Power System

The battery system parameters chosen for HOMER models (Simplified and Advanced) are met by literature presented in this Chapter. The specifications and assumptions adopted for dimensioning Lithium-ion battery systems are summarized in Table 1. The sensitivity analysis is used to estimate some battery system parameters and their results are shown in Chapter 5.

Table 1 – Assumptions and specifications adopted for dimensioning Lithium-ion battery systems applied on Hybrid PSV Power System.

Battery Parameters	LFP	NMC	Item (Results) Chapter 5	Equations	References
Battery Energy Capacity [kWh]	SA ¹	SA ¹	5.2 (<i>SBM</i> ² cases – ΔE and ΔP capacities) 5.3 (All cases ³ – ΔE capacity) 5.5 (Recomm ⁴)	(8)	[74]
Battery Power Rating [kW]	SA ¹	SA ¹	5.2 (<i>SBM</i> ² cases – ΔE and ΔP capacities) 5.4 (All cases ³ – ΔP or ΔC-rate) 5.5 (Recomm ⁴)	(9)	[74]
Nominal C-rate [1/h]	SA ¹	SA ¹	5.2 (<i>SBM</i> ² cases – ΔE and ΔP capacities) 5.4 (All cases ³ – ΔP or ΔC-rate) 5.5 (Recomm ⁴)	(42) or (43)	[31], [39], [56]
Max Discharge C-rate [1/h]	12C	12C	-	(42) or (43)	[75]
Max Charge C-rate [1/h]	4C	4C	-	(42) or (43)	[75]
Round-trip Efficiency [%]	92	94	-	(46) or (47)	[36], [61]
Nominal Voltage [kV] (Battery System)	0.69	0.69	-	-	[58]
Operating Temperature [°C]	20	20	-	-	[34]
Cycle life (100% DoD)	2140	2600	-	(6), (7) or (52)	[61], [62]
Cycle life (80% DoD)	3000	3600	-	(6), (7) or (52)	[61], [62]
Min SoC [%] (80% DoD)	20	20	-	-	Adopted (HOMER)
Min SoC [%] (70% DoD)	30	30	-	-	Adopted (HOMER)
Initial SoC [%]	100	100	-	(1)	Adopted (HOMER)
Serie Batteries (String)	115	115	-	(8), (9)	[36], [74]
Parallel Batteries (Search Space)	SA ¹	SA ¹	-	(8), (9)	[36], [74]

¹SA: Sensitivity Analysis (Results and discussion); ²SBM: Simplified Battery Model;

³All cases: Simplified and Advanced Battery Models; ⁴Recomm: Recommendations for battery operation.

2.8 *Synthesis*

This Chapter presented the main battery technologies characteristics that can be applied to Ships. The battery specifications are usually the same independent of its application. However, when the evaluation of battery systems is deepened, its design and sizing of auxiliary equipment are more detailed depending on application complexity. The Lithium-ion battery systems applied in Ship Power Systems demand a high complexity related to safety characteristics related to *DP* operation, fire safety, and cooling systems. This is demonstrated through the battery operation modes as spinning reserve, peak shaving, or strategic-loading that are important strategies of battery operation for Ship. These solutions are integrated into the *BMS* and its auxiliary components (power electronics, transformer, thermal management, and fire protection system).

The battery durability is also a crucial characteristic for Ship Power Systems and it can be estimated considering the calendar aging and cycle aging. Different indicators are taken into account and their impacts modify the battery expected life. The vessel's demand requires the high energy level that compromises the battery end-of-life, number of cycles, effect of temperature, C-rate, and capacity fade that accelerate the battery cell degradation processes. Based on these aging mechanisms, the battery technologies can be simulated with the computation of the degradation rates and using the single objective approach. This analysis can encompass the estimation of Ah throughput, the cycle life, and the depth-of-discharge for each battery technology, and are essential to define the constraints and assumptions adopted for dimensioning Lithium-ion battery systems used to simulations in this Master's Thesis.

Chapter 3

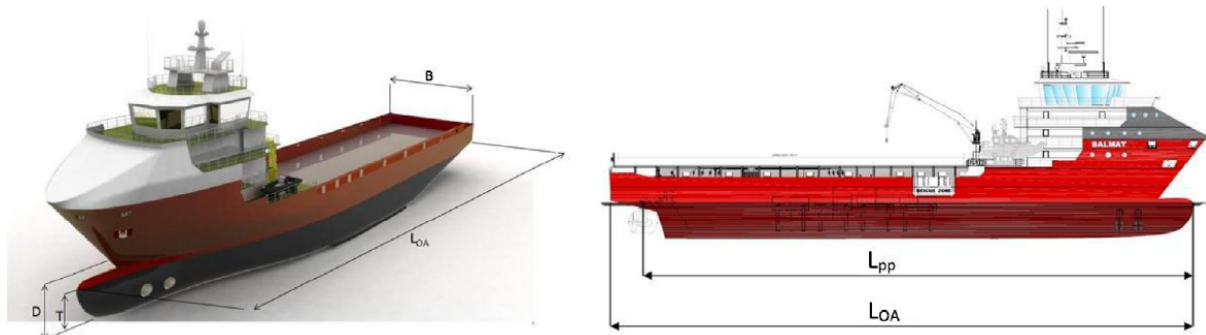
Hybrid Platform Supply Vessel Test System

This chapter intends to show the main aspects of Platform Supply Vessel (*PSV*) as such its operational profile, operation modes, Diesel-electric systems and its Generator-sets configuration. Also are presented the aspects related to emissions, fuel consumption, and efficiency curves performance to the Gen-sets used to simulate.

3.1 PSV Operating Characteristic

Platform Supply Vessel (*PSV*) is a typical ship that provides services to offshore platforms such as personnel, consumables, equipment, participating in rescue and firefighting operations. Figure 17 indicates the main dimensions of a Balmat *PSV*.

Figure 17 – Indication of main Balmat Platform Supply Vessel (*PSV*) dimensions. Beam B; Depth D; Draft T; Length overall L_{OA} ; Length between perpendiculars L_{pp} .



Source: Adapted from [76].

These vessels present stringent Dynamic Positioning (*DP*) capabilities in inching operations, with high values of power reserve in order to prevent from blackout conditions [11].

Besides, *PSV* is robust and it is specially designed to face bad weather conditions for above the 5 Beaufort scale.

In Brazil, for example, the *PSVs* are used as a multitask vessel, thus, they operate with only one cargo type at the time. Furthermore, the most common sizes for *PSV* operating in Brazil are 1500, 3000, and 4500 DWT, where DWT is an abbreviation for the deadweight tonnage and indicate how much weight a ship can carry [77]. Their average dimensions are illustrated in Table 2.

Table 2 – *PSV* 1500, 3000 and 4500 dimensions and their Marine Diesel Oil consumption.

Vessel Type	Length	Width	Deck Area	Useful Deck Area
[DWT]	[m]	[m]	[m ²]	[m ²]
<i>PSV 1500</i>	62	15	394	295
<i>PSV 3000</i>	70	16	575	431
<i>PSV 4500</i>	87	18	880	660

Source: Adapted from [2].

The marine diesel oil consumption is one of the most important factors on the Ship total cost. Depending on operation mode, the fuel consumption is more relevant. According to [77], this consumption is different for each type of *PSV* as can be seen in Table 3.

Table 3 – Marine Diesel Oil consumption per *PSV* according to each operation mode.

Vessel Type	Fuel Consumption [ton/day]		
	[DWT]	in service	in stand by
<i>PSV 1500</i>	11.4	4.3	1.1
<i>PSV 3000</i>	13.3	4.3	1.3
<i>PSV 4500</i>	16.7	5.7	1.3

Source: Adapted from [77].

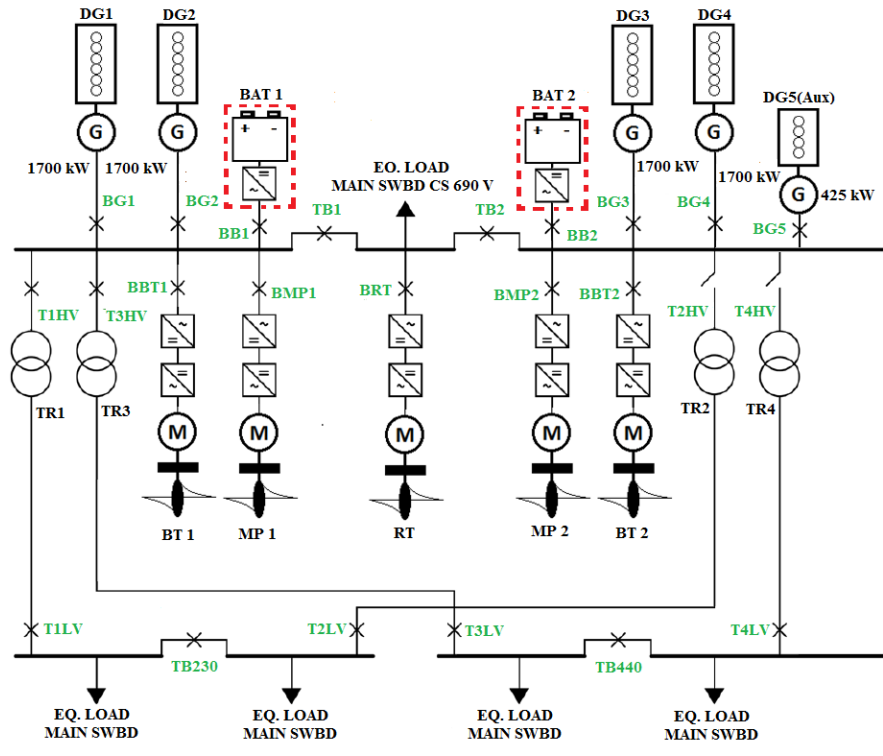
3.2 Diesel-electric systems

The propulsion system can be designed by a hull form of a conceptual design of a *PSV*, where is estimated the vessel resistance. Resistance to advance is estimated for all the speed range (from 1 to 15 knots) for partial load voyage (Transit 1) and high load voyage (Transit 2) conditions [12]. These estimations are based on the statistical methodology proposed by Holprop and Mennen (1982) [78] and Holprop (1984) [79, 80]. However, for this work, the propulsion system is based on the Operational profile for a typical *PSV* and the propeller power

characteristics are considered for each operational mode and mission conditions as can be seen in item 3.3.

Figure 18 illustrates the Single-line Diagram of a typical PSV which include 4 x 1700 kW Diesel Generator-sets (Gen-set) [81] and 1 x 425 kW Auxiliary Gen-set [82]. As mentioned in [83], there is a consensus among the Diesel engine manufacturers that they must be over-dimensioned for their actual use to marine application. Engines are normally oversized mainly due to class requirements and operational profile from the vessel and its DP system. Batteries can be included in the systems and divided following each Bus, for instance, representing two containers.

Figure 18 – Single Diagram for a Typical Platform Supply Vessel.



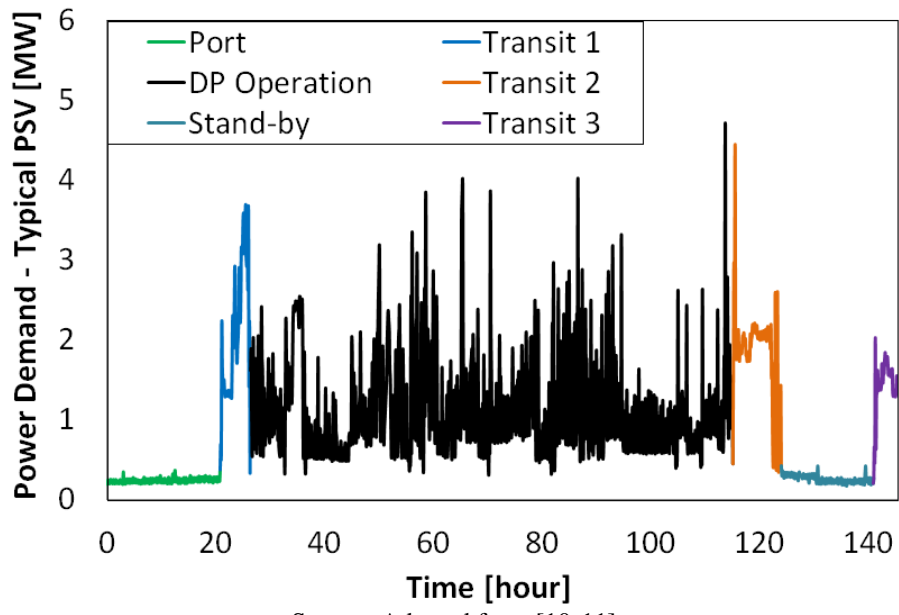
Source: Adapted from [11].

Diesel-electric propulsion system includes two azimuth thruster propellers (MP1 and MP2), two bows (BT1 and BT2), and one azimuth bow retractable thruster (RT) [11]. As can be seen in Figure 18, Diesel Gen-sets (DG1-5) drive the Electric Generator (G) producing electrical power that is supplied to the propulsion motors (M), transferring torque to the propulsion units. The electric motors are driven by power converters which are feed by transformers (TR1-4) [12].

3.3 Typical operational profile of PSV Power System

For analyzing batteries included on the vessels is required a detailed operational profile data because the time-varying power demands indicate the higher potential for energy savings lies [3]. As reported by [11], the operational profile for a typical *PSV* illustrated in Figure 19 was extracted by the Automatic Identification System (*AIS*) during 6 days, with a sampling frequency of 0.2 Hz. This profile shows several peaks due to different vessel operating conditions, that are induced by adverse weather conditions such as waves, currents, and wind. The time series data is plotted for a time-step of 6 minutes, adapting the original curve.

Figure 19 – Operational profile for a typical *PSV* (Total power demand).



Source: Adapted from [10, 11].

For the first 20 hours, *PSV* operates in the Port mode, where its load power is significantly low (i.e. about 300 kW) and a similar situation is presented in the Stand-by mode - between 120 and 140 hours. Rest of mission includes three Transits mode among 21 and 26 hour (Transit 1), 116 and 123 hours (Transit 2), and 141 and 145 hour (Transit 3). The Dynamic Positioning (*DP*) Operation occurs between 27 and 115 hours. This typical *PSV* can operate for 6 days for a cost equal to \$19,605.00, considering the vessel's life as time horizon at 25 years of operation [11].

3.4 Diesel generator-sets

3.4.1 Generator-sets characteristics and specifications

The fuel curve describes the quantity of Diesel that Gen-sets consumes to produce electricity and HOMER software accept the inclusion of the data points of fuel consumption and power output, plotting fuel consumption and efficiency regression curves fitted [25]. The equation of fuel injection (in $L/hour$) to the Gen-set model is given as a quadratic polynomial function of Power output and is valid for the fixed-speed and variable-speed operation, considering different sets of polynomial coefficients [84]. HOMER calculates by Equation 22 the polynomial coefficients after inclusion of data points:

$$F(P_{Gen-set}) = a \cdot P_{Gen-set}^2 + b \cdot P_{Gen-set} + F_0 \quad (22)$$

where $F(P_{Gen-set})[L/hour]$ is fuel consumption as a function of load; a , b and F_0 are the coefficients of the second-order polynomial function estimated by HOMER software, and $P_{Gen-set}[\%]$ is the loading of the Gen-sets as a percentage of the electrical power output [25].

As presented in Figure 20 (d) and (e), the Gen-set efficiency curves are determined as the electrical energy coming out divided by the chemical energy of Diesel going in [25, 54, 85]. This relationship is calculated by Equations 23, 24, 25 and 26:

$$\eta_{Gen-set} = \frac{3.6 \cdot P_{Gen-set}}{\dot{m}_{fuel} \cdot LHV_{fuel}} \quad (23)$$

$$\dot{m}_{fuel} = \rho_{fuel} \cdot F(P_{Gen-set}) \quad (24)$$

$$\dot{m}_{fuel} = \rho_{fuel} \cdot (a \cdot P_{Gen-set}^2 + b \cdot P_{Gen-set} + F_0) \quad (25)$$

$$\eta_{Gen-set} = \frac{3.6 \cdot P_{Gen-set}[kW]}{[\rho_{fuel} \cdot (a \cdot P_{Gen-set}^2[\%] + b \cdot P_{Gen-set}[\%] + F_0[\%])] \cdot LHV_{fuel}} \quad (26)$$

where $\eta_{Gen-set}[\%]$ is Gen-set efficiency; $P_{Gen-set}[kW$ or % load] is electrical power output; $\dot{m}_{fuel}[\text{kg}/\text{h}]$ is mass flow rate of the Diesel fuel; $LHV_{fuel}[\text{MJ}/\text{kg}]$ is the Lower Heating

Value, that is a measure of energy content; ρ_{fuel} is the fuel density in kg/liter; and the factor 3.6 is related to conversion 1 kWh equal 3.6 MJ [25]. The conversion of parameters is based on Diesel fuel of 35° API [16°C (60°F)], a gravity having a Lower Heating Value (*LHV*) of 42.780 MJ/kg (18,390 Btu/lb) when used at 29°C (85°F) and for a fuel density ρ_{fuel} at 0.8389 kg/liter (7.001 lbs/U.S. gal) [81, 82].

According to [76], fuel consumption is directly related to total fuel mass flow rate m_{fuel} and Gen-set power $P_{Gen-set}$ of the system and this is denoted by Equation 27.

$$F(P_{Gen-set}) = \frac{\dot{m}_{fuel}}{P_{Gen-set}^{total}} \quad (27)$$

As a consequence, the total fuel tank capacity V_{tank}^{Ship} [*liter*] is calculated in function of fuel consumption $F(P_{Gen-set})$; fuel density ρ_{fuel} ; total power $P_{Gen-set}^{total}$, and autonomous operation time $t_{autonomous}$, according to Equation 28:

$$V_{tank}^{Ship} = \frac{\dot{m}_{fuel} \cdot t_{autonomous}}{\rho_{fuel}} = \frac{F(P_{Gen-set}) \cdot P_{Gen-set}^{total} \cdot t_{autonomous}}{\rho_{fuel}} \quad (28)$$

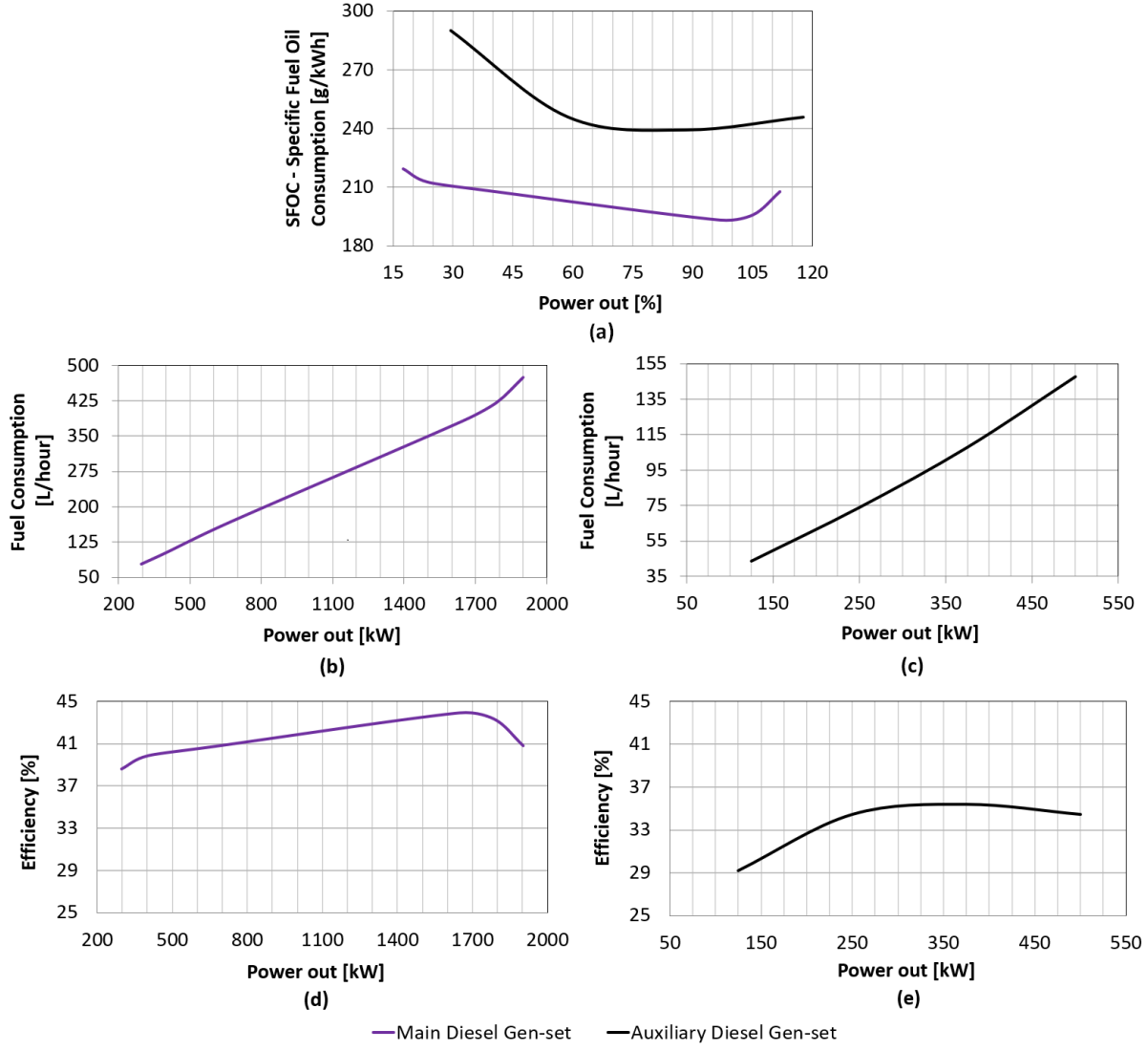
The fuel consumption data points can be used to determine the fuel consumption curve. For each Gen-sets (Main and Auxiliary Gen-sets), a Specific Oil Fuel Consumption (*SOF*_C) curve gives assistance in calculating the fuel consumption. Normally, the Diesel generator manufacturer provides specifications and data about *SFOC* curves that can be included in the HOMER software model. For this work, the curves for Main and Auxiliary Gen-sets are illustrated in Figure 20, where these graphs are adapted from [81, 82] and follow the IMO Tier 2.

Most modern Diesel Gen-sets are turbocharged to supply increased delivered power and more air is required into the cylinders to fuel complete combustion. However, the dynamics of the Gen-sets are slow because the response of the air system is slow, due to the rotating inertia of the turbocharger and the large air receiver volume. The typical transient time scale of the Air during combustion process is in seconds [54].

The Gen-sets should operate with a minimum load, mainly during Port and Stand-by mode conforming to the operational profile from *PSV* (Figure 19). As can be seen in Figure 20 (a), a low load operation is related to a graph area that represents a higher Specific Fuel Consumption.

The minimum load can be defined to Gen-sets following some technical aspects. Usually, the marine engineers operate with Diesel Gen-sets load equal or higher than 50%. However, for some situations, the Gen-sets included in the *PSV* can operate with a load under this percentage. But these low-load operations are recommended for a maximum of 8 hours. This fact is related

Figure 20 – Fuel Consumption curves for Main Gen-sets and Auxiliary Gen-sets. (a) *SFOC* - Specific Fuel Oil Consumption for Main and Auxiliary Marine Engine. (b) Fuel Consumption curve for Main Diesel Engine. (c) Fuel Consumption for Auxiliary Diesel Engine. Efficiency curves. (d) Main Diesel Marine Engine. (e) Auxiliary Diesel Marine Engine.



Source: Based on [81, 82].

to low pressure in the inner part of the engine cylinder, and consequently, the incomplete combustion of Diesel fuel in this one. Whenever the low-load operation lasts for a long time, the Gen-sets (type 4-Stroke-Cycle-Diesel) should be operated for at least 30 minutes for a minimum load at 50%, with the goal of enabling the burning of fuel and soot deposited in the inner part of the engine cylinder. Besides, some manufacturer's confirm that longer periods of low load operations influences in the number of starts/stops for all Gen-sets and in their number of overhaul intervals [83, 86].

The Gen-sets chosen for HOMER model are met by IMO Tier 2 [6, 7] and their specifications are summarized in Table 4.

Table 4 – Manufacturer's Marine Diesel Generator-sets Specification Sheet.

Parameter	Main Gen-set	Auxiliary Gen-set
Engine Model	V-12, 4-Stroke-Cycle-Diesel	Cat® C18 ATAACTM In-line 6, 4-cycle diesel
Emissions	IMO II Compliant	IMO II Compliant
Power Rating [kW (hp)]	1765 (2365)	500 (671)
Frequency [Hz]	60	60
Rotation [rpm]	1800	1800
Bore x Stroke	170.0 mm x 215.0 mm (6.7 in x 8.5 in)	145 mm x 183 mm (5.71 in x 7.2 in)
Fuelling Strategy	Fuel consumption is nominal data with a tolerance of $\pm 3\%$	Low Fuel Consumption
Displacement	58.6 L (3576 in ³)	18.13 L (1106.36 in ³)
Compression Ratio	14.7:1	14.5:1
Oil Change Interval [hour]	1000	-
C RATING	Maximum Continuous Rating — MCR	Maximum Continuous Rating — MCR
Dimensions (Length x Width x Height)	(3153 mm x 2230 mm x 2240 mm)	(5549.9 in x 2055 in x 2739 in)

Source: Adapted from [81, 82].

3.5 Dispatch modeling

In this Master's Thesis, a typical operational profile for *PSV* is replicated for a year. Based on this operation, the HOMER allows estimating some projection, mainly related to battery parameters such as lifetime, number of cycles, energy throughput, fuel costs, and others [25].

In the context of this work, the term "dispatch" is related to control strategies that each Diesel Gen-set and the battery system which can operate integrated and coordinated way whenever there is insufficient energy to supply the power demand of vessel. There is the possibility of using Diesel Gen-sets power to charge the battery systems. Conversely, the battery can minimize the frequency of Gen-sets starts or stops, and the optimized use of diesel fuel. A negative aspect is decreasing of service life (battery wear); electrical losses in the power conversion and battery; and excess of energy that can not be stored in the batteries [25, 27].

This strategy can be implemented in HOMER and it is called Cycle Charging (CC) [25, 27]. It is a dispatch strategy where the Gen-sets ever operate in its maximum power capacity to supply the power demand of vessel. The surplus electrical production is directed to provide power in the order of decreasing priority: (1) Serving the deferrable load; and (2) Charging

battery bank. These previous conditionals are important for simulation of this work. The power demand of *PSV* should be served by Gen-sets and batteries. The CC strategy allows Diesel Gen-sets off during operation; it also allows Gen-sets to operate simultaneously and the Gen-sets capacity less than power demand [25].

During the optimization process [25], the HOMER dispatch Gen-sets and batteries at each time-step following the two-step processes:

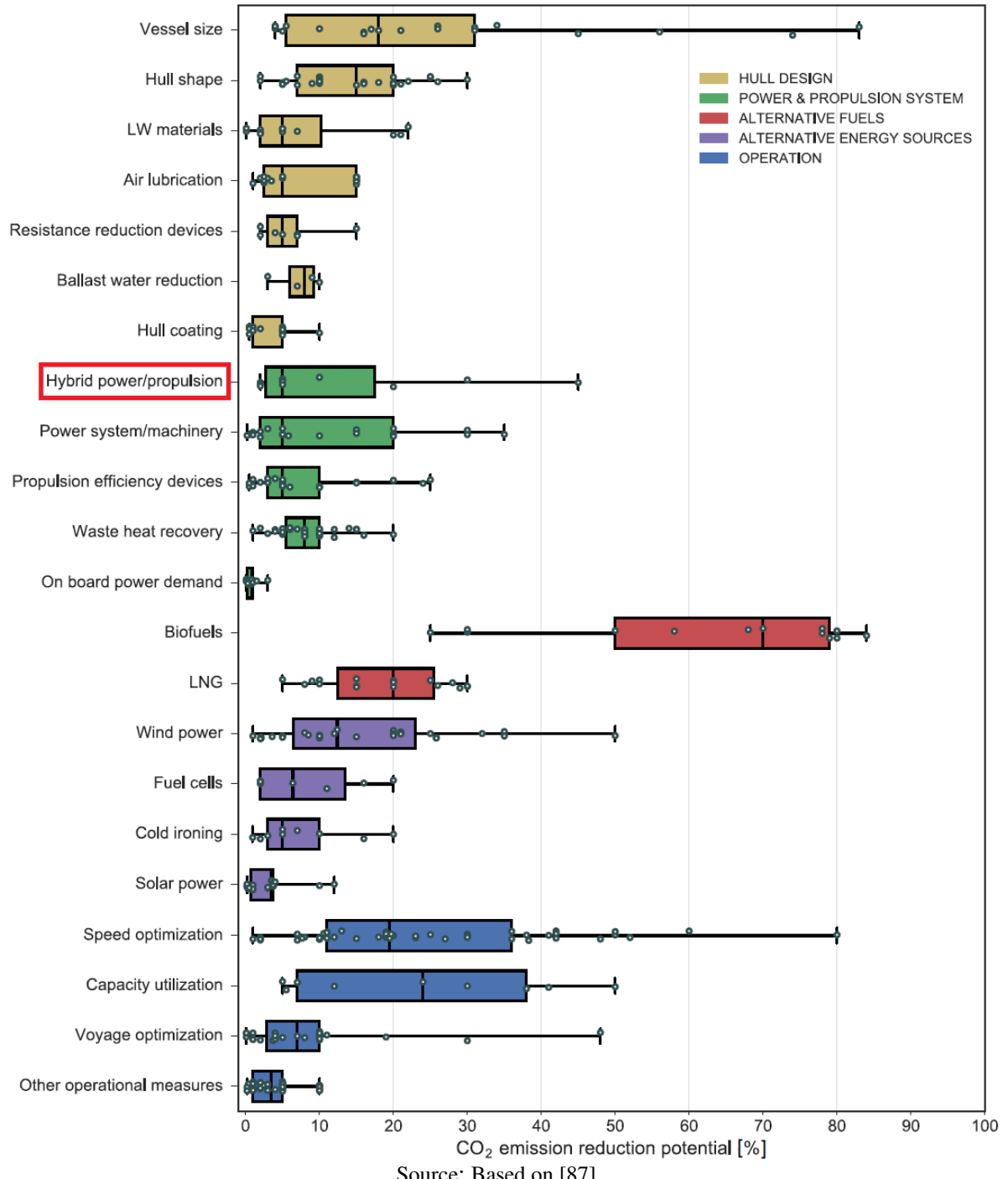
1. HOMER selects the optimal combination of components to serve the power demand of the *PSV* at the least total cost and satisfy the operating reserve requirement. It can be calculated by fixed and marginal cost for each dispatchable energy source;
2. A setpoint State-of-Charge (*SoC*) is applied to the CC controller and when the battery *SoC* is below this setpoint and it is not discharging in the before time step, a new Gen-set will be called upon to serve the power demand of *PSV* and also produce excess electricity to charge the battery. This strategy can also mean that a setpoint at 50% *SoC* – as estimated in this work – allows that the storage system can be discharged or charged when the setpoint is reached.

3.6 Emissions reduction potential in Hybrid Vessels and State of the Art

The potential effect on energy efficiency and emissions reduction can be achieved for several types of measures. According to [87], the reduction in CO_2 emissions from the shipping sector at the fleet level are obtained between 16% and 46%, depending on the calculation method used and considering the final year of scenarios in 2020. Moreover, the potential reduction of emissions also can be estimated by individual measures related to efficient equipment, vessel design, and others. Figure 21 indicate the CO_2 emission reduction potential classified in five main categories of measures: (1) Hull design; (2) Power & propulsion system; (3) Alternative fuels; (4) Alternative energy sources; and (5) Operation.

In this Master's Thesis, the battery study could be included in more than one category. Nevertheless, the reference [87] gives a description of combining batteries with combustion engines as a Hybrid system includes in the Power & propulsion system category (Hybrid power/propulsion subcategory). As highlighted in Figure 21, the CO_2 emission reduction potential in vessels is achieved for the range from 2% to 45%, and these results can be compared with other categories of measures.

Figure 21 – CO_2 emission reduction potential in vessels considering 5 main categories of individual measures.



In the literature, the hybrid vessel often refers to a combination of two or more energy sources such as Diesel Gen-sets, battery, fuel cells, PV systems, and others. The reference [3] proposes the basic and advanced control strategies that slowly change the Diesel Gen-sets loads to modify the Lithium-ion battery's *SoC* or the Gen-sets increase its load when the vessel's demand is high and vice versa. However, this survey does not consider the degradation

mechanisms and only a unique battery capacity is sized. The minimal battery size is estimated for the ship conditions and the economic analysis is verified by costs, savings, and *payback* time. The battery is modeled by Equivalent-circuit and Electrochemical models and a PI-controller is used to determine the Gen-sets load which aims to keep the battery C-rate limit. Consequently, the battery power capacity can be estimated. The basic control requires the discharge C-rate of 2C and the advanced control allows the maximum discharge C-rate at 4C. Other cases are presented in the literature and can be seen in Table 5.

In most of cases presented, the CO_2 emission reduction potential to a range from 2% to 45%, as demonstrated in Figure 21. In some cases researched is not mentioned the optimization strategy used in the simulation as well as the battery power rating and payback. Some works estimate *NPV* and other economic indicators, however, these parameters are based on outdated prices for Ship's equipment. For the 50,000 DWT Open-hatch Dry bulk vessel, the payback lower than 1 year can be considered low. But, the battery energy capacity at 312 kWh and the battery power capacity of 3 x 960 kW are limited for a vessel of 50,000 DWT capacity. Thus, the battery payback is rapidly achieved and, probably, the battery has a low expected life.

For all cases shown in Table 5, the Ship Power Systems are evaluated with Lithium-ion battery or generic battery system, except for *NaS* battery cell. In neither cases, the storage system was simulated considering a specific Lithium-ion battery cell technology (only typical cell), as considered in this Master's Thesis.

Table 5 – Reduction of CO_2 emissions and fuel consumption for several vessels presented in the literature. Optimization strategy, battery capacities, Gen-sets capacity, and Payback for Hybrid Vessel simulated.

Vessel's Name	Type of Vessel	Type of Battery	Optimization Strategy or Software Used	Battery Energy Capacity [kWh]	Battery Power Rating [kW]	Diesel Gen-set Power Rating [kW]	Reduction of CO_2 Emission [%]	Reduction of Fuel Consumption [%]	Payback [year]	Reference
Offshore Support Vessel (OSV)	Oil Tanker	Li-ion	MATLAB/Simulink	80	-	300	15.30	-	-	[84]
Offshore Support Vessel (OSV)	Oil Tanker	<i>Nas</i>	INTLAB-Version 5.5/MATLAB	268	-	2000	74.10	-	-	[71]
Offshore Support Vessel (OSV)	Oil Tanker	Generic	-	500	-	4 x 2000	6.00 - 8.00	-	12.5	[15]
Offshore Support Vessel (OSV)	Oil Tanker	Generic	-	1500	-	2 x 2000	6.00 - 8.00	-	5.0	[15]
50,000 DWT Open-hatch Dry bulk vessel	Ship Crane	Li-ion	Basic and Advanced control strategy (Equivalent-circuit and Electrochemical models)	312	-	3 x 960	30.00	-	<1.0	[3]
Tanker	Oil Tanker	Li-ion	Stochastic effect	1709	-	-	2.97	-	-	[88]
Offshore Support Vessel (OSV)	Oil Tanker	Li-ion	-	2 x 250	1000	4 x 1900	21.00	23.70	6.7	[89]
Hybrid TUG	TUG	Li-ion	-	225	450	$3 \times 1075 + 2 \times 800$	40.00	-	9.0	[89]
Drillship	Offshore Drilling	Li-ion	-	2 x 640	2 x 3850	16 x 880	28.00	55.40	5.00	[89]
Platform Supply Vessel (PSV)	Oil Tanker	Generic	MILP and logic-based algorithm	1000	1000	$2 \times 2350 + 2 \times 994$	-	12.60	-	[86]
Platform Supply Vessel (PSV)	Oil Tanker	Li-ion	-	2000	1540	4 x 1250	-	16.00	-	[90]
Platform Supply Vessel (PSV)	Oil Tanker	Li-ion	Real data and theoretical method of estimating fuel reduction	653	1600	4 x 2010	-	15.00	-	[58]

3.7 *Synthesis*

This Chapter presented the *PSV* Power System and its equipment specifications. Firstly, it is necessary to define the *PSV* operating characteristics and their constraints related to marine Diesel oil consumption and CO_2 emissions. There are several ways to estimate the resistance to advance of vessels and, as consequence, determine the power demand in the Diesel-electric systems, the focus of this dissertation is to use the data adapted from the literature of an operational profile for a typical *PSV*. Although the operational profile is adapted from literature, the sizing of Gen-sets is based on real data of manufactures that following the rules imposed by the International Maritime Organization. Finally, the dimensioning of Gen-sets is important to define the total objective function that includes fuel costs, as can be seen in the next Chapter.

Chapter 4

Cost Analysis Methodology for Battery Aging

Total cost for a conventional vessel and a hybrid vessel can be estimated considering two main economic aspects [3] that must be analyzed:

- Capital costs – initial cost and installation costs of Gen-sets and battery.
- Operational costs – the operational cost for Gen-sets and the evaluation of battery performance to reduced fuel consumption and maintenance during vessel missions.

4.1 Components costs

Cost estimates are allocated as follows: Fixed Operation and Maintenance (*O&M*), battery pack, Power Conversion System Equipment (*PCSEq*), Power Control System (*PCS*), installation, and Balance of System (*BS*). For the battery system, the capital cost is estimated for a storage system by adding the costs of the battery pack, balance of system, power control, and the installation costs [39].

Equipment costs based on the power capacity ratings - such as Gen-sets - are priced in *US\$/kW*, while the battery packs usually are priced in *US\$/kWh*. The storage equipment costs include the DC battery system that incorporates electrolyte, electrode, and battery cells costs. These costs are also related to the costs of assembling components into the system (strings, modules, packs, internal wiring, Battery Management System - *BMS*, temperature, and voltage monitoring equipment) [39].

Installation costs are included in Engineer-Procure-Construct (*EPC*), transportation of all equipment, site design, permitting equipment, installation parts, and labor. Normally, the manufacturers provide these solutions into the containers for the *PSV Power System*. The container is embedded in the *PCSEq* along with packaging, controls, and converter costs. These converter power are priced in *US\$/kW* [39].

PCS is a equipment category that include the cost of high-level controllers required to energy storage systems being implemented to dispatch and operate the Ship Power Systems. Controllers need to combine multiple functions such as understanding the type of charge management required for marine application and battery technology characteristics. In the simulator used in this work, the *PCS* costs are represented by a controller that allow specifying how the system operates during simulation – dispatch strategy. It is possible to define a cost and lifetime for the controller that depends on the sizes of generators, the price of fuel, the *O&M* cost, and battery bank. These Controllers are provided in *US\$/kW* [25, 39].

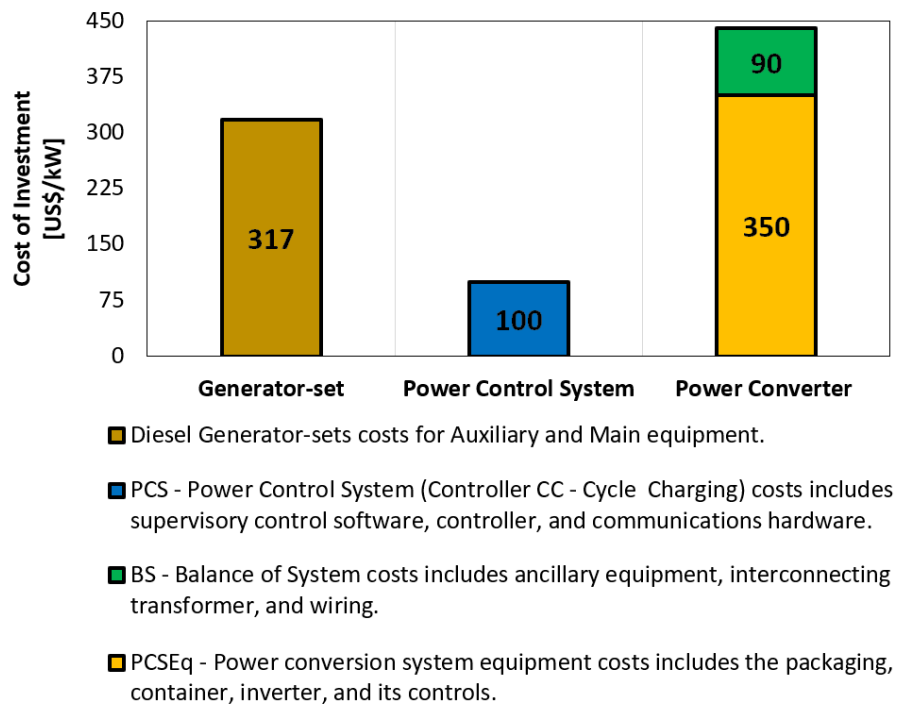
BS costs include additional ancillary equipment, wiring, and interconnecting transformer. It is priced in *US\$/kW* and its cost is proportional to the power capacity of the system. However, for fixed *O&M* costs, the storage technologies do not yet have longer-term operating experience and this theme is currently debated by industry. Consequently, the majority of projects have been including some kind of capacity maintenance agreement that guarantees a fixed level of energy capacity in the battery system over a lifetime project. Especially, tightening of mechanical and electrical connections, maintenance of *HVAC* system, landscaping maintenance, cabinet touch up painting, and cleaning are incorporated in the *O&M* requirements for a storage system. Capacity maintenance agreement cost can be accounted as part of the initial capital or as fixed *O&M*. Note that variable costs are usually negligible for most storage systems, but this variable can consider the inclusion of battery degradation cost [39].

4.1.1 Generator-sets, power converter, and *O&M* costs

Figure 22 shows the cost of investment to Power Control System (*PCS*), Balance of Systems (*BS*), and Conversion System Equipment (*PCSEq*) - converter. The *O&M* cost is 0.5 *US\$/op.hour* and 10 *US\$/year* for Gen-sets, and Power Converter, respectively [91]. According to [92], the average price of diesel fuel was approximately 1.02 *US\$/L* in July 2019, and an

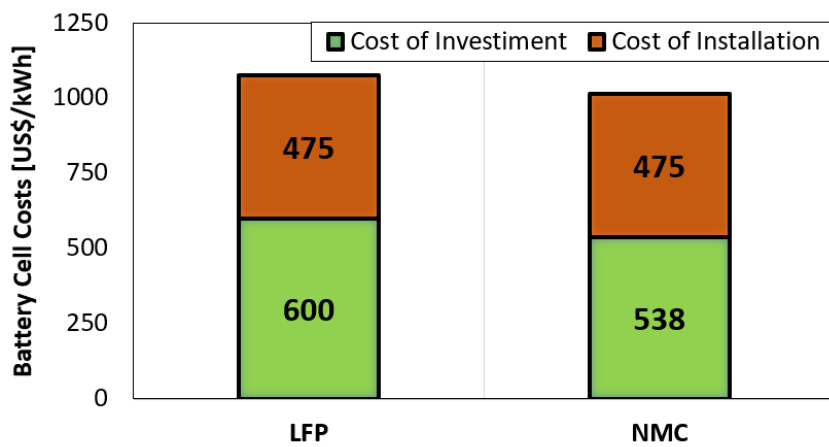
inflation rate about 2% [30]. These data were included on the simulator to extract annual analysis of Ship Power System operation.

Figure 22 – Investment cost estimate for Ship’s Equipment considering Gen-sets, *PCS*, *BS*, and *PCSEq*.



Source: Adapted from [39].

Figure 23 – Battery cell costs for Ship Power System. Cost of investment and installation.



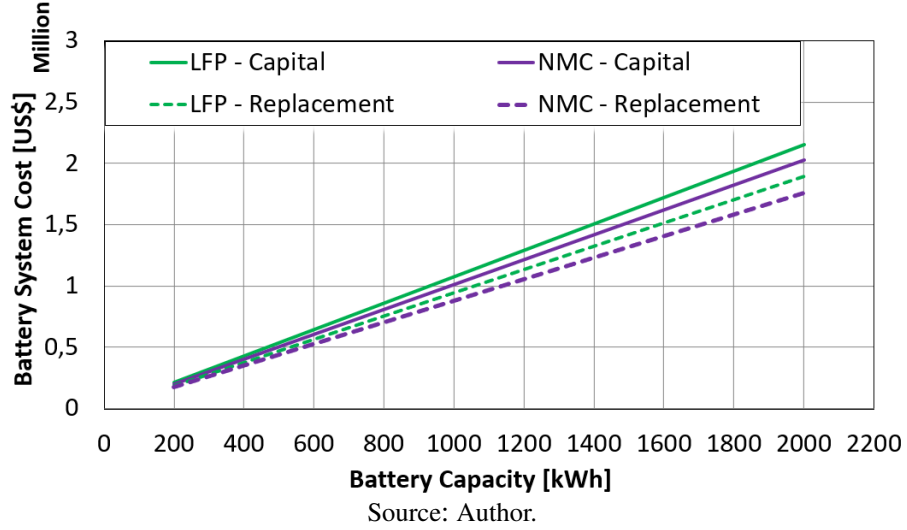
Source: Based on [36], [39], and [93].

4.1.2 Battery costs

Simulator selects the optimal combination of Gen-sets and battery capacity to serve the primary load and the thermal one, where this latter was neglected for all simulation in this work. Accordingly, the software determines the fixed and marginal cost of main Gen-sets, auxiliary Gen-sets, and battery. Gen-sets marginal cost is related to fuel price times fuel curve. Besides, battery fixed cost is zero and its marginal cost is determined to storage wear cost [25]. However, there is not a uniform or industry acceptable methodology for quantifying variable *O&M* as a means of considering degradation processes [39]. Figure 23 summarizes investment, installation, *O&M* cost and total Li-ion battery cells cost for both cells studied.

According to [94], there is an archetypal sigmoid function (S-curve) related to the deployment of several technologies. These curves can map future cost reductions over time and battery prices per year. For Li-ion batteries, the cost projections based on experience rates and S-curve type market growth assumptions for utility-scale storage is $12 \pm 3\%$ on the battery system level (from 2015 to 2040). The annual reduction of prices depends on the type of storage technologies and their applications. However, in the DNV-GL Report presented in [39], the replacement cost was calculated by 10-year cost trends (2016-2026) to *LFP* and *NMC* cells. Based on these DNV-GL Report, it is possible to estimate the decrease in battery cost for each year. The results of replacement cost show an average reduction at 12% and at 13% per year for *LFP* and *NMC* cells, respectively.

Figure 24 illustrates the investment cost and replacement cost for *LFP* and *NMC* cells. These curves are estimated based on Figure 23. According to [27], the battery capital cost depends on its bank sized, but it does not relate to the dispatch strategies – as Cycle-charging, for example. However, the replacement cost depends on the that.

Figure 24 – Battery Cost Curve. Cost of Investment and replacement for *LFP* and *NMC* cells.

4.2 Economic metrics for Lithium-ion batteries performance evaluation

Optimization software presents several economic parameters that can be applied for the interpretation of the results of different cases, sensitivity analysis, and scenarios. This work is focused on integration between battery degradation processes and some economic factors, as can be seen following.

4.2.1 Net Present Value (*NPV*)

The Net Present Value is an investment that allows an evaluation regarding its discounted net present value - related to the investigated investment. According to [29], the *NPV* is the only objective function considered by Optimization software for modeling the energy system. It is composed of the equipment cost, installation cost, replacement cost, and *O&M* costs such as the price of Diesel. This method considers a constant interest rate over the horizon studied that for cases in this work, are analyzed exactly by 30 years. It is calculated by summing up the discounted revenues and costs [25, 30, 91, 95, 96].

$$NPV_{SYSTEM} = \sum_{t=0}^N \frac{(R_t - C_t)}{(1+i)^t} \quad (29)$$

where t is time; N indicate the project lifetime; R_t is the revenue; C_t is the costs, and the interest rate is represented by i . The similar equation is given as [30]:

$$NPV_{SYSTEM} = \frac{(C_{annualized})}{CRF(i,N)} \quad (30)$$

$C_{annualized}$ is total annualized cost; and $CRF(i,N)$ system capital recovery factor calculated by Equation 31 [30]:

$$CRF(i,N) = \frac{i(1+i)^N}{(1+i)^N - 1} \quad (31)$$

The factor $CRF(i,N)$ is usually obtained through Compound Interest Tables such as present in [95], where are used the interest rate i and project lifetime N .

For improving the comparability of different cases analyzed - for this work, for different energy/power capacities; C-rates; *DoD*; battery cells; comparison of methods for battery aging - the NPV can be applied for the interpretation of the results of the economic model. If the NPV is positive, the investment is profitable, because the revenues cover the investment costs and the desired capital return rate. If the NPV is zero, revenues only cover the expenses that are called break-even costs. Finally, for an NPV is lower than zero, a loss occurs because the investment costs and the capital return can not be compensated by the revenues (discounted) [91, 95]. Costs are positive and revenues are negative to NPC (Net Present Cost) and it differs from NPV , in turn, because the signals are inverted.

4.2.2 *CAPEX* and *OPEX*

The Capital Expenditures (*CAPEX*), also known as investment costs, should be paid in the first period. For the cases analyzed in this work, it is considered as investment costs the acquisition of batteries, Gen-sets, converter, and controllers. Besides, the Operational Expenditures (*OPEX*) are related to maintenance and other operational costs and they are supposed to be equal for each period. Some periods might present higher *OPEX* costs than in other periods, despite over the lifetime, the operational expenditures should be leveled out [91, 97, 98].

4.2.3 Internal Rate of Return

Internal Rate of Return (*IRR*) is the interest rate. It is a factor that results in a Net Present Value (*NPV*) equal zero, and it can be calculated through iterative Newton approximation method [25, 91, 95, 96, 99]. The difference between initial cost and the “storage” cost result in yielding the annual savings [100], can be seen in Equation 32:

$$NPV_{SYSTEM} = \sum_{n=0}^N \frac{C_n}{(1+IRR)^n} = 0 \quad (32)$$

where n is the total number of periods (a non-negative integer); N is the total number of periods; and C_n is the cash flow.

4.2.4 Payback and Discounted Payback

In general, a comparison between the Conventional Ship Power System and Hybrid Ship Power System can be estimated by *payback*. The latter calculates how many years to recover an investment. Specifically, the period necessary to recover a battery cost. For this reason, the *payback* shows the number of years it takes for the cumulative income to equal the value of the initial investment [25], in this case, it can be called capital expenditure. Besides, discounted *payback* means how many years the flow cash needs until amortization or the specific year in which accumulated *NPV* reaches the positive value. When one does not achieve into positive value over the lifetime of the project, probably the investment will not pay off [91, 95, 96].

Considering a installation of the battery system on a Hybrid Ship System, the payback period [101] may be calculated using the following the Equation 33.

$$t_{payback} = \frac{A_{pb}}{D_{pb} \cdot (B_{pb} \cdot C_{pb} \cdot E_{pb} + F_{pb} \cdot G_{pb} \cdot H_{pb} \cdot I_{pb}) + (J_{pb} \cdot K_{pb})} \quad (33)$$

where $t_{payback}$ is the payback period in [years]; A_{pb} is the battery initial investment cost [US\$]; B_{pb} is the fuel price [US\$/liter]; C_{pb} is Diesel consumption rate [liter/hour]; D_{pb} is operation of Hybrid PSV Power System [days/yr]; E_{pb} is the vessel operation hours of stand-alone mode [hour/day]; F_{pb} is the stand-connected mode [hour/day]; G_{pb} is the shore connection electricity cost [US\$/kWh]; H_{pb} is the power rating of battery system in [kW]; I_{pb} is the total efficiency of battery system; J_{pb} is the carbon credit in [US\$/ton]; and K_{pb} is the

avoided emission of carbon dioxide given in [ton/years]. In Annex E, the Table 13 details the previous parameters to determine the theoretical payback.

4.2.5 Levelized Cost of Energy (LCOE)

Levelized Cost of Energy (LCOE), also called Levelized Cost of Storage (LCOS), is denominated as the average cost per unit of useful electrical energy (in US\$/kWh or US\$/MWh) of the system as payment for charging and discharging the battery. It can be calculated through the division between the annualized producing cost (total annualized cost deducting the serving cost the thermal load) by the total electric load served [25, 91, 95, 96]. As the cases simulated in this work neglect the temperature effects (thermal load), LCOE can be defined as [29, 91]:

$$LCOE = \frac{C_{total,annualized}}{E_{served}} \quad (34)$$

where $C_{total,annualized}$ is the total annualized cost [US\$/year] and E_{served} is the total electrical load served [kWh/year].

4.3 Objective function

The objective function describes the studied problem to minimize the total cost of the Hybrid Ship Power System, divided by costs from Diesel Gen-sets and battery. This total cost is composed of fuel, installation, replacement, and operating costs [71, 72]. The multi-objective functions are given by Equation 35 and Equation 36:

$$\min(f_1) = C_{Fuel} + C_{battery} \cdot CRF(i, N)_{battery} \quad (35)$$

$$\min(f_2) = \sum_{t_{hour}=1}^{h_{total}} Emission_{Fuel} \cdot F[P_{Gen-set}] \quad (36)$$

where C_{Fuel} is fuel cost, $C_{battery}$ is battery cost, and $Emission_{Fuel}$ [ton] are the CO_2 emissions of cases analysed in this work. According to [73], the operational cost of Gen-sets is

typically considered as its the fuel cost, that can be characterized as a function of $P_{Gen-set}$, and is calculated following the Equation 37:

$$C_{Fuel} = \sum_{t_{hour}=1}^{h_{total}} Price_{Fuel} \cdot F[P_{Gen-set}] \quad (37)$$

where $Price_{Fuel}$ is an average price of diesel fuel [$US\$/Liter$]; $F[P_{Gen-set}]$ in [$Liter/hour$] represents the fuel consumption curve; and $P_{Gen-set}$ is output power of Gen-sets [kW]. These curves can be seen in Figure 20 (b) and (c) for Main and Auxiliary Gen-sets, respectively.

However, a battery is not operated by fuel. The battery energy-charging is similar to refilling fuel for a Gen-set. Thus, the input electricity can be considered as the "fuel consumption" for a battery. Following this analogy [73], the battery and Gen-sets present the same type capital costs (fixed costs) and can be calculated by Equations 38 and 39:

$$C_{Battery} = (C_{investment}^{Battery} + C_{installation}^{Battery}) \cdot E_{Battery}^{capacity} \quad (38)$$

$$C_{Gen-set} = (C_{investment}^{Gen-set} + C_{installation}^{Gen-set}) \cdot P_{Gen-set}^{capacity} \quad (39)$$

where battery costs are calculated in [$US\$/kWh$] and Gen-sets costs are given by [$US\$/kW$]. But the operational cost for the storage system is determined by the price of energy used to charge the battery. If a battery is powered by a microgrid and renewable energy is used to charge the battery, its operational cost can be considered zero [72, 73].

4.4 Sensitivity analysis

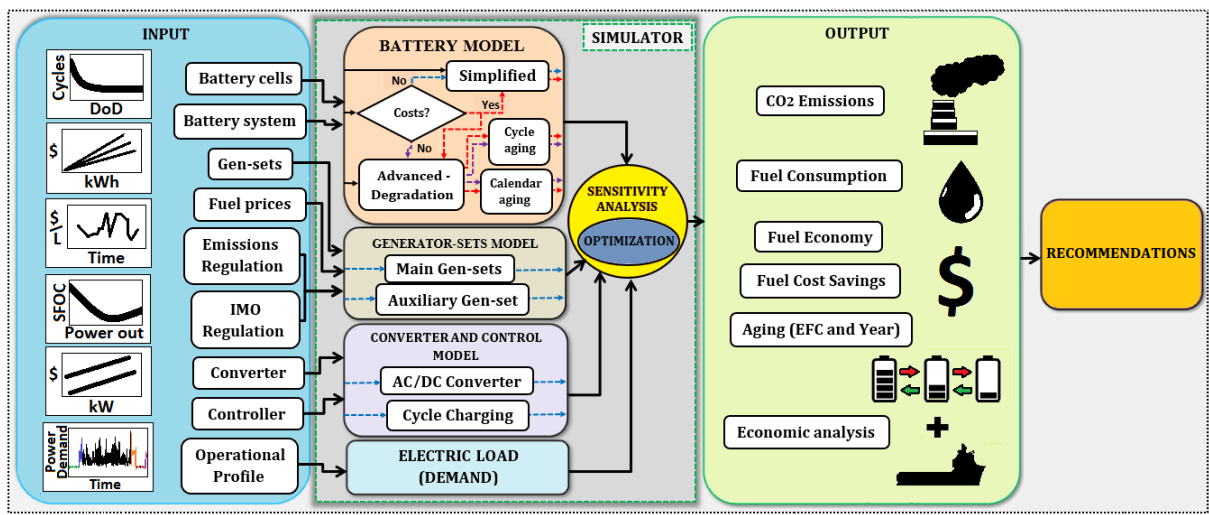
The sensitivity analysis shown in the results and discussion is related to the battery parameters, and the base case (conventional Ship) is compared with the Hybrid vessel without any variation of input economic parameters, where only values per unit are presented. The only exception is the battery cost curve, where the price of the battery system is modified in function of the number of packs.

As mentioned in [30], the software used for this work optimizes the objective function of the total cycle cost of the conventional system and the hybrid one. It runs multiple iterations with ranges of sensitivity variables to evaluate the effect the changes in input parameters may have on the system studied. A list of cases (or optimization result table) for the different system configuration can be ranked from the best to the worst solution, for instance, according to the best

reduction of fuel consumption or lowest *NPV*. Additionally, the software optimizes the system energy using an algorithm called "modified grid search" and allows the sensitivity analysis. According to [26], the optimization algorithm is not detailed in the User Guide because it is one of the main assets of the software.

In addition, the sensitivity analysis is considered for some battery parameters: battery energy capacity ranging from 200 kWh to 2000 kWh (number of battery packs variation or modification of container size), battery power ranging from 200 kW to 2000 kW (or nominal battery C-rate variation), *DoD*, and Round-trip efficiency depending on battery technology. For simulation were considered two Lithium-ion cell technologies: lithium iron phosphate (*LFP*) and lithium nickel cobalt manganese (*NMC*). The sensitivity analysis consists of eight cases considering simplified and advanced battery models: (1) No Aging | No Cost; (2) Aging | Cost; (3) No Aging | No Cost; (4) Aging | No Cost; (5) No Aging | Cost (70% *DoD*); (6) No Aging | Cost (80% *DoD*); (7) Aging | Cost (70% *DoD*); and (8) Aging | Cost (80% *DoD*). The general methodology used in this work can be visualized in Figure 25.

Figure 25 – Flowchart of the proposed method (detailed) on this Master's Thesis considering Optimization software.



Source: Author.

The input data from such analyses are related to the fuel consumption and Specific Fuel Oil Consumption (*SFOC*) curves for Generator-sets, aside from price curves for equipment described in this Chapter. The choice of Diesel Gen-set is based on IMO Regulations, and Typical *PSV* operational profile mentioned in the previous Chapter.

The results (output data) present in the next Chapter are analyzed by the reduction of *CO₂* emissions, fuel consumption, fuel-saving, reduction of fuel cost, expected life, *EFC*, and

economic parameters for both battery cell technologies. Thus, some recommendations for battery operation in *PSV* Power Systems are provide considering each of the four cases simulated.

4.5 *Synthesis*

This Chapter detailed the economic indicators applied to Hybrid vessels and their components. Cost analysis methodology for battery aging is divided into the capital and operational costs. The replacement costs also are estimated for all equipment considered in the simulation. These costs can be allocated to the acquisition of battery systems, *O&M*, power control system, power conversion system equipment, installation, Gen-sets cost, and balance of system. The fuel costs are allocated to the operational costs that frequently are considered zero for renewable sources. The literature reports that there is not industry acceptable methodology for quantifying battery degradation costs. Nevertheless, it is also the point of this work the battery models can be involved in the aging processes and the cost analyzes, simultaneously.

Additionally, when these equipment are sized to the *PSV* Power Systems, some economic indicators can be determined. This Chapter indicates these parameters based on literature related to hybrid systems. The variables *CAPEX*, *OPEX*, *NPV*, and *payback* can be determined to the vessel operating for 30 years. The sensitivity analysis is used to evaluate the impact of battery operation in the output data of HOMER software, and this is indispensable to the results of the simulation presented in the next Chapter.

Chapter 5

Results and Discussion

In this Chapter, the feasibility of Li-ion batteries (*LFP* and *NMC* cells) in Ship Power Systems both from a technical and economic point of view is discussed. It presents the results for the battery aging model (Advanced) and the Simplified model, where the battery degradation processes are disregarded. The application of the battery models is demonstrated through four simulation cases: (1) "No Aging | No Cost"; (2)"Aging | Cost"; (3)"No Aging | Cost"; and (4)"Aging | No Cost". Furthermore, to investigate accurately the cases that involve economic aspect, the effect of the depth-of-discharge is simulated for 70% and 80% *DoD* for the following cases: (1) "No Aging | Cost (70% *DoD*)"; (2)"No Aging | Cost (80% *DoD*)"; (3) "Aging | Cost (70% *DoD*)"; and (4) "Aging | Cost (80% *DoD*)". Thus, these cases studied have the purpose of determining the battery potential in terms of techno-economical and demonstrate the discrepancy between the models used. Table 6 shows the description of cases investigated in this work.

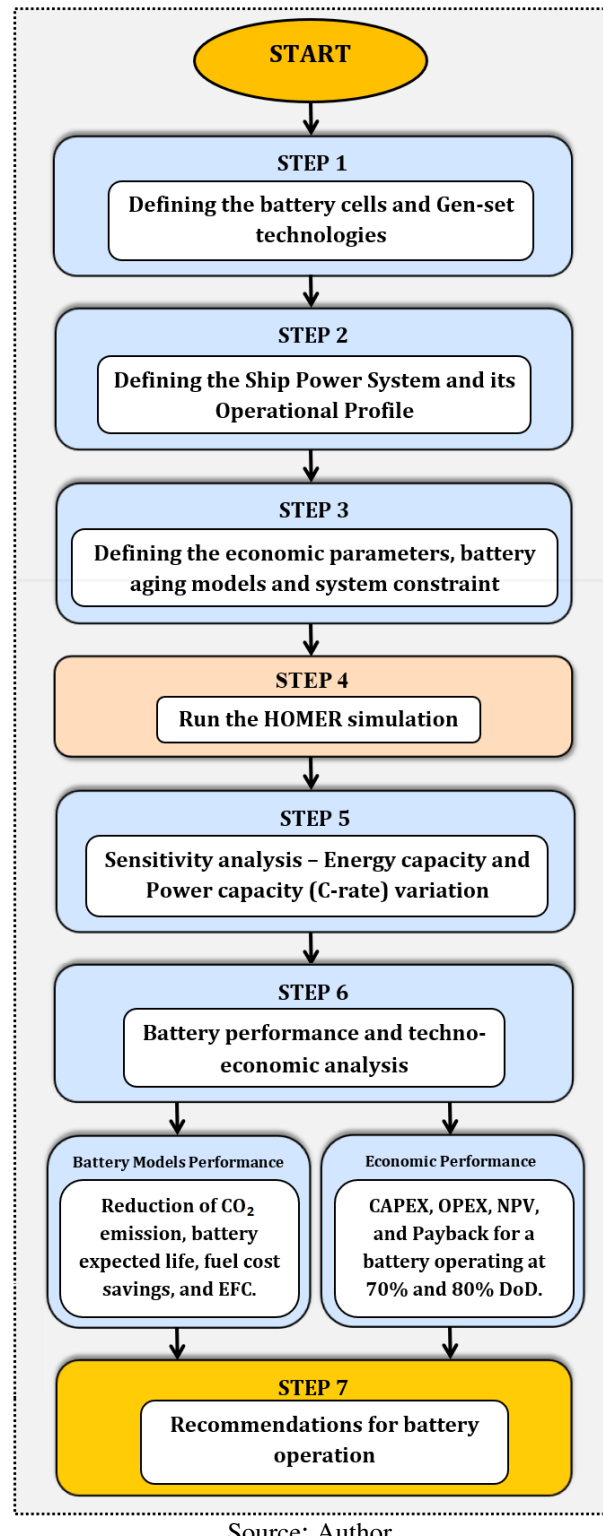
Table 6 – Description of the cases simulated in this Master's Thesis.

Battery Performance Cases (80% <i>DoD</i>)	Description
No Aging No Cost	Battery operating at 80% <i>DoD</i> . Simplified battery model, where the effects of battery degradation are disregarded Battery cost is NOT considered.
Aging Cost	Battery operating at 80% <i>DoD</i> . Advanced battery model, where the effects of battery degradation are regarded Battery cost is considered.
No Aging Cost	Battery operating at 80% <i>DoD</i> . Simplified battery model, where the effects of battery degradation are disregarded Battery cost is considered.
Aging No Cost	Battery operating at 80% <i>DoD</i> . Advanced battery model, where the effects of battery degradation are regarded Battery cost is NOT considered.
Economic Viability Cases	Description
No Aging Cost (70% <i>DoD</i>)	Battery operating at 70% <i>DoD</i> . Simplified battery model, where the effects of battery degradation are disregarded Battery cost is considered.
No Aging Cost (80% <i>DoD</i>)	Battery operating at 80% <i>DoD</i> . Simplified battery model, where the effects of battery degradation are disregarded Battery cost is considered.
Aging Cost (70% <i>DoD</i>)	Battery operating at 70% <i>DoD</i> . Advanced battery model, where the effects of battery degradation are regarded Battery cost is considered.
Aging Cost (80% <i>DoD</i>)	Battery operating at 80% <i>DoD</i> . Advanced battery model, where the effects of battery degradation are regarded Battery cost is considered.

Source: Author.

The flowchart of the entire methodology, simulation process, and data analysis are shown in Figure 26.

Figure 26 – Flowchart of the entire methodology, simulation process, and data analysis.



Source: Author.

Initially, the battery cells and Gen-sets are defined based on the vessel's operational profile and technical requirements (Step 1 and 2). The economic parameters and aging models

are determined by inputs HOMER software and the system constraint is estimated by real conditions presented in the literature and discussed in previous Chapters (Step 3). The results of the HOMER simulation are compared by a sensitivity analysis where the battery energy capacity (for 1000 kW fixed) and battery power capacity (for 1000 kWh fixed) are changed to obtain new data in the output HOMER. These results are presented in the next sections for the following parameters: reduction of CO_2 emission; battery expected life; fuel savings; fuel costs savings; equivalent full cycles (*EFC*); *CAPEX*; *OPEX*; *NPV*; and *payback* (Step 6). Some recommendations for battery operation are based on the best solutions considering each simulation case (Step 7).

The results of the Base Case can be seen in section 5.1. In the section 5.2, the sensitivity analysis for the Simplified battery model is presented. Section 5.3 demonstrates the impact of battery energy capacity, and the effect of battery C-rate variation can be seen in section 5.4. C-rate definition can be seen in the Glossary (page 137). Finally, from section 5.5, the evaluation of battery capacities is shown and recommendations are made for battery operation in *PSV* Power System.

5.1 Base case

The HOMER simulation that does not include the battery system is assumed as the Base Case which can be compared with cases of the vessel powered by the battery. The Base Case represents the typical *PSV* which includes 4 x 1700 kW Diesel Generator-sets (Gen-set) and 1 x 425 kW Auxiliary Gen-set as can be seen in Figure 18. The main results of Base Case analysis are presented in Table 7.

Table 7 – The results of Base Case simulation (Homer software) for CO_2 emissions, fuel consumption, and economic analyses of a Typical *PSV* Power Systems.

Parameter	Base Case (Typical <i>PSV</i> Power System)
CO_2 Emitted [ton/year]	6,209,5
Fuel Consumption [L/year]	2,358,037
<i>NPV</i> [US\$]	-40.767.930,00
<i>CAPEX</i> [US\$]	3.042.412,50
<i>OPEX</i> [US\$]	2.706.284,00

Source: HOMER simulation.

Although there is a *CAPEX* for each system component, the Capital Expenditure indicated from the Table is related to a Ship system *CAPEX*, and can be used to compare the various battery technical options (capacity level). A similar evaluation is shown to *OPEX* (Operating Expenditure), *NPV* (Net Present Value), CO_2 emitted, and fuel consumption. The CO_2 emitted and fuel consumption are measured per year, while the other parameters are measured during 30 years (vessel lifetime).

The section 5.2 demonstrates the effect of modification of the battery energy capacity and C-rate considering only the Simplified Battery Model.

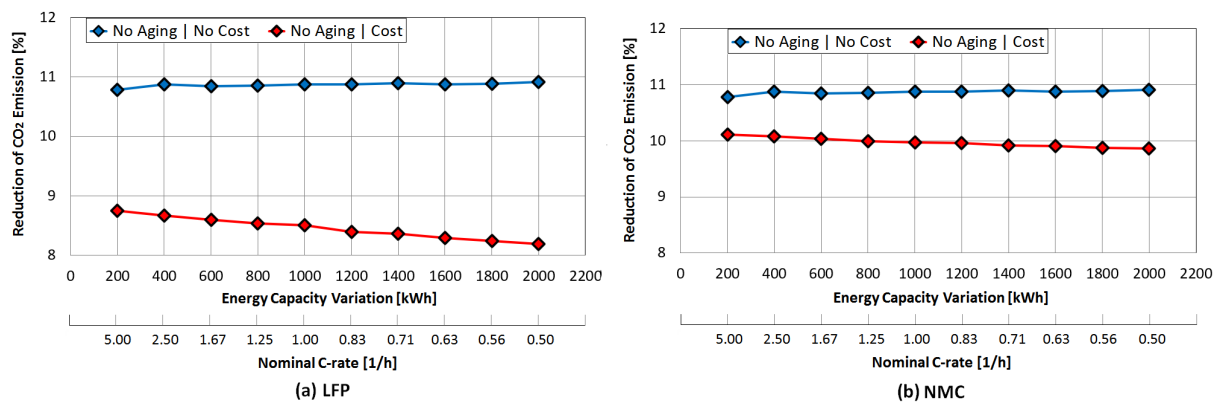
5.2 Sensitivity analysis for Simplified battery model

Sensitivity analysis of battery capacity from 200 kWh to 2000 kWh is subsequently seen for most Figures and it is attributed to the graphs (a) and (b) the results for *LFP* and *NMC* battery cells, respectively. For both graphs, the energy capacity variation is evaluated by a constant power capacity of 1000 kW and it is represented by nominal C-rate (axis X). These same sequences for the presentation of results can be seen in most Figures in the next items.

5.2.1 Pollutant emission estimation (Energy variation)

Figure 27 compares the reduction of CO_2 emissions per year for the *LFP* and *NMC* cells considering only "No Aging" case.

Figure 27 – Reduction of CO_2 for Hybrid PSV Power System with battery included. Sensitivity analysis from 200 to 2000 kWh for battery cell technologies analysed. (a) *LFP* (ΔE capacity). (b) *NMC* (ΔE capacity). The Nominal C-rate (axis X) represents the fixed battery power capacity of 1000 kW.



Source: Author.

In terms of battery system space, battery cell status, and its operation, when the energy capacity is grown, it means that several battery cells are included in the storage system through modules and packs. However, when the power capacity is modified, this can mean a alteration of the battery nominal C-rate. This C-rate variation is presented in item 5.4. As detailed in Figure 27(a), the reduction of CO_2 is calculated in [%] per year, and "No Aging" cases present the best results at 8.7% and 11% per year for "Cost - red points" and "No Cost - blue points" ones, respectively. Note that the "No Cost" case presents the best results because the battery system is operated in better possible conditions with a zero cost. Therefore, maximum battery potential can be extracted for the Ship Power System in this case.

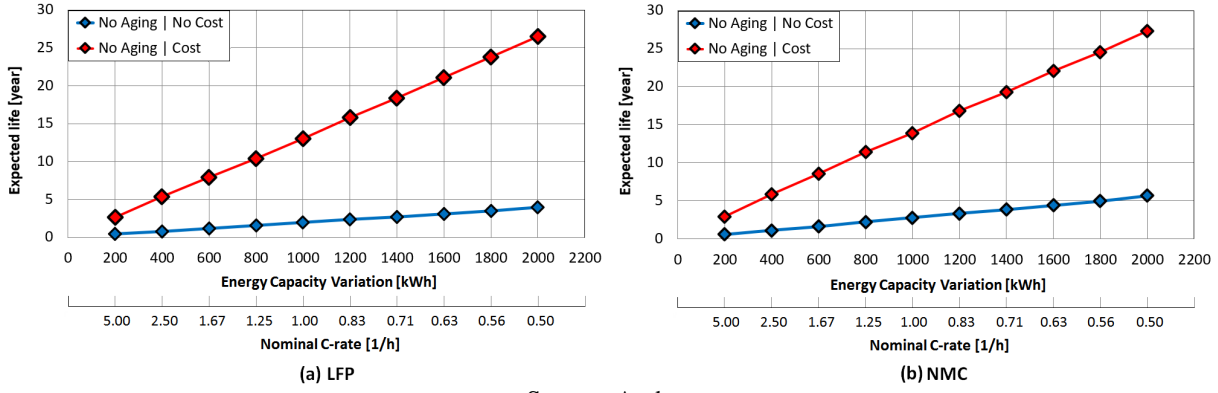
Figure 27 (b) illustrate battery performance for *NMC* cells. The rate of CO_2 emissions present a similar tendency for all cases in comparison with *LFP* cells, except for the "No Aging | cost - red points" case which shows a better performance than a previous cell. Furthermore, it is clear from the graph (b) that a reduction of CO_2 emissions is about 10%, and 11% per year for the most battery capacities analyzed.

The results from such CO_2 emissions analyses should be treated within considerable caution. Each point shown in Figure 27 in % per year is associated with a battery expected life (in years). This can be only seen when absolute numbers of parameters are calculated such as the fuel savings of battery-powered *PSV* that will highlight in the item 5.2.4.

5.2.2 Battery expected life (Energy variation)

From Figure 28 (a), we can observe that normally the expected life is increased with the inclusion of battery energy capacity packs. The similar performance can be seen in Figure 28 (b) for *NMC* battery cell. The expected life is calculated by Wh-throughput (that can be seen in Glossary, page 141). The total battery energy that can be cycled is estimated and the *DoD* determines when the battery system needs to be replaced. Comparing the 27 (a) and 28 (a), note that the battery operating at 1200 kWh has a durability of approximately 15 years and it provides the reduction of CO_2 emissions of 8.4% ("No Aging | Cost"). However, for the same case, the battery capacity at 2000 kWh provides the reduction of CO_2 emissions of 8.2% during about 26 years.

Figure 28 – Battery Expected life (years) for the battery included in the Hybrid PSV Power System. Sensitivity analysis from 200 to 2000 kWh for battery cell technologies analysed. (a) *LFP* (ΔE capacity). (b) *NMC* (ΔE capacity). The Nominal C-rate (axis X) represents the fixed battery power capacity of 1000 kW.

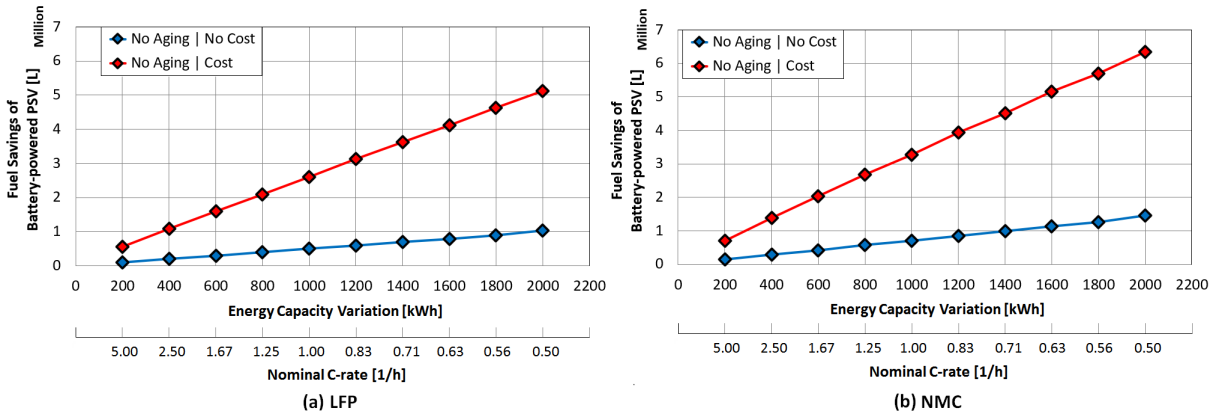


Source: Author.

5.2.3 Reduction of fuel consumption (Energy variation)

Figure 29 presents the Fuel Savings (in millions of Liters) of Battery-powered Hybrid PSV Power Systems. The "No Aging | Cost" case has the best performance in terms of fuel economy from 600 to 2000 kWh. The *LFP* and *NMC* present a similar tendency. Note that when the battery energy capacity is increased, the fuel savings trends also do.

Figure 29 – Fuel Savings (Millions of Liters) of Battery-powered Hybrid PSV Power Systems. Sensitivity analysis from 200 to 2000 kWh for battery cell technologies analysed. (a) *LFP* (ΔE capacity). (b) *NMC* (ΔE capacity). The Nominal C-rate (axis X) represents the fixed battery power capacity of 1000 kW.



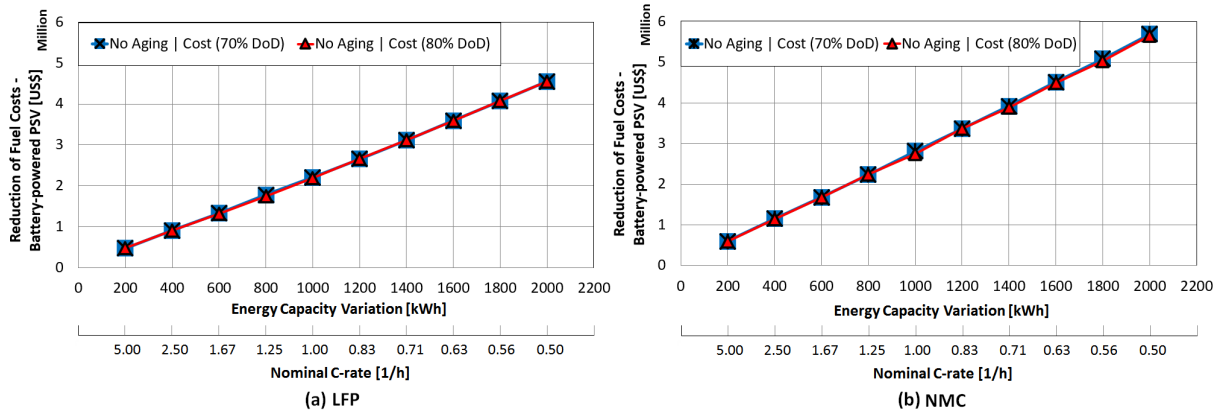
Source: Author.

5.2.4 Fuel costs savings (Energy variation)

Figure 30 pinpoints the reduction of Fuel Costs (in US\$) to Hybrid PSV Power Systems with battery included, and its operating performance is compared to 70% and 80% *DoD*. The *LFP* and *NMC* present a similar tendency. Note that when the battery energy capacity is increased, the fuel costs trends also do. *NMC* battery cell provides a larger fuel economy than *LFP* that can be evidenced by the a shift up in the *NMC* curve in comparison with *LFP* line. The *DoD* does not present impact in the reduction of fuel costs.

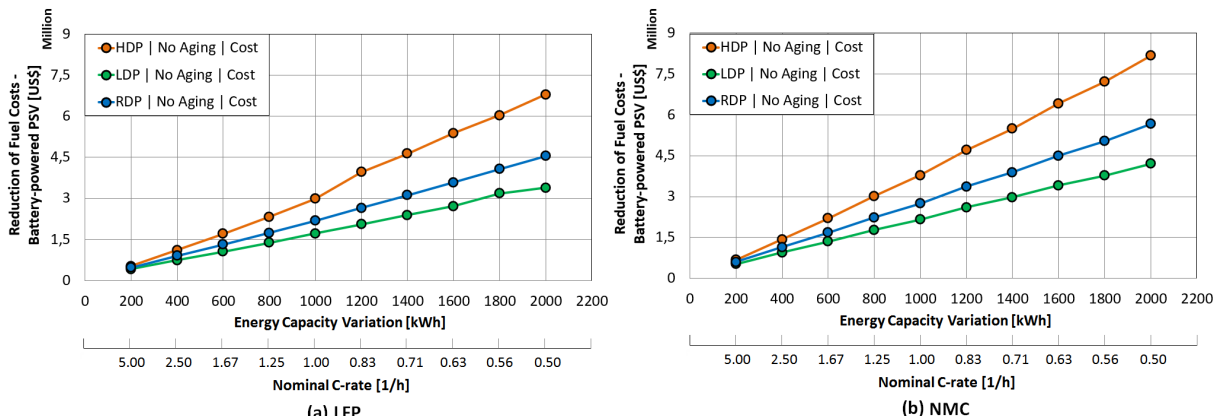
Figure 30 – Reduction of Fuel Costs (in US\$) for Hybrid PSV Power Systems with battery included.

Sensitivity analysis from 200 to 2000 kWh for battery cell technologies analysed. (a) *LFP* (ΔE capacity). (b) *NMC* (ΔE capacity). The Nominal C-rate (axis X) represents the fixed battery power capacity of 1000 kW.



Source: Author.

Figure 31 – Reduction of Fuel Costs (in US\$) for Hybrid PSV Power Systems with battery included. Evaluation was based on Oil price scenarios from 2019 to 2049. *HDP* - High Diesel Price, *RDP* - Reference Diesel Price, and *LDP* - Low Diesel Price. Sensitivity analysis from 200 to 2000 kWh for battery cell technologies analysed. (a) *LFP* (ΔE capacity). (b) *NMC* (ΔE capacity). The Nominal C-rate (axis X) represents the fixed battery power capacity of 1000 kW.



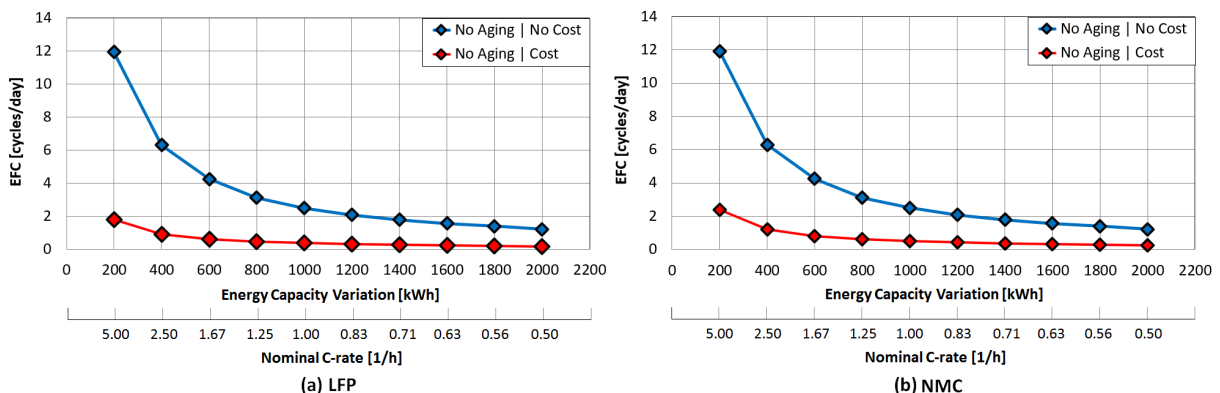
Source: Author.

As highlighted in Figure 31, the reduction of fuel costs (in US\$) to battery-powered PSV can be analyzed by three scenarios considering the Oil price from 2019 to 2049, where *HDP* is an abbreviation for High Diesel Price, *RDP* means Reference Diesel Price, and *LDP* abbreviates Low Diesel Price. Only cost cases were considered for these analyses. These three oil price scenarios are compared and the procedure consists of defining the fuel consumption per year for all capacities range. After that, the oil price yearly is multiplied by the fuel curve until battery End of Life (*EoL*) is reached. Figure 31 demonstrates the reduction of fuel cost provide by each battery capacity simulated for the vessel.

5.2.5 Equivalent Full Cycle (Energy variation)

Figure 32 compares the *EFC* – Equivalent Full Cycle – for each battery capacity evaluated. As detailed in Figure 32 (a) e (b) for *LFP* and *NMC* cells, respectively, there is a decreasing tendency of the *EFC* when battery packs are included in the system, but these cycles can be more prolonged. The battery that operates with high C-rate has an influence on the number of cycles as illustrated in Figure 9 (page 41).

Figure 32 – *EFC* - Equivalent Full Cycles for each battery capacity studied. Sensitivity analysis from 200 to 2000 kWh for battery cell technologies analysed. (a) *LFP* (ΔE capacity). (b) *NMC* (ΔE capacity). The Nominal C-rate (axis X) represents the fixed battery power capacity of 1000 kW.



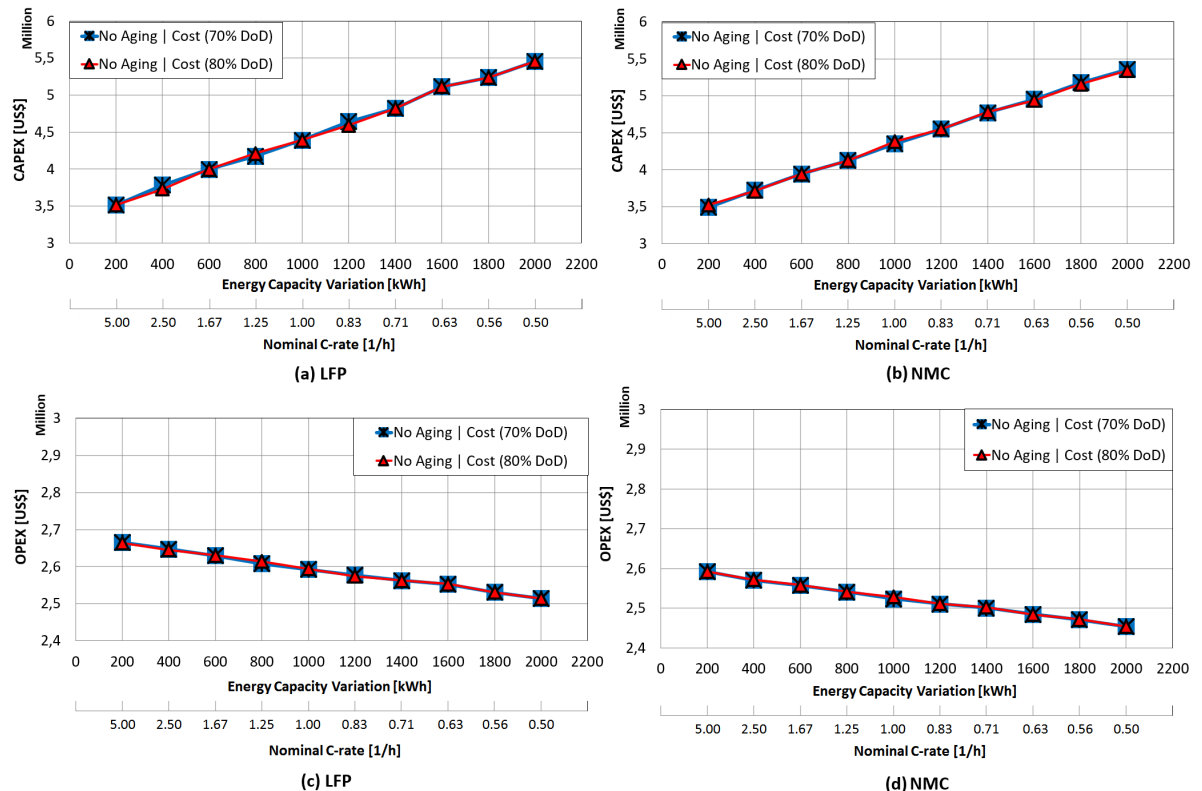
Source: Author.

The "No Aging | No Cost" case represents the best battery performance due to battery operating at zero cost. When the price of battery is included on the simulation "No Aging | Cost", the HOMER optimization process chooses the lower total cost, determined by minimization of the objective function.

5.2.6 Economic analysis (Energy variation) – Hybrid PSV Power System

Figure 33 compares the multiple design configurations of *PSV* with *LFP/NMC* battery cells varying *CAPEX* and *OPEX* scenarios. The discrepancy between *CAPEX* values from the graph and values from the Base Case are battery initial cost, power converter, and power control system. Note that *CAPEX* presents approximately the same curve for all cases simulated. If the battery capacity selected is technically the better, the lowest *CAPEX* option is mostly an adequate choice. However, this evaluation does not allow discovering if a battery should be operated with 70% or 80% *DoD*. The Figure 33 (c) and (d) reveals the minimum *OPEX* linked to the maximum battery energy capacity at 2000 kWh (*LFP* and *NMC* - No Aging).

Figure 33 – Evaluation of *CAPEX* and *OPEX* for Hybrid *PSV* Power System. *CAPEX*. (a) *LFP* (ΔE capacity). Sensitivity analysis from 200 to 2000 kWh for battery cell technologies analysed. (b) *NMC* (ΔE capacity). *OPEX*. (c) *LFP* (ΔE capacity). (d) *NMC* (ΔE capacity). The Nominal C-rate (axis X) represents the fixed battery power capacity of 1000 kW.

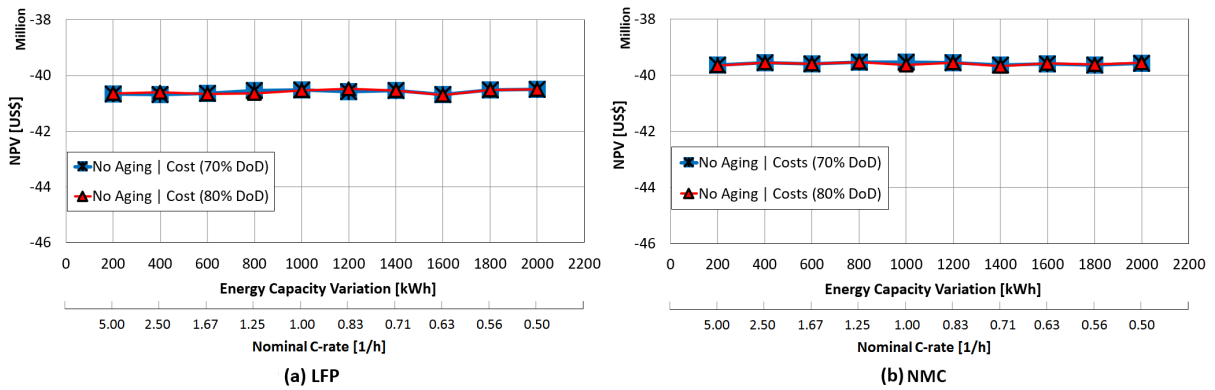


Source: Author.

The results of *NPV* can be seen in Figure 34 and most curves demonstrate that the lowest during life-cycle costs are related to lower battery capacities. For instance, graph (a) for *LFP* cell demonstrates the spend profile during a lifetime project of 30 years represented by its *NPV* from -US\$ 40.5 to -US\$ 41.2 million for a battery at 200 kWh. The *NMC* presents a better economic

performance than *LFP* because NPV_{NMC} is less negative than NPV_{LFP} . Note that the values of $NPVs$ are lower than zero. This results in a loss because the investment costs and the capital return can not be compensated by the revenues (discounted). However, this evaluation should be integrated into other *PSV* operational costs considering the vessel's life as a time horizon at 30 years of operation. The *DoD* does not present an impact in the *CAPEX*, *OPEX*, and *NPV*.

Figure 34 – Evaluation of *NPV* for Hybrid *PSV* system. Sensitivity analysis from 200 to 2000 kWh for battery cell technologies analysed. (a) *LFP* (ΔE capacity). (b) *NMC* (ΔE capacity). The Nominal C-rate (axis X) represents the fixed battery power capacity of 1000 kW.

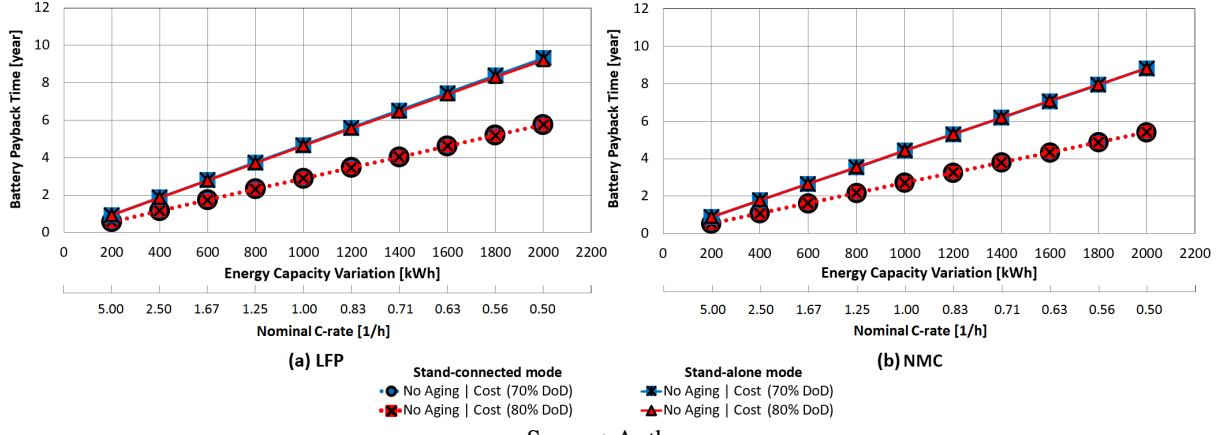


Source: Author.

Payback is determined by Equation 33 and their parameters can be visualized in Table 13 (Annex E). Figure 35 show the theoretical *payback* calculation parameters for *PSV* powered by battery. These results consider the battery operating as stand-alone mode and also stand-connected to the grid when the vessel stays at Port (percentage annual time is approximately 15% of *PSV*'s operational profile or 20 hours per mission in the Port mode). Besides, the effects of Diesel consumption rate, the avoided emission of carbon dioxide, carbon credit, and the number of days per year of *PSV* operation are considered. Graphs (a) and (b) demonstrate a *payback* growth together with energy capacity and the higher value allows to battery return on investment in about 9 years (2000 kWh | 1000 kW). When the same battery is connected to the grid, the battery initial investment is recovered 3 years more rapidly than the battery operating as a stand-alone mode. The *DoD* does not present an impact on the *payback*.

The next items show the sensitivity analysis of battery power capacity variation and its effects in the reduction of CO_2 emissions, battery expected life, fuel consumption, savings fuel costs, *EFC*, and economic analysis of a Hybrid *PSV* Power Systems. In terms of battery operation, this power modification represents the C-rate variation.

Figure 35 – Theoretical *payback* calculation parameters for PSV powered by battery. Sensitivity analysis from 200 to 2000 kWh for battery cell technologies analysed. (a) LFP (ΔE capacity). (b) NMC (ΔE capacity). The Nominal C-rate (axis X) represents the fixed battery power capacity of 1000 kW.

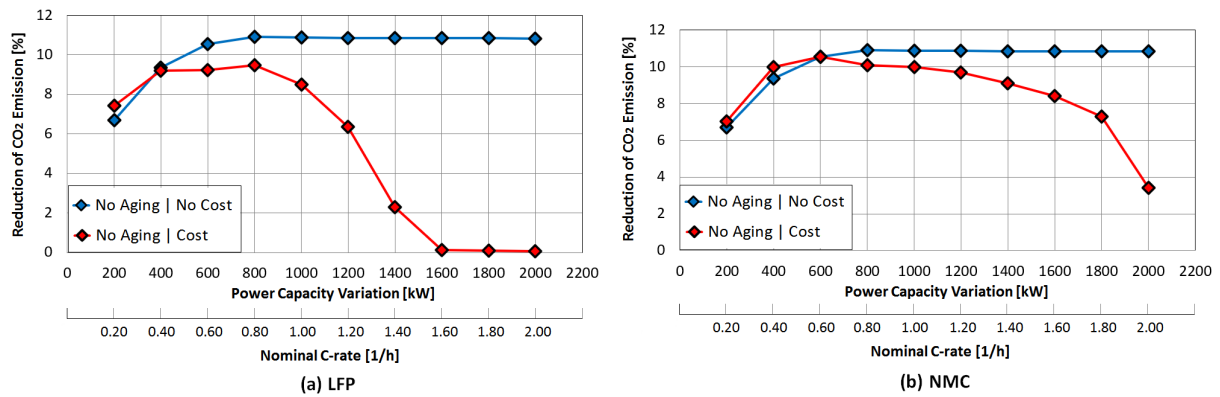


Source: Author.

5.2.7 Pollutant emission estimation (Power variation)

Figure 36 illustrates the reduction of CO_2 emissions per year for sensitivity analysis of battery capacities from 200 kW to 2000 kW. The power capacity variation is evaluated by an energy capacity of 1000 kWh and it can be represented by nominal C-rate (axis X). These same sequences for the presentation of results can be seen in most Figures in the next items.

Figure 36 – Reduction of CO_2 to Hybrid PSV Power System with battery included. Sensitivity analysis from 200 to 2000 kW for battery cell technologies analysed. (a) LFP (ΔP capacity). (b) NMC (ΔP capacity). The Nominal C-rate (axis X) represents the fixed battery energy capacity of 1000 kWh.



Source: Author.

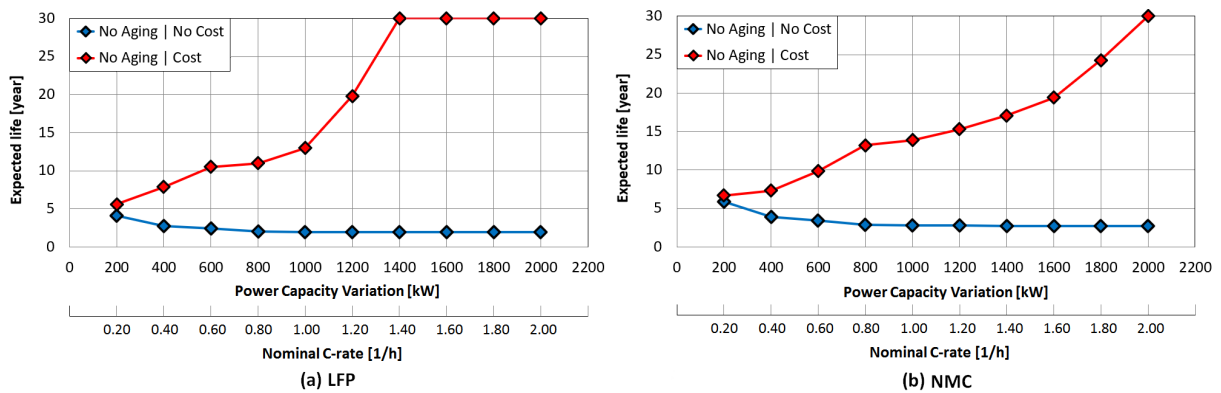
As detailed in Figure 36 (a), the rate of CO_2 emissions decreases when power capacity is increased for "No Aging | Cost" case. However, the rate of emissions is stabilized about 11% for "No Aging | No Cost". In practical terms, these curves indicate when the cost analysis is

considered on simulation, the HOMER software opts to preserve the battery during its lifetime, mainly from the 1600 kW to 2000 kW for *LFP* cell and 2000 kW for *NMC* cell. In high power conditions, the battery operational costs tend to increase significantly and the battery system operation is avoided.

5.2.8 Battery expected life (Power variation)

Figure 37 (a) details the expected life in function of power capacity variation. "No Aging | No Cost" case indicates that expected life is approximately constant for all power range. The similar performance can be seen in Figure 37 (b) for *NMC* battery cell. The better battery lifespan is observed in "No Aging | Cost", mainly for power capacity upper of 1200 kW (or C-rate higher than 1.2C). The expected life is different between the two types of battery cells because the *LFP* is not used to operate from 1600 to 2000 kW, thus, these battery capacities have the durability of 30 year. This effect is not observed to *NMC* battery cells.

Figure 37 – Battery Expected life (years) to Hybrid PSV Power System with battery included. Sensitivity analysis from 200 to 2000 kW for battery cell technologies analysed. (a) *LFP* (ΔP capacity). (b) *NMC* (ΔP capacity). The Nominal C-rate (axis X) represents the fixed battery energy capacity of 1000 kWh.



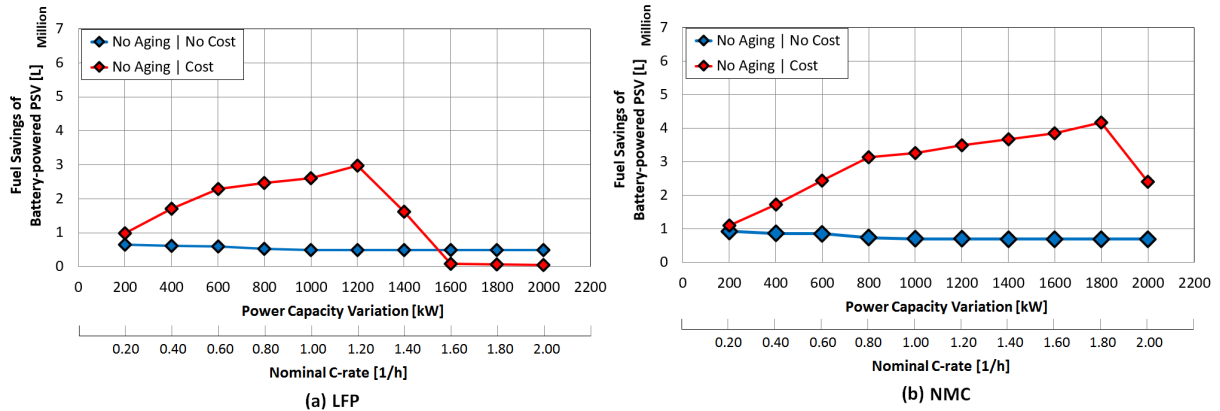
Source: Author.

5.2.9 Reduction of fuel consumption (Power variation)

Figure 38 shows Fuel Savings (in millions of Liters) of Battery-powered Hybrid PSV Power Systems. The "No Aging | Cost" case the best performance in terms of fuel economy. The *LFP* and *NMC* cells present similar tendency except for observation of graphs (a) and (b) that indicate a decrease of fuel savings to high C-rates (from 1.40 to 2 C for *LFP* cell, and 2C for

NMC cell for the case that involves "Cost"). In most of the power capacities analyzed, the "No Aging | No Cost" case presents low fuel savings.

Figure 38 – Fuel Savings (Millions of Liters) of Battery-powered Hybrid *PSV* Power Systems. Sensitivity analysis from 200 to 2000 kW for battery cell technologies analysed. (a) *LFP* (ΔP capacity). (b) *NMC* (ΔP capacity). The Nominal C-rate (axis X) represents the fixed battery energy capacity of 1000 kWh.

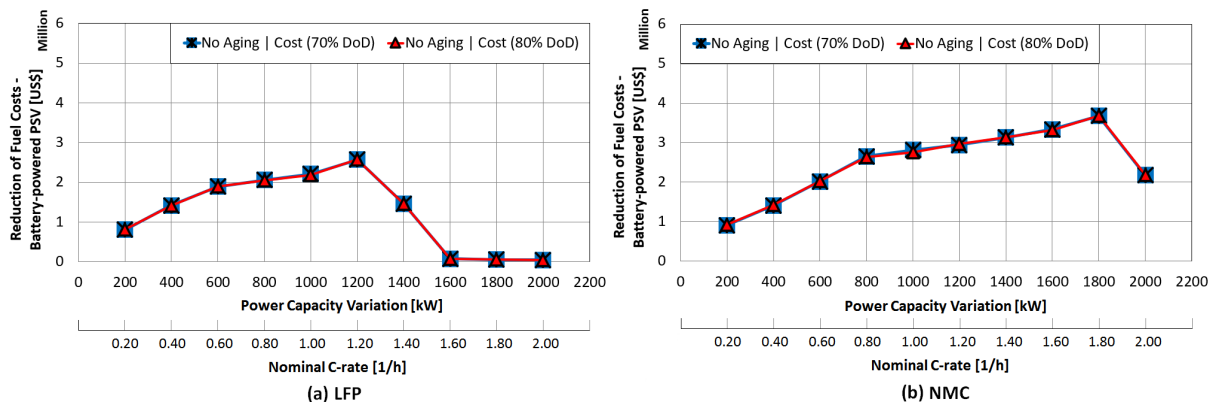


Source: Author.

5.2.10 Fuel costs savings (Power variation)

Figure 39 pinpoints the reduction of Fuel Costs (in US\$) to Hybrid *PSV* Power Systems with battery included, and its operate performance is compared to 70% and 80% *DoD* (Depth-of-discharge). The cost was included in all analyses. The results demonstrate that "No Aging" cases present the same reduction of fuel costs for all range of capacities.

Figure 39 – Reduction of Fuel Costs (in US\$) to Hybrid *PSV* Power Systems with battery included. Sensitivity analysis from 200 to 2000 kW for battery cell technologies analysed. (a) *LFP* (ΔP capacity). (b) *NMC* (ΔP capacity). The Nominal C-rate (axis X) represents the fixed battery energy capacity of 1000 kWh.

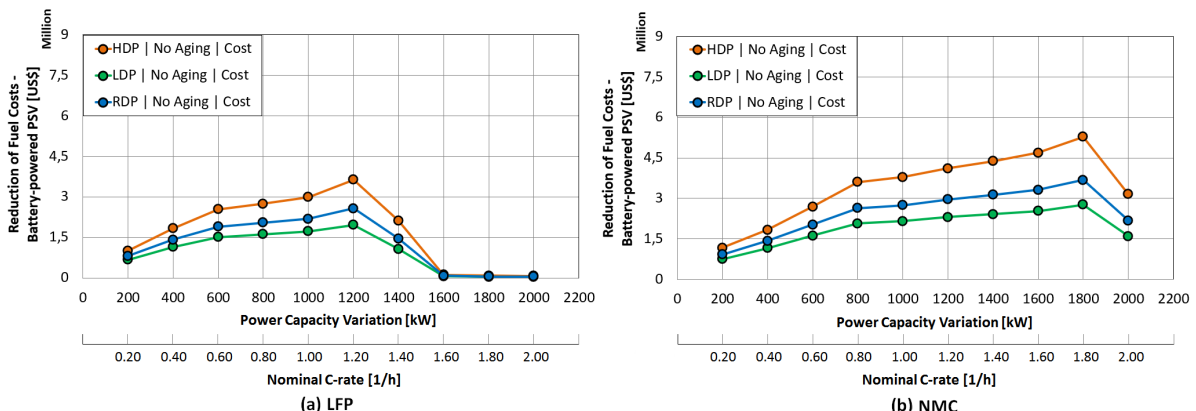


Source: Author.

The reduction of fuel costs (in US\$) to battery-powered PSV can be analyzed by three scenarios considering the Oil price from 2019 to 2049, where *HDP* is an abbreviation for High Diesel Price, *RDP* means Reference Diesel Price, and *LDP* abbreviates Low Diesel Price. Only cost cases were considered for these analyses. "No Aging" battery models are compared and the procedure consists of defining the fuel consumption per year for all capacities range. After that, the oil price yearly is multiplied by the fuel curve until battery *EoL* is reached. The *EoL* definition is described in the Glossary (page 137). Figure 40 demonstrates the reduction of fuel cost provide by each battery capacity simulated for the vessel.

Figure 40 (a) indicates the best results at 1200 kW or C-rate at 1.2C. Above this capacity, the battery reduces its performance. Besides, the Figure 40 (b) details a decrease of battery performance when it operates with C-rate at 2C (1000 kWh | 2000 kW). This mean that the best option to battery capacity is at 1000 kWh | 1800 kW.

Figure 40 – Reduction of Fuel Costs (in US\$) to Hybrid PSV Power Systems with battery included. Evaluation was based on Oil price scenarios from 2019 to 2049. *HDP* - High Diesel Price, *RDP* - Reference Diesel Price, and *LDP* - Low Diesel Price. Sensitivity analysis from 200 to 2000 kW for battery cell technologies analysed. (a) *LFP* (ΔP capacity). (b) *NMC* (ΔP capacity). The Nominal C-rate (axis X) represents the fixed battery energy capacity of 1000 kWh.

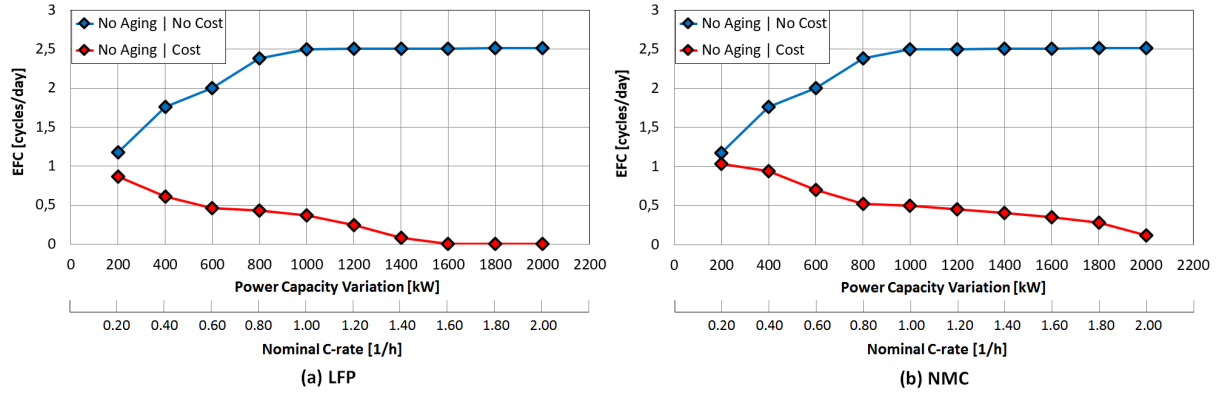


Source: Author.

5.2.11 Equivalent Full Cycle (Power variation)

Figure 41 compares the *EFC* - Equivalent Full Cycle - for each battery capacity evaluated. As detailed in the graph (a) e (b), the *EFC* tend to growing when the battery is operated to high C-rates for "No Cost" case, whereas the same behaviour is not observed when the analyses of cost are considered because the battery is preserved to the Ship operation (due to high operational costs).

Figure 41 – *EFC* - Equivalent Full Cycles for each battery capacity studied. Sensitivity analysis from 200 to 2000 kW for battery cell technologies analysed. (a) *LFP* (ΔE capacity). (b) *NMC* (ΔE capacity). The Nominal C-rate (axis X) represents the fixed battery energy capacity of 1000 kWh.



Source: Author.

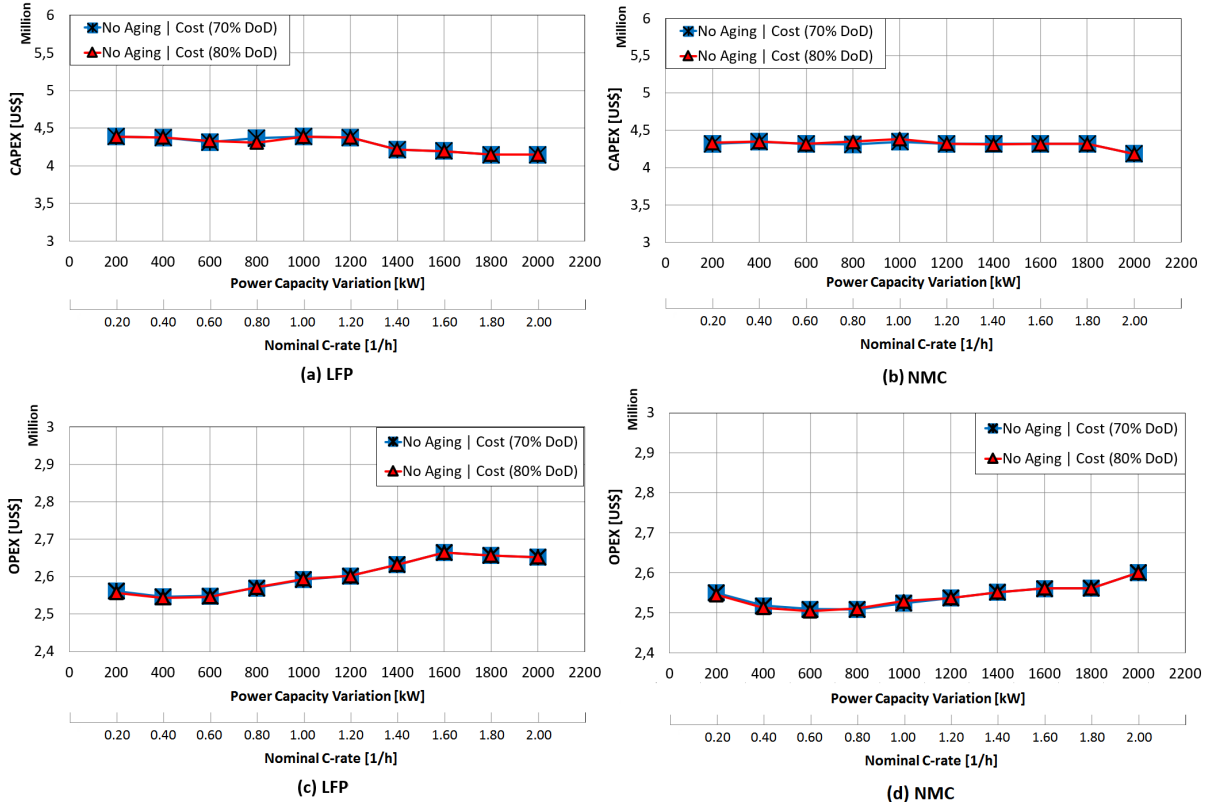
5.2.12 Economic analysis (Power variation) – Hybrid PSV Power System

Figure 42 compares the multiple design configurations of *PSV* with *LFP/NMC* battery cells varying *CAPEX* and *OPEX* scenarios. The discrepancy between *CAPEX* values from the graph and values from the Base Case are battery initial cost, power converter, and power control system. If the battery capacity selected is technically the best, the lowest *CAPEX* option is mostly an adequate choice. However, this evaluation does not allow discovering if a battery should be operated with 70% or 80% *DoD*. When battery C-rate is varied as shown in Figure 42 (a) and (b), the system *CAPEX* is similar for all cases analyzed and the data tend to stay between 4 and 4.5 million dollars, considering the battery energy capacity as constant (1000 kWh) for this sensitivity analysis.

The minimum system *CAPEX* can be associated with high *OPEX* when there is the high fuel consumption of Gen-sets or high maintenance requirements during the lifetime of the *PSV* operation. Figure 42 (c) and (d) shows a evaluation of *OPEX* costs for Hybrid *PSV* Power System considering "No Aging" battery cases. The graphs demonstrate that the *OPEX* is identical to both *DoD* cases and the lower *OPEX* linked to the battery power capacity at 600 kW (*LFP* and *NMC* - "No Aging").

OPEX may not necessarily be the best economic parameter for decision-makers to choose the optimum cost solution, mainly if the project storage system operations duration are different. This means that an evaluation of *CAPEX* and *OPEX* separately may hide the best solution. The results of *NPV* can be seen in Figure 43 and the curves demonstrate that the lowest costs during

Figure 42 – Evaluation of *CAPEX* and *OPEX* for Hybrid PSV Power System. *CAPEX*. Sensitivity analysis from 200 to 2000 kW for battery cell technologies analysed. (a) *LFP* (ΔP capacity). (b) *NMC* (ΔP capacity). *OPEX*. (c) *LFP* (ΔP capacity). (d) *NMC* (ΔP capacity). The Nominal C-rate (axis X) represents the fixed battery energy capacity of 1000 kWh.



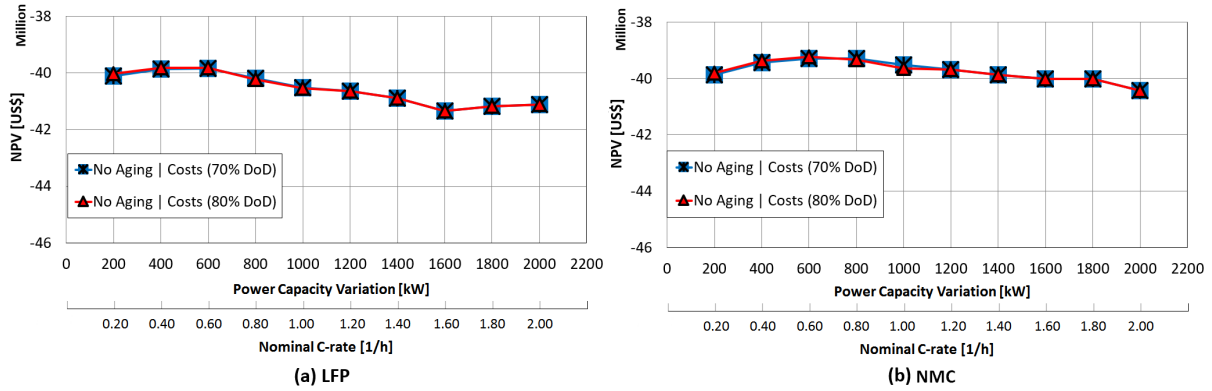
Source: Author.

life-cycle are related to lower battery capacities. As illustrated in the graph (a) for *LFP* cell, the spend profile during a lifetime project of 30 years represented by its *NPV* about -US\$ 40.0 million for a battery at 200 kW / 1000 kWh, while the maximum power capacity of 2000 kW / 1000 kWh presents the *NPV* about -US\$ 41.0 million. As shown in Figure 43 (b), the *NMC* cell presents the similar trend than *LFP* cell. The minimum *NPV* is achieved for 600 kW / 1000 kWh (C-rate at 0.60C).

Note that the values of *NPVs* are lower than zero. This results in a loss because the investment costs and the capital return can not be compensated by the revenues (discounted). However, this evaluation should be integrated into other *PSV* operational costs considering the vessel's life as a time horizon at 30 years of operation.

Figure 44 present the theoretical *payback* calculation parameters for *PSV* powered by battery. These results consider the battery operating as stand-alone mode and also stand-connected to the grid when the vessel stays at Port. Graphs (a) and (b) present a *payback* decrease together with power capacity and the higher value allow to battery return on investment in about 4.5 years

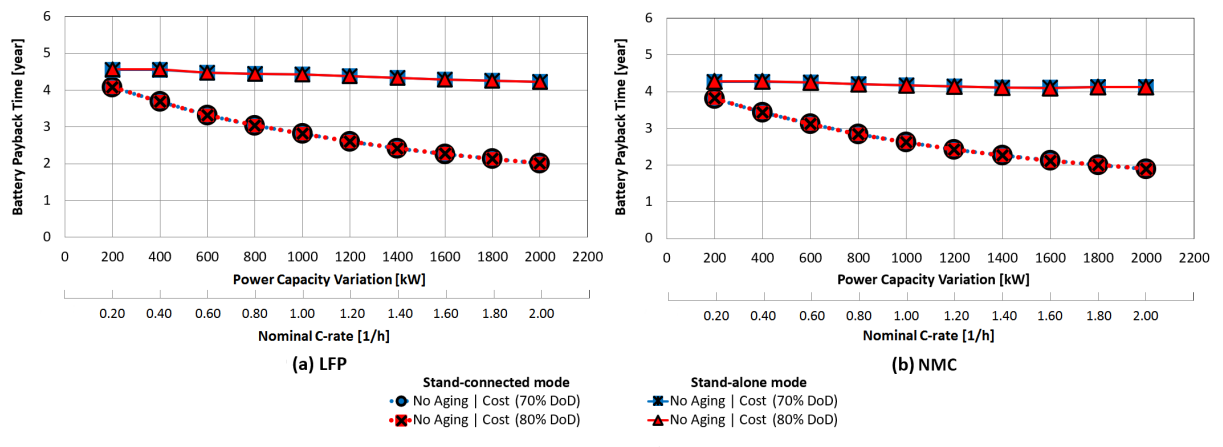
Figure 43 – Evaluation of *NPV* for Hybrid PSV system. Sensitivity analysis from 200 to 2000 kW for battery cell technologies analysed. (a) *LFP* (ΔP capacity). (b) *NMC* (ΔP capacity). The Nominal C-rate (axis X) represents the fixed battery energy capacity of 1000 kWh.



Source: Author.

(*LFP*). Regardless of *DoD* that the battery has been operating, the same results are achieved for mode operation. However, the *payback* is approximately constant for stand-alone mode, while it decreases for stand-connected to the grid. Specifically, a battery of 1000 kWh will present a similar *payback* regardless of power battery capacity if it is operating in the stand-connected to the grid. For the same battery, in turn, the *payback* decrease when it is connected to the grid, demonstrating that is more advantage charge battery in the port for investment return.

Figure 44 – Theoretical *payback* calculation parameters for PSV powered by battery. Sensitivity analysis from 200 to 2000 kW for battery cell technologies analysed. (a) *LFP* (ΔP capacity). (b) *NMC* (ΔP capacity). The Nominal C-rate (axis X) represents the fixed battery energy capacity of 1000 kWh.



Source: Author.

Section 5.3 demonstrates the impact of battery energy capacity variation with the inclusion of degradation models. Similarly, section 5.4 shows the impact of battery C-rate variation (modification of power) with the inclusion of degradation models.

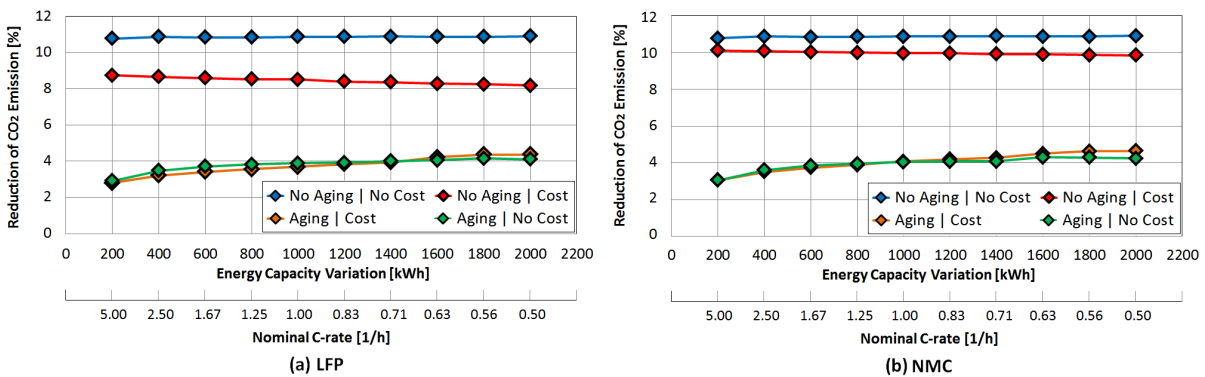
5.3 Impact of battery energy capacity variation

This section shows the results and discussion of the impact of battery energy capacity variation (and power capacity fixed in 1000 kW) for reduction of CO_2 emissions, expected life, fuel consumption, savings fuel costs, EFC , and economic analysis of a Hybrid PSV Power Systems, where the battery system is installed and compared with a Conventional PSV Power Systems, denominated Base Case.

5.3.1 Pollutant emission estimation

The reduction of CO_2 emissions per year for sensitivity analysis of battery capacity from 200 kWh to 2000 kWh can be seen in Figure 45. The graphs (a) and (b) show the results for *LFP* and *NMC* battery cells, respectively. For both graphs, the energy capacity variation is evaluated by a constant power capacity of 1000 kW and it is represented by nominal C-rate (axis X). These same sequences for the presentation of results can be seen in most Figures in the next items. Basically, these cases analyzed are distinguished among costs included, advanced battery model (aging effect is considered), simplified battery model (aging effect is not considered), and costs not included in the simulation.

Figure 45 – Reduction of CO_2 to Hybrid PSV Power System with battery included. Sensitivity analysis from 200 to 2000 kWh for battery cell technologies analysed. (a) *LFP* (ΔE capacity). (b) *NMC* (ΔE capacity). The Nominal C-rate (axis X) represents the fixed battery power capacity of 1000 kW.



Source: Author.

As detailed in Figure 45 (a), the reduction of CO_2 is calculated in [%] per year, and "No Aging" cases present the best results around 8.7% and 11%/yr for "Cost - red points" and "No Cost - blue points" ones, respectively. Besides, the "Aging" cases show the performance in the reduction of CO_2 between 3% and 4.5%.

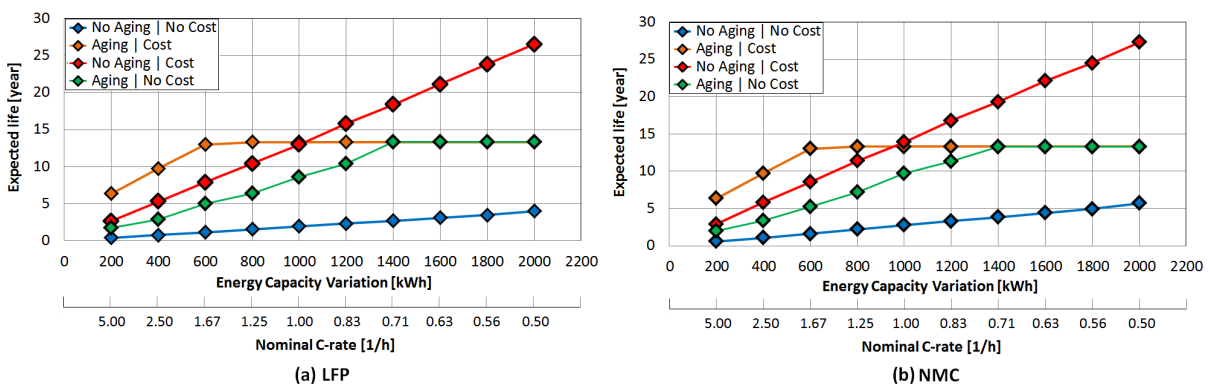
Figure 45 (b) highlights the battery performance for *NMC* cells. The rate of CO_2 emissions present a similar tendency for all cases in comparison with *LFP* cells, except for the "No Aging | Cost - red points" case which shows a better performance than a previous cell. Furthermore, it is clear from the graph (b) that the reduction of CO_2 emissions is about 10% and 11% per year for the most battery capacities analyzed.

The results from such CO_2 emissions analyses should be treated within considerable caution. Each point shown in Figure 45 in % per year is associated with a battery expected life (in years). This can be only seen when absolute numbers of parameters are calculated such as the fuel savings of battery-powered *PSV* that will highlight in the item 5.3.3.

5.3.2 Battery expected life

From Figure 46 (a), we can observe that normally the expected life is increased with the inclusion of battery energy capacity packs. However, note that the "Aging | Cost" case presents constant expected life from 600 to 2000 kWh, and from 1400 kWh to 2000 kWh, the expected life is not also modified for the "Aging | No Cost" case. The similar performance can be seen in Figure 46 (b) for *NMC* battery cell.

Figure 46 – Battery Expected life (years) to Hybrid *PSV* Power System with battery included. Sensitivity analysis from 200 to 2000 kWh for battery cell technologies analysed. (a) *LFP* (ΔE capacity). (b) *NMC* (ΔE capacity). The Nominal C-rate (axis X) represents the fixed battery power capacity of 1000 kW.

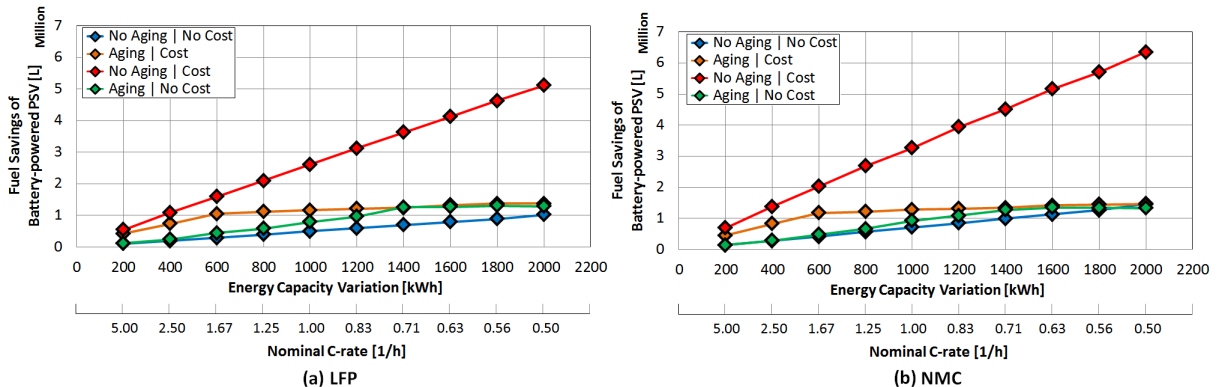


Source: Author.

5.3.3 Reduction of fuel consumption

Figure 47 shows Fuel Savings (in millions of Liters) of Battery-powered Hybrid PSV Power Systems. The "No Aging | Cost" case has the best performance in terms of fuel economy from 1200 to 2000 kWh. The *LFP* and *NMC* present a similar tendency. Note that when the battery energy capacity is increased, the fuel savings trends also do. For cases that fuel consumption present constant approximate performance, the battery expected life follow the same trend.

Figure 47 – Fuel Savings (Millions of Liters) of Battery-powered Hybrid PSV Power Systems. Sensitivity analysis from 200 to 2000 kWh for battery cell technologies analysed. (a) *LFP* (ΔE capacity). (b) *NMC* (ΔE capacity). The Nominal C-rate (axis X) represents the fixed battery power capacity of 1000 kW.



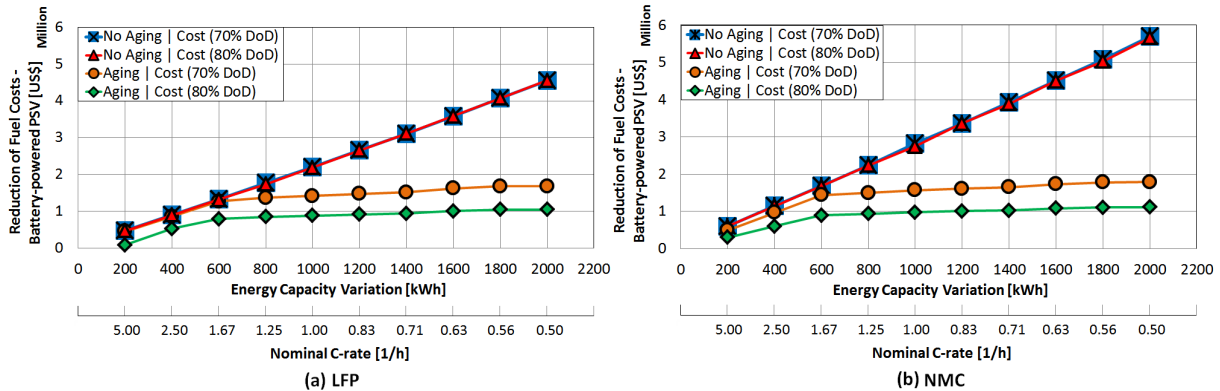
Source: Author.

5.3.4 Fuel costs savings

Figure 48 pinpoints the reduction of Fuel Costs (in US\$) to Hybrid PSV Power Systems with battery included, and its operating performance is compared to 70% and 80% *DoD*. The curves are distinguished between "Aging" and "No Aging" cases. The cost was included in all analyses. The results demonstrate that 70% *DoD* presents the best performance for "Aging" cases, but "No Aging" ones present the same reduction of fuel costs for all range of capacities. *LFP* and *NMC* cells can be differentiated by the performance from 200 to 600 kWh, where the *LFP* indicates identical fuel economy among 70%, 80% (No Aging), and 70% *DoD* (Aging). Above 800 kWh, there is a large discrepancy between "No Aging" and "Aging" cases that can reach 450% for *NMC* cell. This is also denoted by an economy approximately US\$ 5.5 million

(No Aging) in comparison of about US\$ 1.0 million (Aging at 80% DoD) for 2000 kWh capacity in Figure 48 (b).

Figure 48 – Reduction of Fuel Costs (in US\$) to Hybrid PSV Power Systems with battery included. Sensitivity analysis from 200 to 2000 kWh for battery cell technologies analysed. (a) LFP (ΔE capacity). (b) NMC (ΔE capacity). The Nominal C-rate (axis X) represents the fixed battery power capacity of 1000 kW.

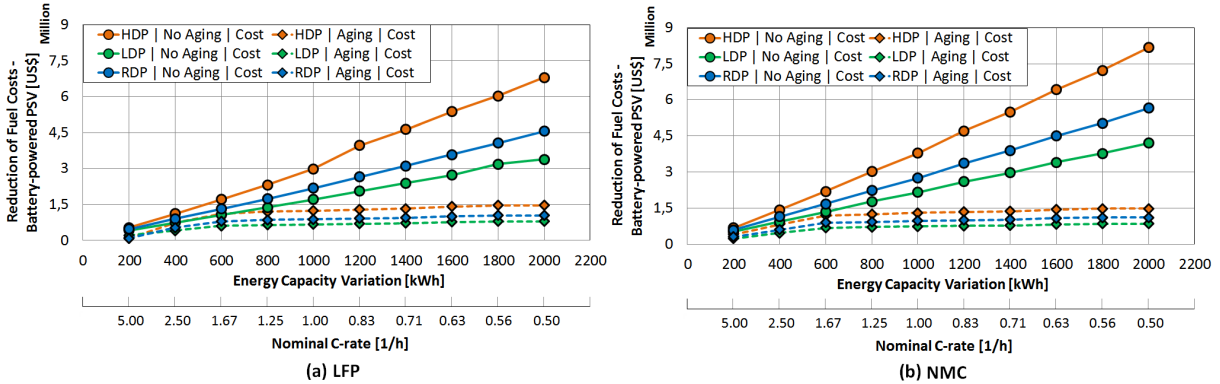


Source: Author.

As highlighted in Figure 49, the reduction of fuel costs (in US\$) to battery-powered PSV can be analyzed by three scenarios considering the Oil price from 2019 to 2049, where *HDP* is an abbreviation for High Diesel Price, *RDP* means Reference Diesel Price, and *LDP* abbreviates Low Diesel Price. Only cost cases were considered for these analyses. "No Aging" and "Aging" battery models are compared and the procedure consists of defining the fuel consumption per year for all capacities range. After that, the oil price yearly is multiplied by the fuel curve until battery End of Life (*EoL*) is reached. Figure 49 demonstrates the reduction of fuel cost provide by each battery capacity simulated for the vessel.

It is clear from Figure 49 (a) and (b) that there is a large discrepancy between "No Aging" and "Aging" cases. For instance, a capacity of 2000 kWh results in a decrease in fuel cost about US\$ 7.0 million when battery degradation is disregarded. However, the same energy capacity shows a decrease in fuel cost about US\$ 1.5 million for a battery evaluated by the degradation model.

Figure 49 – Reduction of Fuel Costs (in US\$) to Hybrid PSV Power Systems with battery included. Evaluation was based on Oil price scenarios from 2019 to 2049. *HDP* - High Diesel Price, *RDP* - Reference Diesel Price, and *LDP* - Low Diesel Price. Sensitivity analysis from 200 to 2000 kWh for battery cell technologies analysed. (a) *LFP* (ΔE capacity). (b) *NMC* (ΔE capacity). The Nominal C-rate (axis X) represents the fixed battery power capacity of 1000 kW.

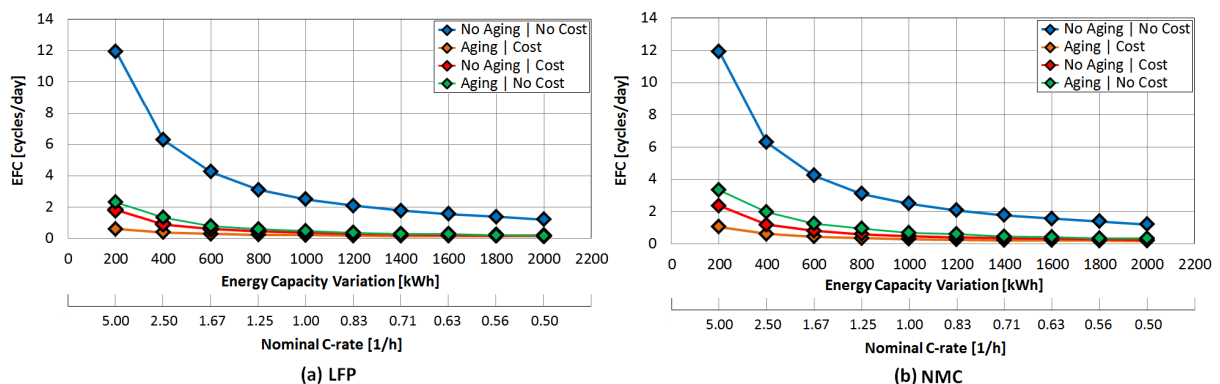


Source: Author.

5.3.5 Equivalent Full Cycle

Figure 50 compares the *EFC* – Equivalent Full Cycle – for each battery capacity evaluated. As detailed in Figure 50 (a) e (b) for *LFP* and *NMC* cells, respectively, there is a decreasing tendency of the *EFC* when battery packs are included in the system, but these cycles can be more prolonged.

Figure 50 – *EFC* - Equivalent Full Cycles for each battery capacity studied. Sensitivity analysis from 200 to 2000 kWh for battery cell technologies analysed. (a) *LFP* (ΔE capacity). (b) *NMC* (ΔE capacity). The Nominal C-rate (axis X) represents the fixed battery power capacity of 1000 kW.

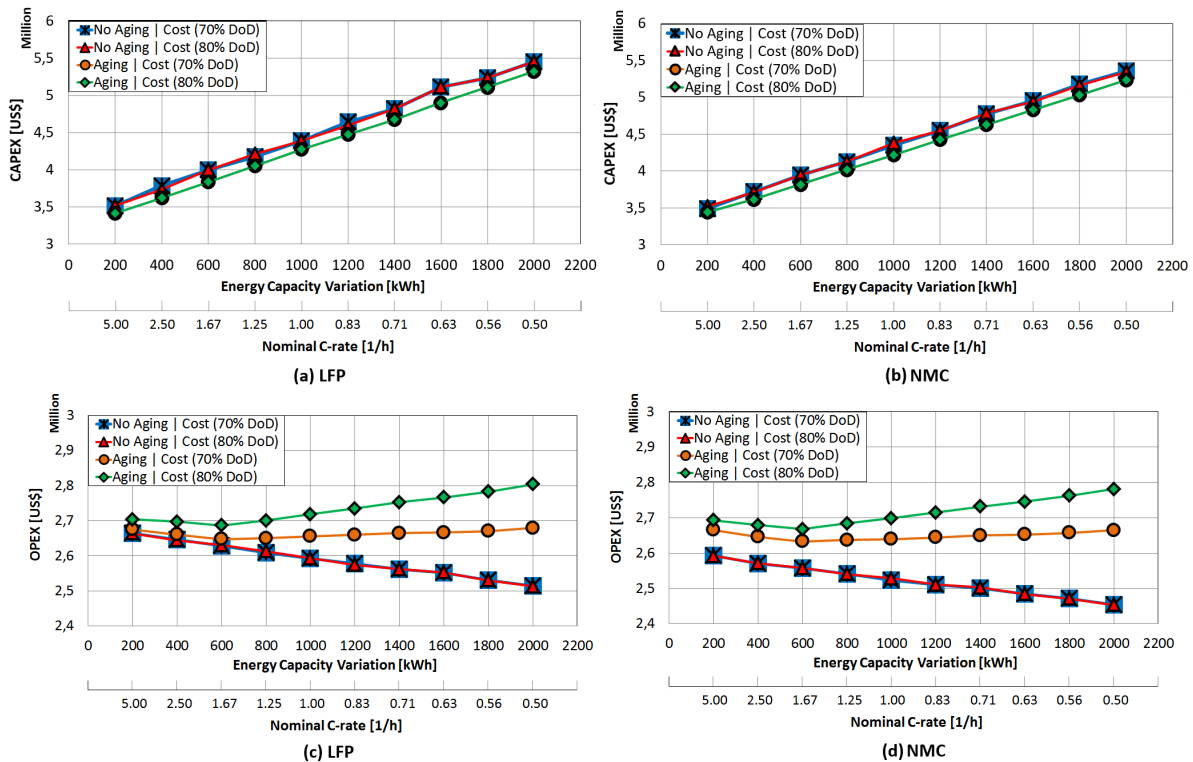


Source: Author.

5.3.6 Economic analysis – Hybrid PSV Power System

Figure 51 highlights the multiple design configurations of *PSV* with *LFP/NMC* battery cells varying *CAPEX* and *OPEX* scenarios. Note that *CAPEX* presents approximately the same curve for all cases simulated. If the battery capacity selected is technically the better, the lowest *CAPEX* option is mostly an adequate choice. However, this evaluation does not allow discovering if a battery should be operated with 70% or 80% *DoD*.

Figure 51 – Evaluation of *CAPEX* and *OPEX* for Hybrid *PSV* Power System. *CAPEX*. (a) *LFP* (ΔE capacity). (b) *NMC* (ΔE capacity). *OPEX*. (c) *LFP* (ΔE capacity). (d) *NMC* (ΔE capacity). The Nominal C-rate (axis X) represents the fixed battery power capacity of 1000 kW.



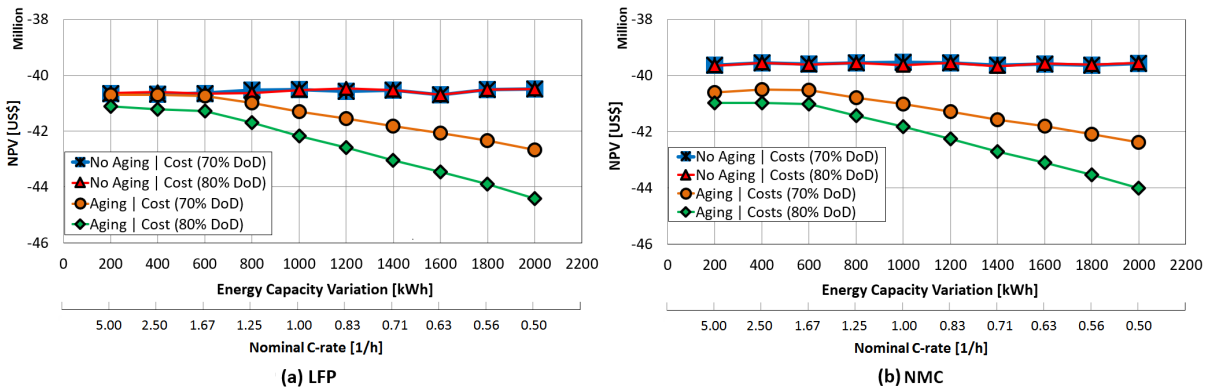
Source: Author.

The minimum system *CAPEX* can be associated with high *OPEX* when there is the high fuel consumption of Gen-sets or high maintenance requirements during the lifetime of the *PSV* operation. Figure 51 (c) and (d) shows a evaluation of *OPEX* costs for Hybrid *PSV* Power System considering "Aging" and "No Aging" battery cases. The former denotes an *OPEX* that is distinguished between values of Depth-of-discharge, whereby at 70% *DoD* presents the lower *OPEX*, and the latter demonstrates that the *OPEX* is identical to both *DoD* cases, but is evident that the *OPEX* is the best in comparison with battery "Aging" cases. Consequently, the Figure 51 (c) and (d) reveals the minimum *OPEX* related to the maximum battery energy capacity at 2000

kWh (*LFP* and *NMC* - No Aging). The lower *OPEX* for Aging simulation was obtained in 600 kWh (70% *DoD*).

OPEX may not necessarily be the best economic parameter for decision-makers to choose the optimum cost solution, mainly if the project of the storage system operations duration is different. This means that an evaluation of *CAPEX* and *OPEX* separately may hide the best solution. The results of *NPV* can be seen in Figure 52 and the curves demonstrate that the lowest costs during the lifetime are related to lower battery capacities. For instance, graph (a) for *LFP* cell illustrates the spend profile during a lifetime project of 30 years represented by its *NPV* from -US\$ 40.5 to -US\$ 41.2 million for a battery at 200 kWh. Conversely, for the battery energy capacity at 2000 kWh, the "No Aging" cases; "Aging" case of 70% *DoD*; and 80% *DoD* indicate a *NPV* about -US\$ 41.5 million, -US\$ 43.8 million, and -US\$ 44.5 million, respectively. Besides, the battery operating at 70% *DoD* is the cheapest solution in most of the cases simulated.

Figure 52 – Evaluation of *NPV* for Hybrid *PSV* system. Sensitivity analysis from 200 to 2000 kWh for battery cell technologies analysed. (a) *LFP* (ΔE capacity). (b) *NMC* (ΔE capacity). The Nominal C-rate (axis X) represents the fixed battery power capacity of 1000 kW.

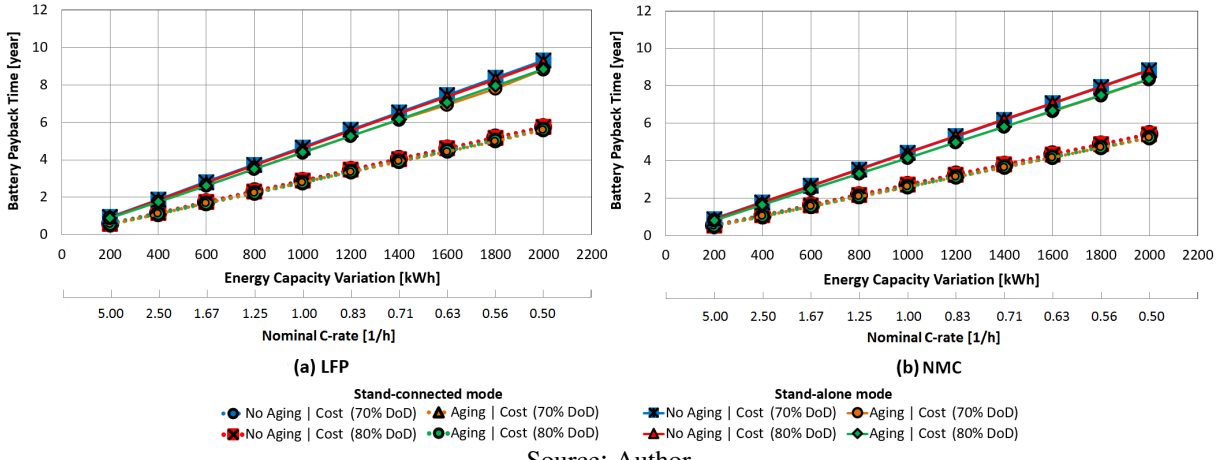


Source: Author.

Figure 53 indicate the theoretical *payback* calculation parameters for *PSV* powered by battery. These results consider the battery operating as stand-alone mode and also stand-connected to the grid when the vessel stays at Port.

Figures 53 (a) and (b) indicate a *payback* increase together with growing the number of battery packs and the higher capacity value allows to return on investment between 8 and 9 years when the battery is disconnected to grid. Nevertheless, when the same battery system is connected to the grid, the *payback* time decrease between 5 and 6 years. Regardless of *DoD* that the battery has been operating, the same results are achieved for both mode operation. The *payback* time for *NMC* battery system is slightly lower than the *LFP*.

Figure 53 – Theoretical *payback* calculation parameters for *PSV* powered by battery. Sensitivity analysis from 200 to 2000 kWh for battery cell technologies analysed. (a) *LFP* (ΔE capacity). (b) *NMC* (ΔE capacity). The Nominal C-rate (axis X) represents the fixed battery power capacity of 1000 kW.



Source: Author.

5.4 Impact of battery C-rate variation

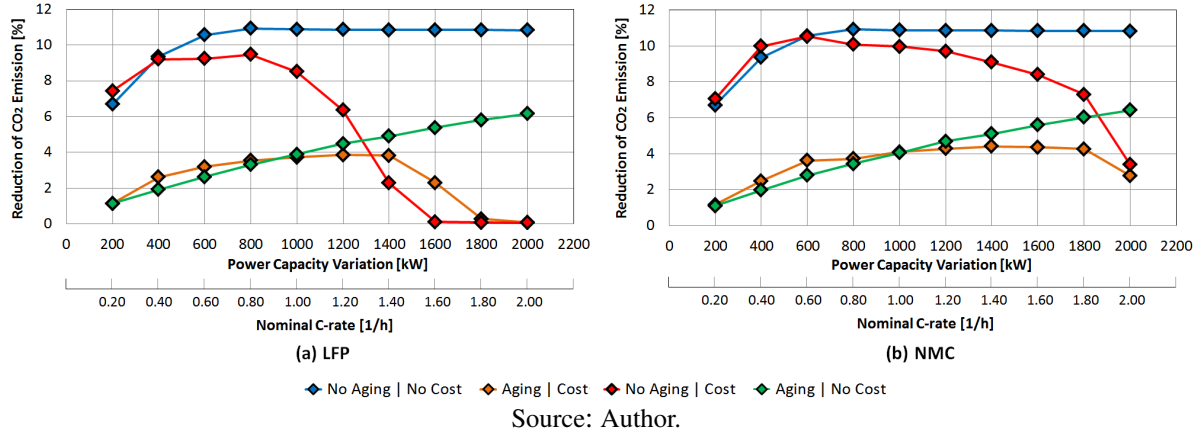
This section shows the sensitivity analysis of battery power capacity variation and its effects in the reduction of CO_2 emissions, battery expected life, fuel consumption, savings fuel costs, *EFC*, and economic analysis of a Hybrid *PSV* Power Systems. In operational terms of battery, this power alteration represents the C-rate variation.

5.4.1 Pollutant emission estimation

Figure 54 illustrates the reduction of CO_2 emissions per year for sensitivity analysis of battery capacities from 200 kWh to 2000 kWh, and from 200 kW to 2000 kW. The graphs (a) and (b) show the results for *LFP* and *NMC* cells, respectively. The power capacity variation is evaluated by an energy capacity of 1000 kWh and it can be represented by nominal C-rate (axis X). These same sequences for the presentation of results can be seen in most Figures in the next items.

As can be seen in Figure 54 (a), the rate of CO_2 emissions decreases when power capacity is increased for "No Aging | Cost" and "Aging | Cost" cases. However, the rate of emissions is grown for "Aging | No Cost" and is stabilized around 11% for "No Aging | No Cost". In practical terms, these curves indicate that when the cost analysis is considered on simulation, the HOMER software opts to preserve the battery during its lifetime. As the power capacity grows, the results

Figure 54 – Reduction of CO_2 to Hybrid PSV Power System with battery included. Sensitivity analysis from 200 to 2000 kW for battery cell technologies analysed. (a) LFP (ΔP capacity). (b) NMC (ΔP capacity). The Nominal C-rate (axis X) represents the fixed battery energy capacity of 1000 kWh.



Source: Author.

of optimization reveal that the battery does not use in the Hybrid Ship Power System due to its high cost.

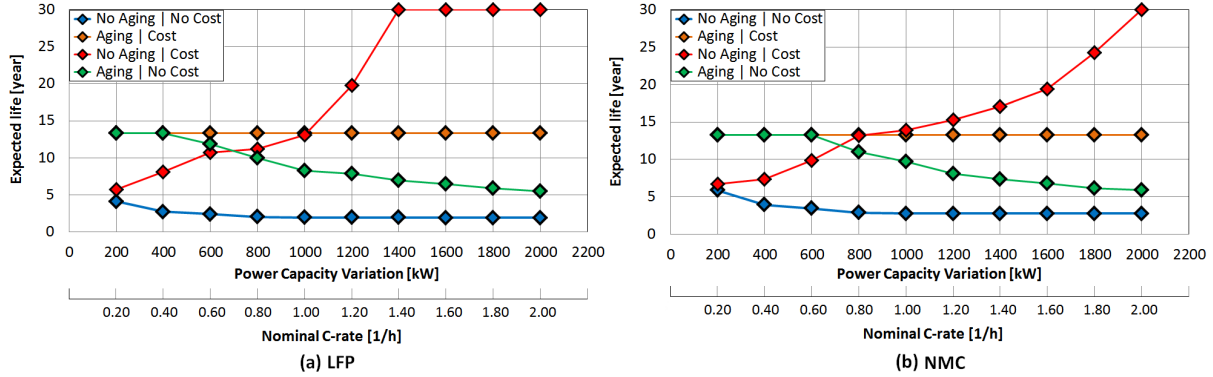
As detailed in Figure 54 (b), the rate of CO_2 emissions caused by NMC battery present a similar tendency for all cases in comparison with LFP cells, except for the "No Aging | Cost - red points" and "Aging | Cost - orange points" cases which shows a better performance than a previous cell.

The results from such CO_2 emissions analyses should be treated within considerable caution. Each point shown in Figure 54 in % per year is associated with a battery expected life (in years). This can be only seen when absolute numbers of parameters are calculated such as the fuel savings of battery-powered PSV that will highlight in the item 5.4.3.

5.4.2 Battery expected life

Figure 55 (a) shows the expected life in function of power capacity variation. "Aging | Cost" case indicates that expected life is constant for all power range. The similar performance can be seen in Figure 55 (b) for NMC battery cell. The better battery lifespan is observed in "No Aging | Cost", mainly for power capacity upper of 1200 kW (or C-rate higher than 1.2C).

Figure 55 – Battery Expected life (years) to Hybrid PSV Power System with battery included. Sensitivity analysis from 200 to 2000 kW for battery cell technologies analysed. (a) *LFP* (ΔP capacity). (b) *NMC* (ΔP capacity). The Nominal C-rate (axis X) represents the fixed battery energy capacity of 1000 kWh.

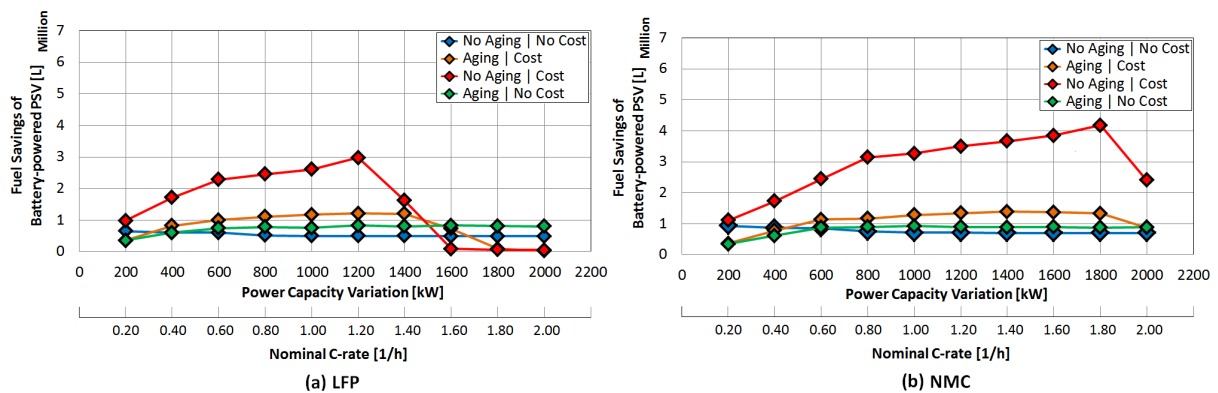


Source: Author.

5.4.3 Reduction of fuel consumption

Figure 56 shows Fuel Savings (in millions of Liters) of Battery-powered Hybrid PSV Power Systems. The "No Aging | Cost" case has the best performance in terms of fuel economy. The *LFP* and *NMC* cells present similar tendency except for observation of graphs (a) and (b) that indicate a decrease of fuel savings to high C-rates (from 1.40 to 2 C for *LFP* cell, and 2C for *NMC* cell for all case that involves "Cost"). In most of the power capacities analyzed, the "No Aging | No Cost" case presents low fuel savings. However, this low economy allows this battery model to provide the best performance in terms of reduction of CO_2 emissions for PSV.

Figure 56 – Fuel Savings (Millions of Liters) of Battery-powered Hybrid PSV Power Systems. Sensitivity analysis from 200 to 2000 kW for battery cell technologies analysed. (a) *LFP* (ΔP capacity). (b) *NMC* (ΔP capacity). The Nominal C-rate (axis X) represents the fixed battery energy capacity of 1000 kWh.



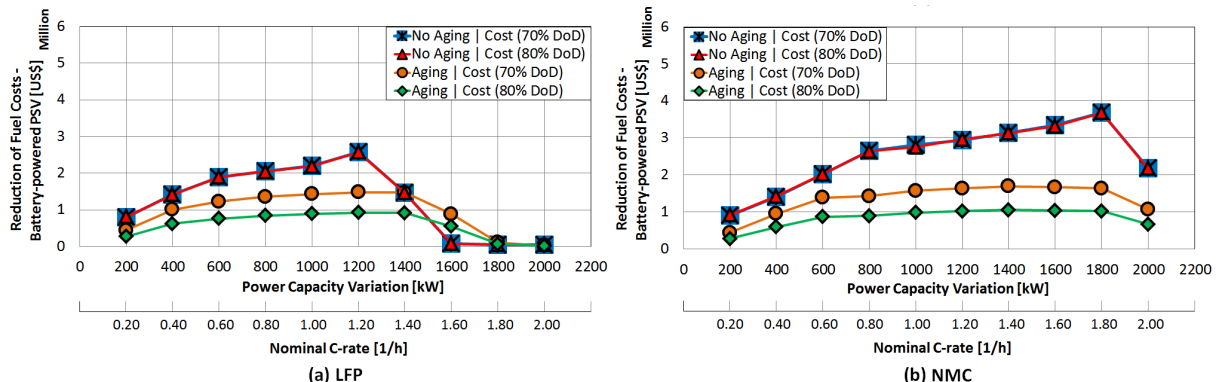
Source: Author.

5.4.4 Fuel costs savings

Figure 57 pinpoints the reduction of Fuel Costs (in US\$) to Hybrid PSV Power Systems with battery included, and its operating performance is compared to 70% and 80% *DoD* (Depth-of-discharge). The curves are distinguished between "Aging" and "No Aging" cases. The cost was included in all analyses. The results demonstrate that 70% *DoD* presents the best performance for "Aging" cases, but "No Aging" ones present the same reduction of fuel Costs for all range of capacities. *LFP* and *NMC* cells can be differentiated by the performance from 200 to 600 kWh, where the *LFP* indicates identical fuel economy among 70%, 80% (No Aging), and 70% *DoD* (Aging). *NMC* shows a higher discrepancy among "Aging" and "No Aging" cases. For instance, the 1800 kW case presents a large discrepancy between "No Aging" and "Aging" cases that can reach about 4.5 times.

Figure 57 – Reduction of Fuel Costs (in US\$) to Hybrid PSV Power Systems with battery included.

Sensitivity analysis from 200 to 2000 kW for battery cell technologies analysed. (a) *LFP* (ΔP capacity). (b) *NMC* (ΔP capacity). The Nominal C-rate (axis X) represents the fixed battery energy capacity of 1000 kWh.

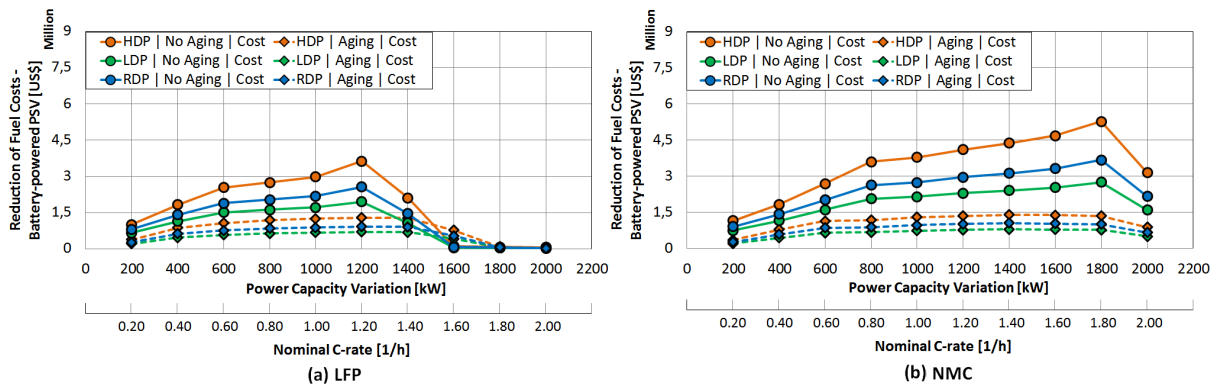


Source: Author.

The reduction of fuel Costs (in US\$) to battery-powered PSV can be analyzed by three scenarios considering the Oil price from 2019 to 2049, where *HDP* is an abbreviation for High Diesel Price, *RDP* means Reference Diesel Price, and *LDP* abbreviates Low Diesel Price. Only cost cases were considered for these analyses. "No Aging" and "Aging" battery models are compared and the procedure consists of defining the fuel consumption per year for all capacities range. After that, the oil price yearly is multiplied by the fuel curve until battery *EoL* is reached. Figure 58 demonstrates the reduction of fuel cost provide by each battery capacity simulated for the vessel.

Figure 58 (a) indicates the best results at 1200 kW or C-rate at 1.2C. Above this capacity, the battery reduces its performance in terms of fuel economy. Besides, Figure 58 (b) details a decrease of battery performance when it operates with C-rate at 2C (1000 kWh | 2000 kW). Thus, the best option to battery capacity is of 1000 kWh | 1800 kW.

Figure 58 – Reduction of Fuel Costs (in US\$) to Hybrid PSV Power Systems with battery included. Evaluation was based on Oil price scenarios from 2019 to 2049. *HDP* - High Diesel Price, *RDP* - Reference Diesel Price, and *LDP* - Low Diesel Price. Sensitivity analysis from 200 to 2000 kW for battery cell technologies analysed. (a) *LFP* (ΔP capacity). (b) *NMC* (ΔP capacity). The Nominal C-rate (axis X) represents the fixed battery energy capacity of 1000 kWh.

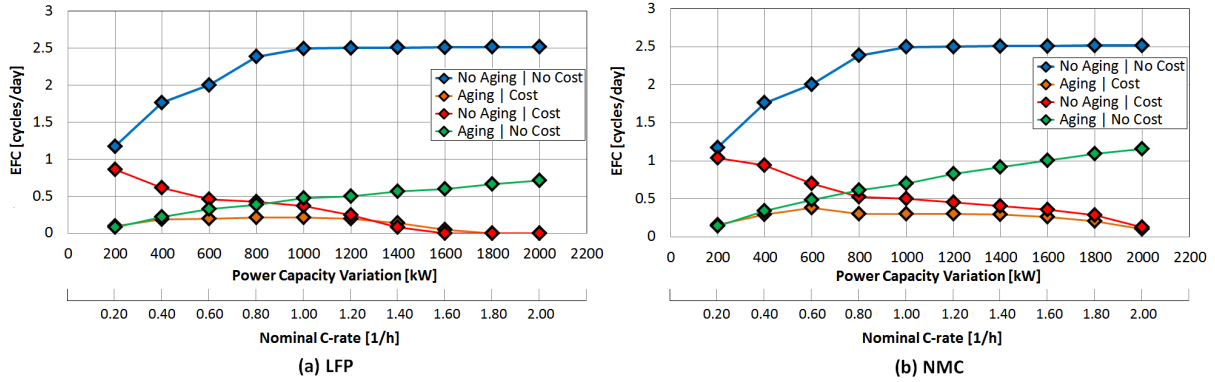


Source: Author.

5.4.5 Equivalent Full Cycle

Figure 59 compares the *EFC* - Equivalent Full Cycle - for each battery capacity evaluated. As detailed in graph (a) e (b), the *EFC* tends to grow when the battery is operated to high C-rates for "No Cost" cases, whereas the same behavior is not observed when the battery is preserved during the operation on the Ship due to high operational costs ("Cost" cases).

Figure 59 – *EFC* - Equivalent Full Cycles for each battery capacity studied. Sensitivity analysis from 200 to 2000 kW for battery cell technologies analysed. (a) *LFP* (ΔP capacity). (b) *NMC* (ΔP capacity). The Nominal C-rate (axis X) represents the fixed battery energy capacity of 1000 kWh.



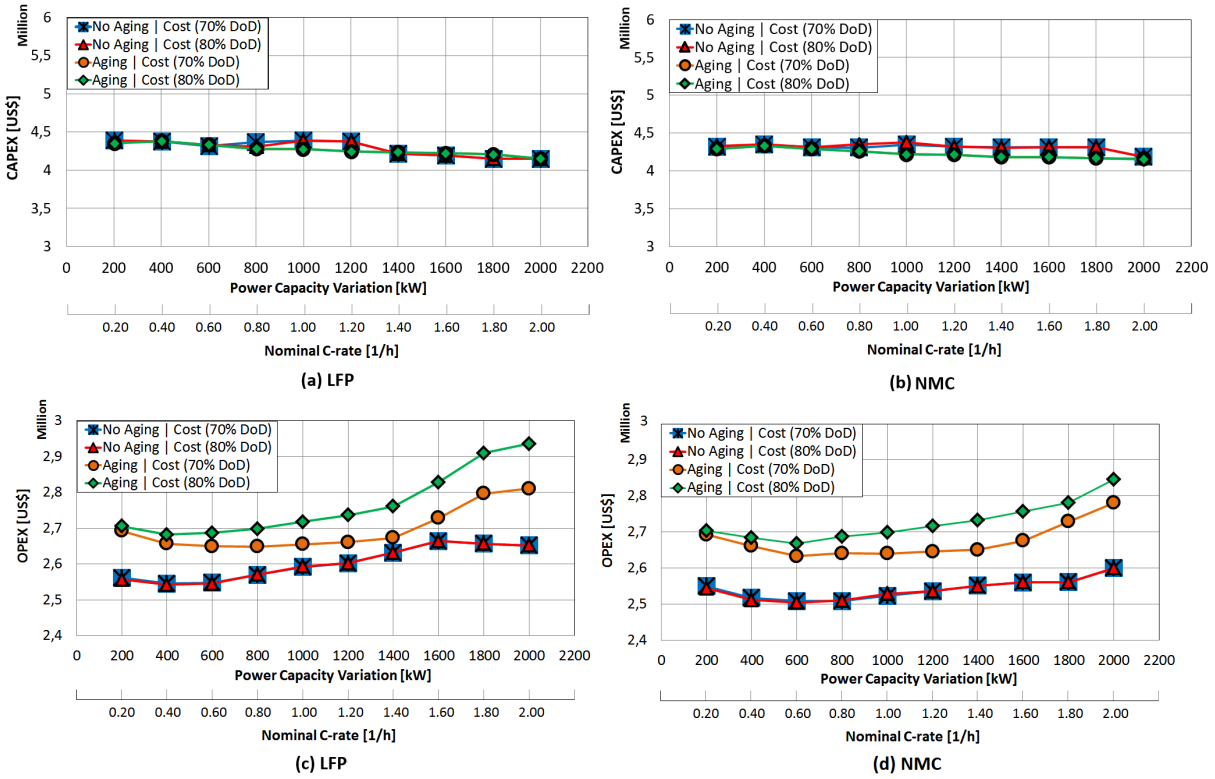
Source: Author.

5.4.6 Economic analysis – Hybrid PSV Power System

Figure 60 compares the multiple design configurations of *PSV* with *LFP/NMC* battery cells varying *CAPEX* and *OPEX* scenarios. The discrepancy between *CAPEX* values from the graph and values from the Base Case are battery initial cost, power converter, and power control system. If the battery capacity selected is technically the better, the lowest *CAPEX* option is mostly an adequate choice. However, this evaluation does not allow discovering if a battery should be operated with 70% or 80% *DoD*. It is clear from Figures 60 (a) and (b) that when battery C-rate is varied, the *PSV* system *CAPEX* is similar for all cases analyzed and the data trend to stay between 4 and 4.5 million dollars, considering the energy capacity as constant for this sensitivity analysis.

The minimum system *CAPEX* can be associated with high *OPEX* when there is a high fuel consumption of Gen-sets or high maintenance requirements during the lifetime of the *PSV* operation. Figure 60 (c) and (d) present a evaluation of *OPEX* costs for Hybrid *PSV* Power System considering "Aging" and "No Aging" battery cases. The former denotes an *OPEX* that is distinguished between values of Depth-of-discharge, whereby at 70% *DoD* presents the lower *OPEX*, and the latter demonstrates that the *OPEX* is identical to both *DoD* cases, but is evident that the *OPEX* is the best in comparison with battery "Aging" cases. Consequently, the Figure 60 (c) and (d) reveals the minimum *OPEX* linked to the maximum battery power capacity at 2000 kWh (*LFP* and *NMC* - No Aging). The lower *OPEX* for Aging simulation was obtained in 600 kW (70% *DoD*). Figure 60 (d) indicate that lower *OPEX* is achieved to C-rates lower than 1C

Figure 60 – Evaluation of *CAPEX* and *OPEX* for Hybrid PSV Power System. *CAPEX*. (a) *LFP* (ΔP capacity). (b) *NMC* (ΔP capacity). *OPEX*. (c) *LFP* (ΔP capacity). (d) *NMC* (ΔP capacity). The Nominal C-rate (axis X) represents the fixed battery energy capacity of 1000 kWh.

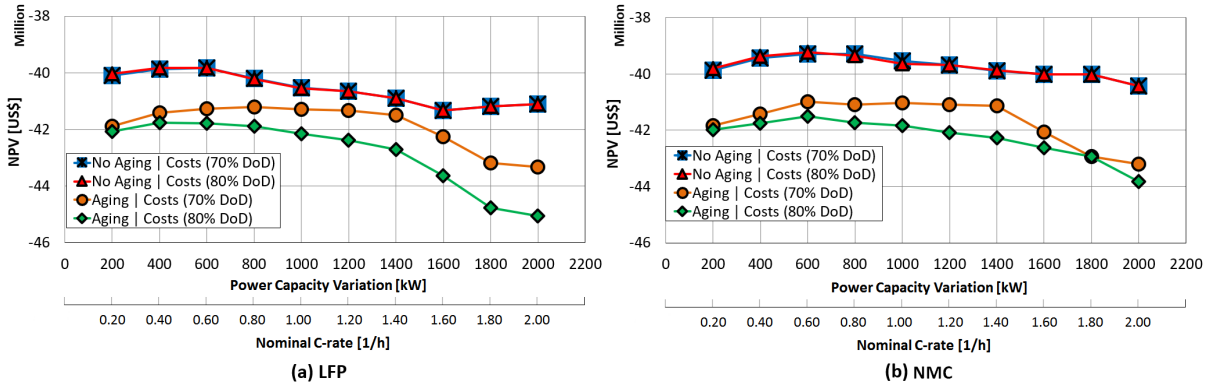


Source: Author.

for "No Aging" cases. However, the "Aging" cases show the lower *OPEX* is obtained to range from 400 to 1400 kW (70% *DoD*) for *LFP* cell – graph (c) and (d). To *NMC* battery cell, the best performance is achieved to range from 600 and 1400 kW.

OPEX may not necessarily be the best economic parameter for decision-makers to choose the optimum cost solution, mainly if the project storage system operations duration are different. This means that an evaluation of *CAPEX* and *OPEX* separately may hide the best solution. The results of *NPV* can be seen in Figure 61 and most curves demonstrate that the lowest during life-cycle costs are related to lower battery capacities. For instance, the graph (a) for *LFP* cell pinpoints the spend profile during a lifetime project of 30 years represented by its *NPV* from -US\$ 40.0 to -US\$ 42.0 million for a battery at 200 kW. Conversely, for the battery power capacity at 2000 kW, the "No Aging" cases; "Aging" case of 70% *DoD*; and 80% *DoD* indicate a *NPV* about -US\$ 41.5 million, -US\$ 43.2 million, and -US\$ 45.0 million, respectively. Besides, the battery operating at 70% *DoD* is the cheapest solution in most of the cases simulated ("Aging" cases).

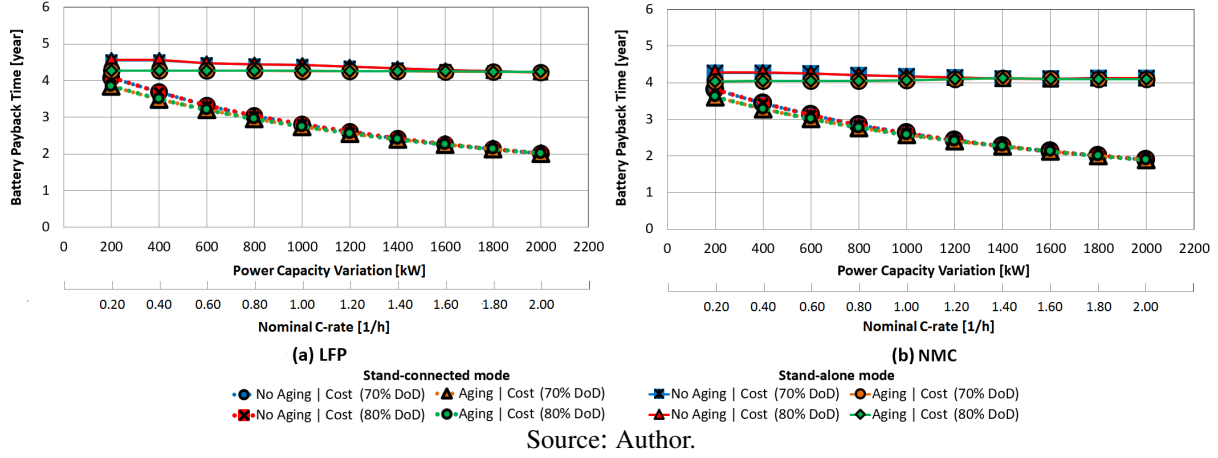
Figure 61 – Evaluation of *NPV* for Hybrid *PSV* system. Sensitivity analysis from 200 to 2000 kW for battery cell technologies analysed. (a) *LFP* (ΔP capacity). (b) *NMC* (ΔP capacity). The Nominal C-rate (axis X) represents the fixed battery energy capacity of 1000 kWh.



Source: Author.

Figure 62 illustrates the theoretical *payback* calculation parameters for *PSV* powered by battery. These results consider the battery operating as stand-alone mode and also stand-connected to the grid when the vessel stays at Port. Figures 62 (a) and (b) show a *payback* decrease together with power capacity and the higher value allow to battery return on investment between 4.5 and 5.5 years. Regardless of *DoD* that the battery has been operating, the same results are achieved for each mode operation. The "No Aging" cases present the *payback* time slightly larger than "Aging" cases from 200 to 1400 kW and from 200 to 1200 kW for batteries *LFP* and *NMC*, respectively. After that, all cases achieve an equivalent performance. Note that it is more favourable operate the battery in the stand-connected to the grid mode in terms of *payback* time. However, this condition is achievable when the Shore connection electricity cost is more attractive than fuel cost due to Ship operation.

Figure 62 – Theoretical *payback* calculation parameters for PSV powered by battery. Sensitivity analysis from 200 to 2000 kW for battery cell technologies analysed. (a) LFP (ΔP capacity). (b) NMC (ΔP capacity). The Nominal C-rate (axis X) represents the fixed battery energy capacity of 1000 kWh.



5.5 Recommendations for battery operation in the hybrid PSV power system

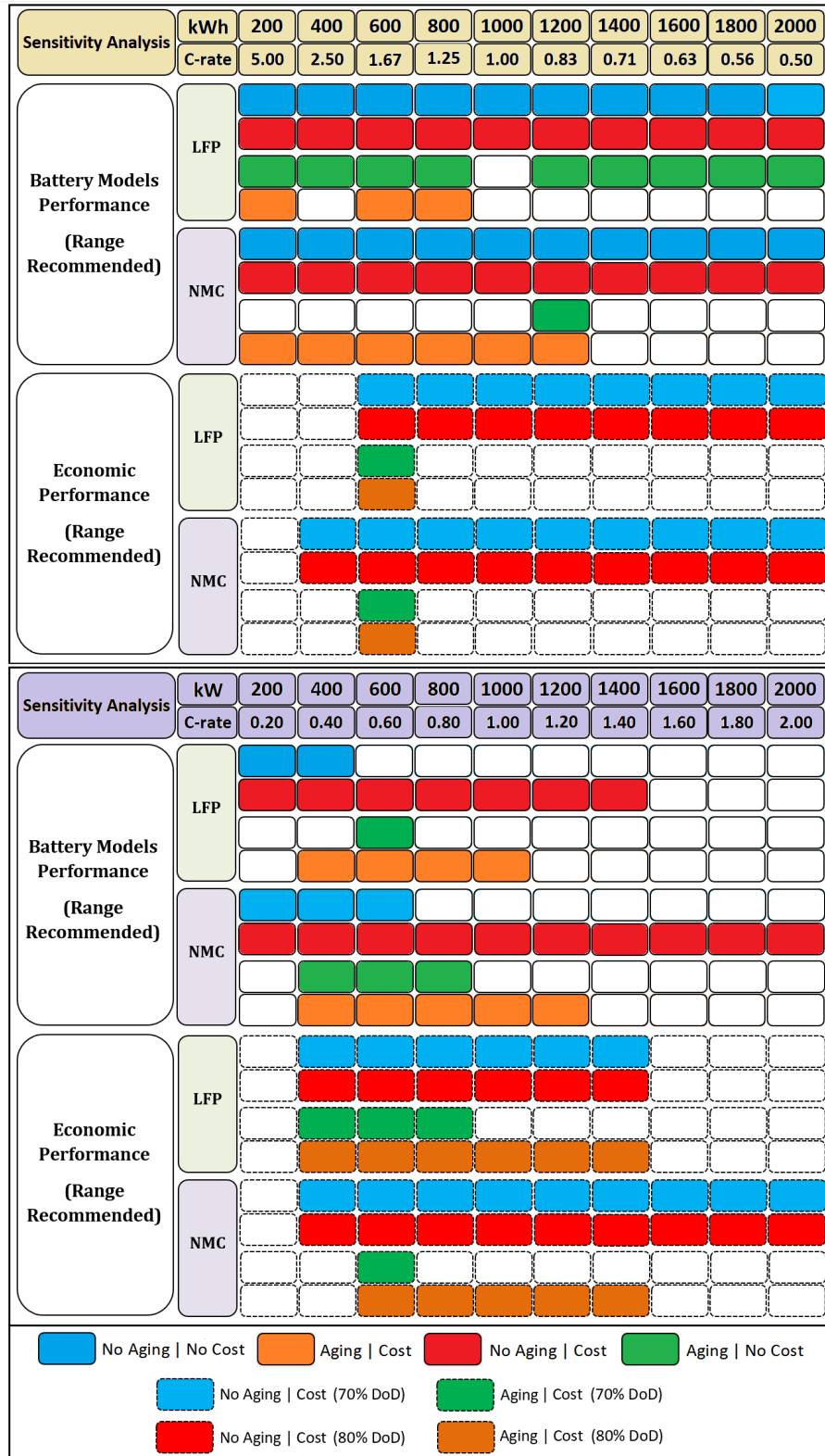
Based on the results previously presented, this work proposes recommendations to battery capacity operation range that attend the most of battery indicators simulated. The procedure is divided into four-step and each of which consists of verifying the battery model's performance and economic performance considering the impact of energy variation and the effect of battery power capacity variation (or the battery operating at different C-rates). The parameters should be compared with some technical restrictions found in the literature and others adopted in this work. The battery model's performance range is analyzed through a reduction of CO_2 emission, expected life, reduction of fuel consumption, and EFC , whereas the economic performance range is evaluated by the reduction of fuel costs, $CAPEX$, $OPEX$, and NPV . A general recommendation is shown at the end of each analysis and the cases studied (Table 6) in the previous sections are separately presented.

The economical restrictions consist of a search for energy and power intervals associated with lower costs. Conversely, the technical restrictions for the battery model's performance range can be found in the literature reported in the previous Chapters of this Master's Thesis. The reduction of CO_2 emission is restricted to values from 2% to 45% per year [87]. The battery expected life is acceptable for higher than 10 years and 3,000 cycles of life [57]. For EFC is adopted a value to upper the 0.50 cycles per day, and the range to fuel economy (in US\$) is chosen to intervals that exceed the battery's initial cost for each capacity analyzed.

The results of recommendations for battery operation are detailed from Figure 65 to Figure 68 (see Annex A on page 131). Figure 63 summarizes the best results of battery capacity range for *LFP* and *NMC* cells considering the battery model's performance and its economic viability. Note that battery cells studied present different performances in most cases. The economic criteria tend to select the lower battery capacity range. However, technical battery performance tends to present higher battery capacity ranges. The integration among the indicators analyzed is made after the application of restriction for each parameter. The battery capacity ranges that attend the restrictions and the intervals repeated are selected. Annex A presents the results at the end of each Figure and this process is repeated again two times to obtain the Figure 63 and Figure 64.

Clearly, the batteries simulated to "No Aging" cases can operate in the wide energy/power range. Besides, Figure 63 reveals that there is no difference between battery performance for 70 and 80% *DoD* when the battery degradation is disregarded except for the *NMC* battery model's performance (power variation cases). According to economic performance, this discrepancy between the *DoD* values is observed only in the "Aging" cases, where the battery operating with *DoD* at 70% present the lower energy/power ranges. In addition, the battery *NMC* system can be operated to a larger interval of energy/power capacities than the *LFP* technology, mainly when the economic indicators are considered.

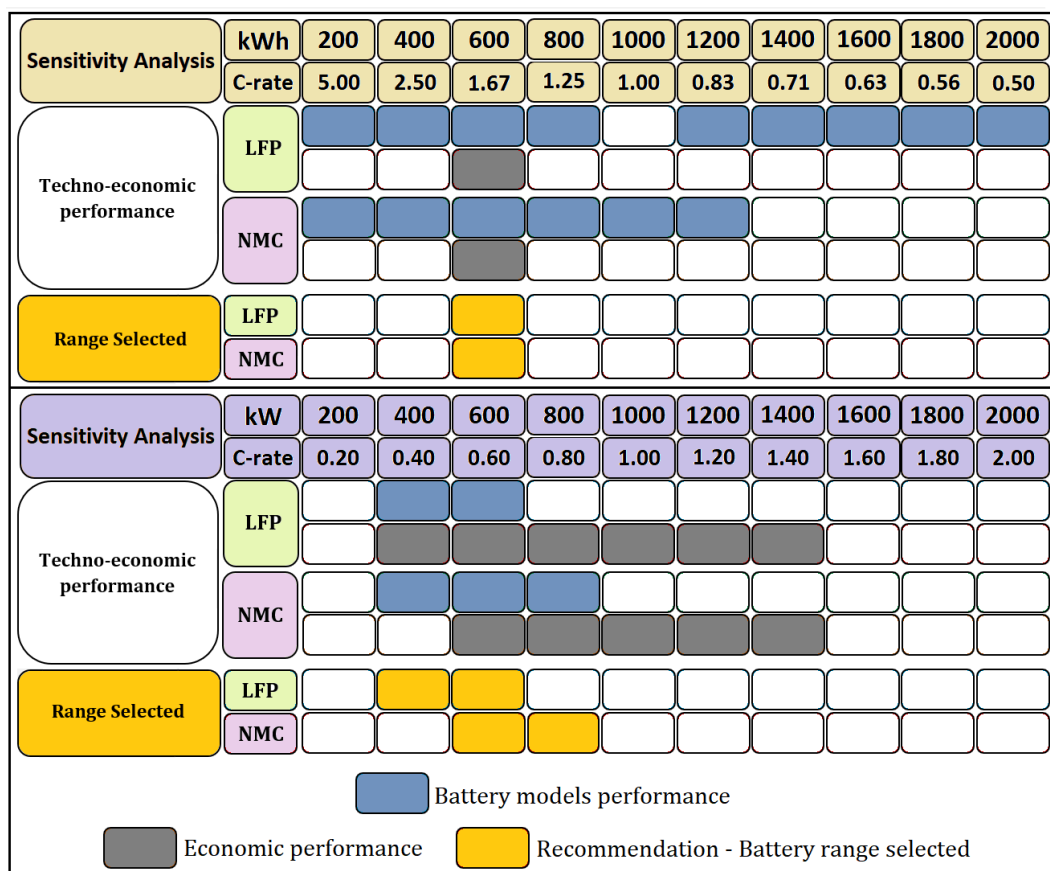
Figure 63 – Integrated solution for the battery models performance and economic viability. Part 1 – Range recommended for battery energy capacity variation from 200 to 2000 kWh (Sensitivity analysis). Nominal C-rate represents the fixed battery power capacity of 1000 kW. Part 2 – Similar to the Sensitivity analysis of battery power capacity variation.



Source: Author.

The results of the integrated solution of battery cases are demonstrated in Figure 64. *LFP* and *NMC* battery systems operate more efficiently at 600 kWh (1000kW). At this point, the *OPEX* and *NPV* are minimum for most cases analyzed. The same procedure can be applied to the battery power capacity variation as can be observed in the second part of Figure 64. Range acceptable of the *LFP* battery system is contained within the interval between the 400 and 600 kW (correspondingly, the C-rate from 0.40 to 0.60C), and the C-rate interval between 0.60 and 0.80C (from 600 to 800 kW) for *NMC* battery.

Figure 64 – Recommendation – Range selected integrating all cases simulated. The Nominal C-rate represents the fixed battery power capacity at 1000 kW or fixed battery energy capacity at 1000 kWh, depending on the sensitivity analysis selected.



Source: Author.

5.6 Synthesis

This Chapter showed the simulation of a typical *PSV* Power System including Main/Auxiliary Gen-sets, Power converter, and Lithium-ion batteries (*LFP* and *NMC* cells). The sensitivity analysis was divided among eight cases considering simplified and advanced battery models, and some cases involved the costs together with the evaluation of *DoD* change.

Simulation analyses show the impact on fuel consumption and CO_2 emissions of different characteristics such as rated battery power and rated battery energy capacity, *DoD*, C-rate, and type of battery cells chosen. *NMC* cells presented the best performance of most analyzed parameters.

Sensitivity analysis clearly proved that there is a difference between the battery models used in HOMER software. The battery model that does not consider the aging processes presents a technical performance better than the model simulated for degradation. A similar evaluation demonstrates that the battery model that does not consider economic aspects is better technically than the battery with an economic model. A battery model can be considered better technically than other models if the parameters such as emissions, fuel consumption, expected life, and *EFC* present better performance. In fact, the price of battery systems and the aging processes are disregarded in the simulation of the "No Aging | No Cost" case and it implies the maximum battery system performance. Therefore, this case can be used as a maximum performance reference model, and its application is not recommended to evaluate technically and economically the battery system for a Ship Power System based on the real conditions.

When the power capacity (C-rate variation) is evaluated, the HOMER tends to preserve the battery that is not operated on the Ship, mainly when high battery power capacities are included in *PSV*. Probably, when the battery capital cost is growing (by the increase of packs in the storage system), the total cost function is impacted and the optimization opts to operate the Auxiliary Gen-sets with lower operational costs. Similarly, the increase of power battery capacity induces the growth of operational costs of the *PSV* Power System and the battery is also not used in the operation.

Moreover, it more advantageous to operate the batteries with a Depth-of-discharge of 70% than 80% if we consider expected life, reduction of fuel costs, *OPEX*, and *NPV*. *CAPEX* presented the same value for all cases studied. This parameter is not adequate to compare the different battery models studied. The point of maximum *CAPEX* is achieved when a high battery

capacity (2000 kWh) is included in the system. However, this point does not necessarily reflect on the reduction of the vessel's operational costs (*OPEX*).

The *NPV* integrates the *CAPEX* and *OPEX* of each Ship equipment. When the *NPV* is analyzed, the battery with high values of energy/power capacity results in a decrease of *NPV* (value more negative). The same battery capacity can provide a reduction of fuel cost in US\$ 7 million if degradation processes are disregarded, or result in an economy of US\$ 1.5 million when the aging is considered.

Payback varies in direct proportion with energy capacity and inversely proportional to the power variation (or C-rate). The battery *payback* time is approximately 9 years for an energy capacity of 2000 kWh if it is operated only in the stand-alone mode. The same capacity presents the *payback* time of 6 years if the battery to be connected to the grid (when the Ship stays in the Port).

Finally, this work estimated the battery capacities operation acceptable range that attends the most of battery models studied. *LFP* and *NMC* cells were estimated a battery capacity of 600 kWh (1000 kW). However, for the battery at 1000 kWh, the C-rate was recommended to the range from 0.40 to 0.60C (from 400 to 600 kW) for the *LFP* battery system and to the range from 0.60 to 0.80C (from 600 to 800 kW) for *NMC* cells.

Chapter 6

Final Remarks

This Master's Thesis presented the techno-economic evaluation of Typical *PSV* Power Systems powered by the battery system. Revisiting the previous Chapters, the main battery technologies characteristics were shown in Chapter 2. *PSV* Power Systems and their equipment specifications were presented in Chapter 3, while the economic indicators applied on Hybrid vessels and their individual components were detailed in Chapter 4. Results and discussions were outlined in Chapter 5 and it started showing the details of the cases related to battery models (Simplified and Advanced) sized as simulator input data. Section 5.1 showed the results of the Base Case simulated on the HOMER Energy Software. Section 5.2 demonstrated the impact of battery energy and power capacities in several indicators of Ship operation such as reduction of CO_2 emissions, battery expected life, fuel consumption, *EFC*, *CAPEX*, *OPEX*, *NPV*, and *payback*. In sections 5.3 and 5.4, the same procedure of the previous section was adopted, however, these sections considered the effect of degradation processes together with economic indicators. Finally, section 5.5 proposed the recommendations for range selection considering the battery operation in the *PSV*. This recommendation was based on the results of the previous sections.

This work contributed to the detailed simulation of the *LFP* and *NMC* cells through the technical dimensioning of battery and its economic estimate, considering also the *DoD* curves, *SoC*, round-trip efficiency, C-rates, and input data for the HOMER related to Generator-sets, power converter, controller, and *PSV*'s operational profile. Some combinations of the two battery models were presented and the results demonstrated a high discrepancy among cases studied, considering the same battery capacity.

The Lithium-ion *NMC* battery system presented the techno-economic performance slightly higher than the *LFP* cell due to the superior number of cycles and lower cost. The battery model that does not consider the aging processes presents a technical performance better than the model simulated for degradation. This means that there is no capacity fade for the Simplified model and during its lifetime, the total amount of energy expected to store and deliver (Energy-throughput or Turnovers) is used by the model. A similar evaluation demonstrates that the battery model that does not consider economic aspects is technically better in terms of the reduction of emissions and *EFC* than the battery with an economic model. Actually, "No Cost" cases disregard the price of battery systems and, consequently, the best energy storage system performance is obtained. Besides, it is more advantageous to operate the batteries with depth-of-discharge of 70% than 80% if we consider expected life, reduction of fuel costs, *OPEX*, and *NPV*. The battery *payback* was considered attractive when the storage system operated connected in the grid during harbor operations. Moreover, this work estimated the acceptable range of energy capacity and C-rate that attends most of the indicators to battery models studied.

"No Aging | No Cost" case is indicated for the applications that require investigation about the maximum technical potential of the battery system. This case can be used as a maximum performance reference model. Nevertheless, the "Aging | Cost" case is adequate to evaluate technically and economically the battery system for the Ship Power System specific. As a consequence, this case can be used to make decisions most closely reflected the real vessel operating conditions, considering battery cell degradation and equipment costs. The battery operational costs and its initial costs should be evaluated with data closest possible to the reality because the optimization process may opt to preserve the battery system during the operation to minimize the objective function (total costs) if the energy storage is economically oversized.

Two intermediate cases can be considered in the simulations depending on the level of detail obtained data. For instance, the "Aging | No Cost" case can be applied to the computational simulations where the evaluation in terms of battery cells is relevant (the best alternative between *LFP* and *NMC* cells to attend the vessel project requirements). Several battery cell technologies can be chosen by this case such as presented in Chapter 2. Thus, the "No Aging | Cost" case is appropriate to the needs of economic assessment integrated with the maximum technical potential of the battery system.

The understanding of the selection process of battery system characteristic parameters has been further improved considering the integrated solution for all previous simulated cases. On the development of the integrated method used to propose recommendations for battery

system operating on the vessel, the simulation demonstrated the result of the battery capacity at 600 kWh (1000 kW) for both cell technologies. However, for the battery at 1000 kWh, the C-rate was recommended to the range from 0.40 to 0.60C (from 400 to 600 kW) for the *LFP* battery system and to the range from 0.60 to 0.80C (from 600 to 800 kW) for *NMC* cell.

Future works can be directed to perform a similar analysis to the battery models taken into account the impact of temperature, depth-of-discharge, and other battery cell technologies. It should also be assessed the influence of the temperature in the combined model that includes calendar aging and cycle aging. Furthermore, the optimization method can be entail refining using another simulator integrated to HOMER, because it is not clear what the optimization processes it is based on. Finally, the Generator-sets and other Ship's equipment models can be sized with up-to-date data that take into consideration the more efficient fuels, and equipment that provide the reduction of emissions and fuel consumption as LNG, fuel cells, PV systems, and modern converters.

6.1 *List of Publications*

- **Conference Contribution (Lead Author)**

Vale, R. J., Peralta, C. O., Vieira, G. T. T., Salles, M. B. C., and Carmo, B. S. (2018, October). Assessment of CO₂ Emissions on Platform Supply Vessels for Distinct Battery Dispatch. In 2018 7th International Conference on Renewable Energy Research and Applications (ICRERA) (pp. 1287-1291). IEEE.

- **Conference Contribution (Co-Author)**

Nishimoto, K., Sampaio, C. M., Vale, R. J., and Ruggeri, F. (2019, September). Numerical Simulation of Hybrid Platform Supply Vessel (PSV) Fuel Consumption for the Pre-Salt Layer in Brazil. In Practical Design of Ships and Other Floating Structures (pp. 478-497). Springer, Singapore.

- **Peer-Reviewed Journal Contributions (Co-Author)**

Peralta P, C. O., Vieira, G. T., Meunier, S., Vale, R. J., Salles, M. B., and Carmo, B. S. (2019). Evaluation of the CO₂ emissions reduction potential of Li-ion batteries in ship power systems. *Energies*, 12(3), 375.

Bibliography

- [1] BENNABI, N. *et al.* Hybrid propulsion systems for small ships: Context and challenges. In: IEEE. **2016 XXII International Conference on Electrical Machines (ICEM)**. [S.l.], 2016. p. 2948–2954. Cited 2 time(s) on page 25 and 30.
- [2] MUTARRAF, M. *et al.* Energy storage systems for shipboard microgrids—a review. **Energies**, Multidisciplinary Digital Publishing Institute, v. 11, no. 12, p. 3492, 2018. Cited 4 time(s) on page 25, 26, 27, and 57.
- [3] OVRUM, E.; BERGH, T. Modelling lithium-ion battery hybrid ship crane operation. **Applied Energy**, Elsevier, v. 152, p. 162–172, 2015. Cited 11 time(s) on page 25, 26, 29, 30, 39, 40, 48, 59, 65, 67, and 69.
- [4] GL, D. **MARITIME FORECAST TO 2050—Energy Transition Outlook 2020**. [S.l.], 2020. Cited on page(s) 26.
- [5] BUHAUG, Ø. *et al.* Second IMO Greenhouse gas study. **International Maritime Organization, London**, 2009. Cited on page(s) 26.
- [6] GEERTSMA, R. *et al.* Design and control of hybrid power and propulsion systems for smart ships: A review of developments. **Applied Energy**, Elsevier, v. 194, p. 30–54, 2017. Cited 4 time(s) on page 26, 27, 29, and 62.
- [7] SHI, Y. Greenhouse gas emissions from international shipping: the response from china's shipping industry to the regulatory initiatives of the international maritime organization. **The International Journal of Marine and Coastal Law**, Brill Nijhoff, v. 29, no. 1, p. 77–115, 2014. Cited 2 time(s) on page 26 and 62.
- [8] KANDA, W.; KIVIMAA, P. What opportunities could the covid-19 outbreak offer for sustainability transitions research on electricity and mobility? **Energy Research & Social Science**, Elsevier, v. 68, p. 101666, 2020. Cited on page(s) 26.
- [9] STEFFEN, B. *et al.* Navigating the clean energy transition in the covid-19 crisis. **Joule**, Elsevier, 2020. Cited on page(s) 26.
- [10] VÁSQUEZ, C. A. M. **A methodology to select the electric propulsion system for Platform Supply Vessels (PSV)**. 2014. PhD Thesis (PhD) — Universidade de São Paulo. Cited 2 time(s) on page 27 and 59.
- [11] BOVERI, A. *et al.* Optimal sizing of energy storage systems for shipboard applications. **IEEE Transactions on Energy Conversion**, IEEE, v. 34, no. 2, p. 801–811, 2018. Cited 4 time(s) on page 27, 56, 58, and 59.

- [12] VÁSQUEZ, C. A. M. Evaluation of medium speed diesel generator sets and energy storage technologies as alternatives for reducing fuel consumption and exhaust emissions in electric propulsion systems for psvs. **Ship Science and Technology**, Corporación de Ciencia y Tecnología para el desarrollo de la Industria . . ., v. 9, no. 18, p. 49–62, 2016. Cited 4 time(s) on page 27, 57, 58, and 148.
- [13] SKJONG, E. *et al.* The marine vessel's electrical power system: From its birth to present day. IEEE, 2015. Cited on page(s) 28.
- [14] ORGANIZATION, I. M. **International Convention for the Prevention of Pollution from Ships**. [S.I.]: Regulations for the Prevention by Garbage from Ships London, 1986. Cited on page(s) 29.
- [15] LINDSTAD, H. E.; ESKELAND, G. S.; RIALLAND, A. Batteries in offshore support vessels—pollution, climate impact and economics. **Transportation Research Part D: Transport and Environment**, Elsevier, v. 50, p. 409–417, 2017. Cited 2 time(s) on page 29 and 67.
- [16] MIYAZAKI, M. R.; SØRENSEN, A. J.; VARTDAL, B. J. Hybrid marine power plants model validation with strategic loading. **IFAC-PapersOnLine**, Elsevier, v. 49, no. 23, p. 400–407, 2016. Cited on page(s) 29.
- [17] MIYAZAKI, M. R.; SØRENSEN, A. J.; VARTDAL, B. J. Reduction of fuel consumption on hybrid marine power plants by strategic loading with energy storage devices. **IEEE Power and Energy Technology Systems Journal**, IEEE, v. 3, no. 4, p. 207–217, 2016. Cited 3 time(s) on page 29, 39, and 40.
- [18] KORKMAZ, S. A.; CERİT, A. G. Applications of fuel cell technologies in ships and a system dynamics approach. **Proceedings Book**, İstanbul University, p. 42, 2016. Cited on page(s) 30.
- [19] OVRUM, E.; DIMOPOULOS, G. A validated dynamic model of the first marine molten carbonate fuel cell. **Applied thermal engineering**, Elsevier, v. 35, p. 15–28, 2012. Cited on page(s) 30.
- [20] CHIN, C. S. *et al.* Customizable battery power system for marine and offshore applications: Trends, configurations, and challenges. **IEEE Electrification Magazine**, IEEE, v. 7, no. 4, p. 46–55, 2019. Cited on page(s) 30.
- [21] OSCAR, S. Medium speed and high speed engines in marine hybrid applications. Åbo Akademi, 2018. Cited on page(s) 30.
- [22] SIDDAIAH, R.; SAINI, R. A review on planning, configurations, modeling and optimization techniques of hybrid renewable energy systems for off grid applications. **Renewable and Sustainable Energy Reviews**, Elsevier, v. 58, p. 376–396, 2016. Cited on page(s) 30.
- [23] P, C. O. P. *et al.* Evaluation of the co2 emissions reduction potential of li-ion batteries in ship power systems. **Energies**, Multidisciplinary Digital Publishing Institute, v. 12, no. 3, p. 375, 2019. Cited 2 time(s) on page 30 and 38.
- [24] HOEDEMAKER, S. ten C. **Battery aging in full electric ships: an assessment of the relationship between battery size, charging strategy and battery lifetime**. 2017. Master's Thesis (Master) — Delft University of Technology. Cited on page(s) 30.

- [25] ENERGY, H. Homer pro version 3.7 user manual. **HOMER Energy: Boulder, CO, USA**, 2016. Cited 16 time(s) on page 32, 45, 48, 49, 51, 60, 61, 63, 64, 70, 72, 73, 75, 76, 136, and 141.
- [26] JAUROLA, M. *et al.* Optimising design and power management in energy-efficient marine vessel power systems: a literature review. **Journal of Marine Engineering & Technology**, Taylor & Francis, v. 18, no. 2, p. 92–101, 2018. Cited 3 time(s) on page 32, 48, and 78.
- [27] BARLEY, C. D.; WINN, C. B. Optimal dispatch strategy in remote hybrid power systems. **Solar Energy**, Elsevier, v. 58, no. 4-6, p. 165–179, 1996. Cited 3 time(s) on page 32, 63, and 72.
- [28] MANWELL, J. F.; MCGOWAN, J. G. Lead acid battery storage model for hybrid energy systems. **Solar Energy**, Elsevier, v. 50, no. 5, p. 399–405, 1993. Cited 4 time(s) on page 32, 49, 51, and 52.
- [29] CLARKE, D. P.; AL-ABDELI, Y. M.; KOTHAPALLI, G. Multi-objective optimisation of renewable hybrid energy systems with desalination. **Energy**, Elsevier, v. 88, p. 457–468, 2015. Cited 3 time(s) on page 32, 73, and 76.
- [30] OLATOMIWA, L. Optimal configuration assessments of hybrid renewable power supply for rural healthcare facilities. **Energy Reports**, Elsevier, v. 2, p. 141–146, 2016. Cited 7 time(s) on page 32, 71, 73, 74, 77, 147, and 148.
- [31] HILL, D.; MILLS-PRICE, M. **Energy 2018 Battery Performance Scorecard**. [S.I.]: DNV-GL, 2018. Cited 7 time(s) on page 34, 35, 42, 43, 54, 137, and 140.
- [32] HILL, D.; KLEINBERG, M.; LIND, E. **Energy 2019 Battery Performance Scorecard**. [S.I.]: DNV-GL, 2019. Cited 2 time(s) on page 34 and 35.
- [33] UNIVERSITY, B. **Summary Table of Li-based batteries (BU-216): learn the key feature Li-ion in a summary table**. 2016. Available from: <<https://batteryuniversity.com>>. Cited 4 time(s) on page 34, 143, 144, and 145.
- [34] GLOBAL, L. **Technical Notes - Lithium-ion Batteries Part I: General Overview and 2019 Update**. [S.I.], 2019. 12 p. Cited 3 time(s) on page 34, 54, and 145.
- [35] DEVIC, A.-C. *et al.* **Battery Energy Storage**. [S.I.], 2018. 17 p. Cited 2 time(s) on page 35 and 36.
- [36] RALON, P. *et al.* Electricity storage and renewables: costs and markets to 2030. **International Renewable Energy Agency (IRENA): Abu Dhabi, UAE**, 2017. Cited 8 time(s) on page 35, 37, 54, 71, 144, 145, 147, and 150.
- [37] MJØS, N. *et al.* **DNV GL Handbook for Maritime and Offshore Battery Systems**. [S.I.]: Tekn. rapp. DNV-GL, des, 2016. Cited on page(s) 35.
- [38] GL, D. **MARITIME FORECAST TO 2050—Energy Transition Outlook 2019**. [S.I.], 2018. Cited 2 time(s) on page 35 and 36.
- [39] KLEINBERG, M. **Battery energy storage study for the 2017 IRP**. [S.I.]: Pacificorp, 2016. Cited 12 time(s) on page 35, 36, 54, 69, 70, 71, 72, 137, 140, 144, 147, and 148.

- [40] GLOBAL, L. **Technical Notes - Lithium-ion Batteries Part II: Safety.** [S.I.], 2019. 9 p. Cited 2 time(s) on page 35 and 36.
- [41] ZHANG, R. *et al.* State of the art of lithium-ion battery soc estimation for electrical vehicles. **Energies**, Multidisciplinary Digital Publishing Institute, v. 11, no. 7, p. 1820, 2018. Cited on page(s) 36.
- [42] HU, X. *et al.* Technological developments in batteries: a survey of principal roles, types, and management needs. **IEEE Power and Energy Magazine**, IEEE, v. 15, no. 5, p. 20–31, 2017. Cited on page(s) 36.
- [43] SHIPPING, A. B. of. **Use of Lithium Bateries in the Marine and Offshore Industries.** 2017. Available from: <https://ww2.eagle.org/en/rules-and-resources/rules-and-guides.html?q=Guide+for+use+of+Lithium+batteries+in+the+Marine+and+Offshore+Industries#/content/dam/eagle/rules-and-guides/current/other/275_lithiumbatteries_marineoffshore_2017>. Cited 4 time(s) on page 36, 37, 38, and 39.
- [44] SHIPPING, A. B. of. **Use of Lithium Bateries in the Marine and Offshore Industries.** 2020. Available from: <https://ww2.eagle.org/en/rules-and-resources/rules-and-guides.html?q=Guide+for+use+of+Lithium+batteries+in+the+Marine+and+Offshore+Industries#/content/dam/eagle/rules-and-guides/current/other/275_lithiumbatteries_marineoffshore_2017>. Cited 3 time(s) on page 37, 38, and 39.
- [45] ENERGY, C. **Energy Containerized.** 2015. Available from: <<https://corvusenergy.com/containerized-energy-storage-system>>. Cited on page(s) 38.
- [46] CHANSON, C.; WIAUX, J. Safety of lithium-ion batteries. **The European Association for Advanced Rechargeable Batteries**, 2013. Cited on page(s) 38.
- [47] PATEL, M. R. **Shipboard electrical power systems.** [S.I.]: Crc Press, 2011. Cited 2 time(s) on page 39 and 49.
- [48] LUO, X. *et al.* Overview of current development in electrical energy storage technologies and the application potential in power system operation. **Applied energy**, Elsevier, v. 137, p. 511–536, 2015. Cited on page(s) 39.
- [49] DAS, C. K. *et al.* Overview of energy storage systems in distribution networks: Placement, sizing, operation, and power quality. **Renewable and Sustainable Energy Reviews**, Elsevier, v. 91, p. 1205–1230, 2018. Cited on page(s) 39.
- [50] LASSELLE, S.; VALØEN, L.; GUNDERSEN, B. Life cycle analysis of batteries in maritime sector. In: **Maritime Battery Forum.** [s.n.], 2016. v. 1. Available from: <https://www.nho.no/siteassets/nhos-filer-ogbilder/filer-ogdokumenter/nox-fondet/dette-er-nox-fondet/presentasjoner-og-rapporter/lifecycle-analysisfor-batteries-in-maritime-sector_final_v_0>. Cited on page(s) 39.
- [51] SHI, Y. *et al.* Using battery storage for peak shaving and frequency regulation: Joint optimization for superlinear gains. **IEEE Transactions on Power Systems**, IEEE, v. 33, no. 3, p. 2882–2894, 2017. Cited on page(s) 40.

- [52] TRAFFIC, M. **Live Map**. 2020. Available from: <<https://www.marinetraffic.com/>>. Cited on page(s) 41.
- [53] BØ, T. I. Scenario-and optimization-based control of marine electric power systems. NTNU, 2016. Cited on page(s) 41.
- [54] BØ, T. I. *et al.* Marine vessel and power plant system simulator. **IEEE Access**, IEEE, v. 3, p. 2065–2079, 2015. Cited 3 time(s) on page 41, 60, and 61.
- [55] RUFER, A. **Energy Storage: Systems and Components**. [S.l.]: CRC Press, 2017. Cited 3 time(s) on page 42, 44, and 138.
- [56] MAHESHWARI, A. Modelling, aging and optimal operation of lithium-ion batteries. Technische Universiteit Eindhoven, 2018. Cited 9 time(s) on page 42, 43, 46, 47, 48, 49, 54, 137, and 140.
- [57] NITTA, N. *et al.* Li-ion battery materials: present and future. **Materials today**, Elsevier, v. 18, no. 5, p. 252–264, 2015. Cited 3 time(s) on page 43, 47, and 112.
- [58] MJØLHUS, L. B. F. **Evaluation of Hybrid Battery System for Platform Support Vessels**. 2017. Master's Thesis (Master) — University of Stavanger, Norway. Cited 5 time(s) on page 43, 54, 67, 140, and 150.
- [59] TEAM, M. *et al.* A guide to understanding battery specifications. December, 2008. Cited 5 time(s) on page 43, 51, 136, 138, and 140.
- [60] REDDY, T. B. **Linden's handbook of batteries**. [S.l.]: McGraw-hill New York, 2011. v. 4. Cited 6 time(s) on page 43, 48, 51, 136, 138, and 140.
- [61] PETERS, J. F. *et al.* The environmental impact of li-ion batteries and the role of key parameters—a review. **Renewable and Sustainable Energy Reviews**, Elsevier, v. 67, p. 491–506, 2017. Cited 3 time(s) on page 45, 54, and 144.
- [62] YING, W. *et al.* Stochastic coordinated operation of wind and battery energy storage system considering battery degradation. **Journal of Modern Power Systems and Clean Energy**, Springer, v. 4, no. 4, p. 581–592, 2016. Cited 2 time(s) on page 45 and 54.
- [63] XU, B. *et al.* Modeling of lithium-ion battery degradation for cell life assessment. **IEEE Transactions on Smart Grid**, IEEE, v. 9, no. 2, p. 1131–1140, 2018. Cited 2 time(s) on page 45 and 136.
- [64] AN, S. J. *et al.* The state of understanding of the lithium-ion-battery graphite solid electrolyte interphase (sei) and its relationship to formation cycling. **Carbon**, Elsevier, v. 105, p. 52–76, 2016. Cited 3 time(s) on page 46, 47, and 48.
- [65] BIRKL, C. R. *et al.* Degradation diagnostics for lithium ion cells. **Journal of Power Sources**, Elsevier, v. 341, p. 373–386, 2017. Cited on page(s) 46.
- [66] HESSE, H. C. *et al.* Lithium-ion battery storage for the grid—a review of stationary battery storage system design tailored for applications in modern power grids. **Energies**, Multidisciplinary Digital Publishing Institute, v. 10, no. 12, p. 2107, 2017. Cited 2 time(s) on page 47 and 144.

- [67] HOLTSTIEGE, F. *et al.* Pre-lithiation strategies for rechargeable energy storage technologies: Concepts, promises and challenges. **Batteries**, Multidisciplinary Digital Publishing Institute, v. 4, no. 1, p. 4, 2018. Cited on page(s) 47.
- [68] WANG, Z. *et al.* Application of stabilized lithium metal powder (slmp®) in graphite anode—a high efficient prelithiation method for lithium-ion batteries. **Journal of Power Sources**, Elsevier, v. 260, p. 57–61, 2014. Cited on page(s) 48.
- [69] MAMUN, A.; SIVASUBRAMANIAM, A.; FATHY, H. K. Collective learning of lithium-ion aging model parameters for battery health-conscious demand response in datacenters. **Energy**, Elsevier, v. 154, p. 80–95, 2018. Cited on page(s) 48.
- [70] CHAPRA, S. C.; CANALE, R. P. *et al.* **Numerical methods for engineers**. [S.l.]: Boston: McGraw-Hill Higher Education,, 2010. Cited on page(s) 48.
- [71] WEN, S. *et al.* Allocation of ess by interval optimization method considering impact of ship swinging on hybrid pv/diesel ship power system. **Applied energy**, Elsevier, v. 175, p. 158–167, 2016. Cited 3 time(s) on page 48, 67, and 76.
- [72] LAN, H. *et al.* Optimal sizing of hybrid pv/diesel/battery in ship power system. **Applied energy**, Elsevier, v. 158, p. 26–34, 2015. Cited 5 time(s) on page 48, 76, 77, 144, and 145.
- [73] NGUYEN, T. A.; CROW, M. Stochastic optimization of renewable-based microgrid operation incorporating battery operating cost. **IEEE Transactions on Power Systems**, IEEE, v. 31, no. 3, p. 2289–2296, 2015. Cited 3 time(s) on page 48, 76, and 77.
- [74] PATEL, M. **Shipboard propulsion, power electronics, and ocean energy**. [S.l.]: Crc Press, 2012. Cited 3 time(s) on page 50, 54, and 139.
- [75] SYSTEMS, S. P. **Products: Spear's Trident family of advanced lithium ion battery storage systems for marine propulsion**. 2019. Available from: <<https://www.spearpowersystems.com/products/>>. Cited on page(s) 54.
- [76] BALDASANO, M. C. Díaz-de *et al.* Conceptual design of offshore platform supply vessel based on hybrid diesel generator-fuel cell power plant. **Applied energy**, Elsevier, v. 116, p. 91–100, 2014. Cited 2 time(s) on page 56 and 61.
- [77] MORAES, A. C.; MOITA, J. V.; CAPRACE, J. D. A discrete-event simulation approach for platform support vessels operations under stochastic effects. In: SOBENA. **2016 XXVII International Congress on Waterborne Transportation, Shipbuilding and Offshore Constructions**. [S.l.], 2018. Cited on page(s) 57.
- [78] HOLTROP, J.; MENNEN, G. An approximate power prediction method. 1982. Cited on page(s) 57.
- [79] HOLTROP, J. A statistical re-analysis of resistance and propulsion data. **Int Shipbuild Prog**, v. 31, p. 272–276, 1984. Cited on page(s) 57.
- [80] LINDSTAD, H.; JULLUMSTRØ, E.; SANDAAS, I. Reductions in cost and greenhouse gas emissions with new bulk ship designs enabled by the panama canal expansion. **Energy Policy**, Elsevier, v. 59, p. 341–349, 2013. Cited on page(s) 57.

- [81] CATERPILLAR. **Marine Engine - Diesel Generator Sets. Model Cat® C3512C HD V-12, 4-Stroke-Cycle-Diesel.** 2019. Available from: <https://www.cat.com/en_US/products/new/power-systems/marine-power-systems/high-performance-propulsion-and-maneuvering-solutions/18408746.html>. Cited 4 time(s) on page 58, 61, 62, and 63.
- [82] CATERPILLAR. **Marine Engine - Diesel Generator Sets. Model Cat® C18 ATAAC™ In-line 6, 4-cycle diesel.** 2019. Available from: <https://www.cat.com/en_ID/products/new/power-systems/electric-power/diesel-generator-sets/3449712859459755.html>. Cited 4 time(s) on page 58, 61, 62, and 63.
- [83] TUFTE, E. D. **Impacts of low load operation of modern four-stroke diesel engines in generator configuration.** 2014. Master's Thesis (Master) — Institutt for marin teknikk. Cited 2 time(s) on page 58 and 62.
- [84] ZAHEDI, B.; NORUM, L. E.; LUDVIGSEN, K. B. Optimized efficiency of all-electric ships by dc hybrid power systems. **Journal of Power Sources**, Elsevier, v. 255, p. 341–354, 2014. Cited 2 time(s) on page 60 and 67.
- [85] KWASIECKYJ, B. Hybrid propulsion systems. efficiency analysis and design methodology of hybrid propulsion systems. **TU Delft, SDPO**, v. 13, 2013. Cited on page(s) 60.
- [86] SKJONG, E. *et al.* Approaches to economic energy management in diesel–electric marine vessels. **IEEE Transactions on Transportation Electrification**, IEEE, v. 3, no. 1, p. 22–35, 2017. Cited 2 time(s) on page 62 and 67.
- [87] BOUMAN, E. A. *et al.* State-of-the-art technologies, measures, and potential for reducing ghg emissions from shipping—a review. **Transportation Research Part D: Transport and Environment**, Elsevier, v. 52, p. 408–421, 2017. Cited 3 time(s) on page 64, 65, and 112.
- [88] WEN, S. *et al.* Optimal sizing of hybrid energy storage sub-systems in pv/diesel ship power system using frequency analysis. **Energy**, Elsevier, v. 140, p. 198–208, 2017. Cited on page(s) 67.
- [89] DAVION, H. **Offshore Oil & Gas Vessels with Hybrid Power: opportunities and barriers in maritime rule structures for Hybrid electric power for backup, propulsion, and drilling.** [S.l.], 2016. Cited on page(s) 67.
- [90] HEIAN, M. J. **Factors influencing machinery system selection for complex operational profiles.** 2014. Master's Thesis (Master) — Institutt for marin teknikk. Cited 2 time(s) on page 67 and 150.
- [91] VONSIEN, S.; MADLENER, R. Cost-effectiveness of li-ion battery storage with a special focus on photovoltaic systems in private households. FCN Working Paper, 2018. Cited 5 time(s) on page 70, 73, 74, 75, and 76.
- [92] PRICES, G. P. **Diesel prices, liter, July 2019 - Average price of diesel around the world.** 2019. Available from: <https://www.globalpetrolprices.com/diesel_prices/>. Cited 2 time(s) on page 70 and 150.

- [93] KEMPENER, R.; BORDEN, E. Battery storage for renewables: Market status and technology outlook. **International Renewable Energy Agency (IRENA), Abu Dhabi**, 2015. Cited 5 time(s) on page 71, 143, 144, 145, and 147.
- [94] SCHMIDT, O. *et al.* The future cost of electrical energy storage based on experience rates. **Nature Energy**, Nature Publishing Group, v. 2, no. 8, p. 17110, 2017. Cited on page(s) 72.
- [95] BLANK, L.; TARQUIN, A. **Engineering economy**. [S.l.]: McGraw-Hill, 2005. Cited 4 time(s) on page 73, 74, 75, and 76.
- [96] QIU, Y. *et al.* Techno-economic analysis of pv systems integrated into ship power grid: A case study. **Energy Conversion and Management**, Elsevier, v. 198, p. 111925, 2019. Cited 3 time(s) on page 73, 75, and 76.
- [97] BUCCI, V. *et al.* Inland waterway gas-fueled vessels: Casm-based electrification of a push-boat for the european network. **IEEE Transactions on Transportation Electrification**, IEEE, v. 2, no. 4, p. 607–617, 2016. Cited on page(s) 74.
- [98] HORVATH, S.; FASIHI, M.; BREYER, C. Techno-economic analysis of a decarbonized shipping sector: Technology suggestions for a fleet in 2030 and 2040. **Energy Conversion and Management**, Elsevier, v. 164, p. 230–241, 2018. Cited on page(s) 74.
- [99] DEDES, E. K.; HUDSON, D. A.; TURNOCK, S. R. Assessing the potential of hybrid energy technology to reduce exhaust emissions from global shipping. **Energy policy**, Elsevier, v. 40, p. 204–218, 2012. Cited on page(s) 75.
- [100] NEUBAUER, J. **Battery lifetime analysis and simulation tool (BLAST) documentation**. [S.l.], 2014. Cited on page(s) 75.
- [101] LEE, K.-J. *et al.* Hybrid photovoltaic/diesel green ship operating in standalone and grid-connected mode—experimental investigation. **Energy**, Elsevier, v. 49, p. 475–483, 2013. Cited 2 time(s) on page 75 and 150.
- [102] ONORI, S. *et al.* A new life estimation method for lithium-ion batteries in plug-in hybrid electric vehicles applications. **International Journal of Power Electronics**, Inderscience Publishers Ltd, v. 4, no. 3, p. 302–319, 2012. Cited 2 time(s) on page 137 and 141.
- [103] DIORIO, N. *et al.* **Technoeconomic modeling of battery energy storage in SAM**. [S.l.], 2015. Cited on page(s) 138.
- [104] LYU, Z. **Concept Design of Hybrid Crane Vessel: Feasibility study of utilizing electric energy storage technology**. 2016. Master's Thesis (Master) — Delft University of Technology. Cited on page(s) 139.
- [105] MIYAZAKI, M. R. *et al.* Hybrid modeling of strategic loading of a marine hybrid power plant with experimental validation. **IEEE Access**, IEEE, v. 4, p. 8793–8804, 2016. Cited on page(s) 140.
- [106] HAN, X. *et al.* Cycle life of commercial lithium-ion batteries with lithium titanium oxide anodes in electric vehicles. **Energies**, Multidisciplinary Digital Publishing Institute, v. 7, no. 8, p. 4895–4909, 2014. Cited 2 time(s) on page 144 and 145.

- [107] BERCKMANS, G. *et al.* Cost projection of state of the art lithium-ion batteries for electric vehicles up to 2030. **Energies**, Multidisciplinary Digital Publishing Institute, v. 10, no. 9, p. 1314, 2017. Cited on page(s) 145.
- [108] UNIVERSITY, B. **BU-802b: What does Elevated Self-discharge Do? Learn about an often ignored characteristic of batteries.** 2018. Available from: <https://batteryunivesty.com/learn/article/elevating_self_discharge>. Cited on page(s) 145.
- [109] KONIAK, M.; CZEREPICKI, A. Selection of the battery pack parameters for an electric vehicle based on performance requirements. In: IOP PUBLISHING. **IOP Conference Series: Materials Science and Engineering**. [S.l.], 2017. v. 211, no. 1, p. 012005. Cited on page(s) 145.
- [110] RITARI, A. *et al.* Hybrid electric topology for short sea ships with high auxiliary power availability requirement. **Energy**, Elsevier, v. 190, p. 116359, 2020. Cited on page(s) 150.
- [111] PERČIĆ, M.; ANČIĆ, I.; VLADIMIR, N. Life-cycle cost assessments of different power system configurations to reduce the carbon footprint in the croatian short-sea shipping sector. **Renewable and Sustainable Energy Reviews**, Elsevier, v. 131, p. 110028, 2020. Cited on page(s) 150.

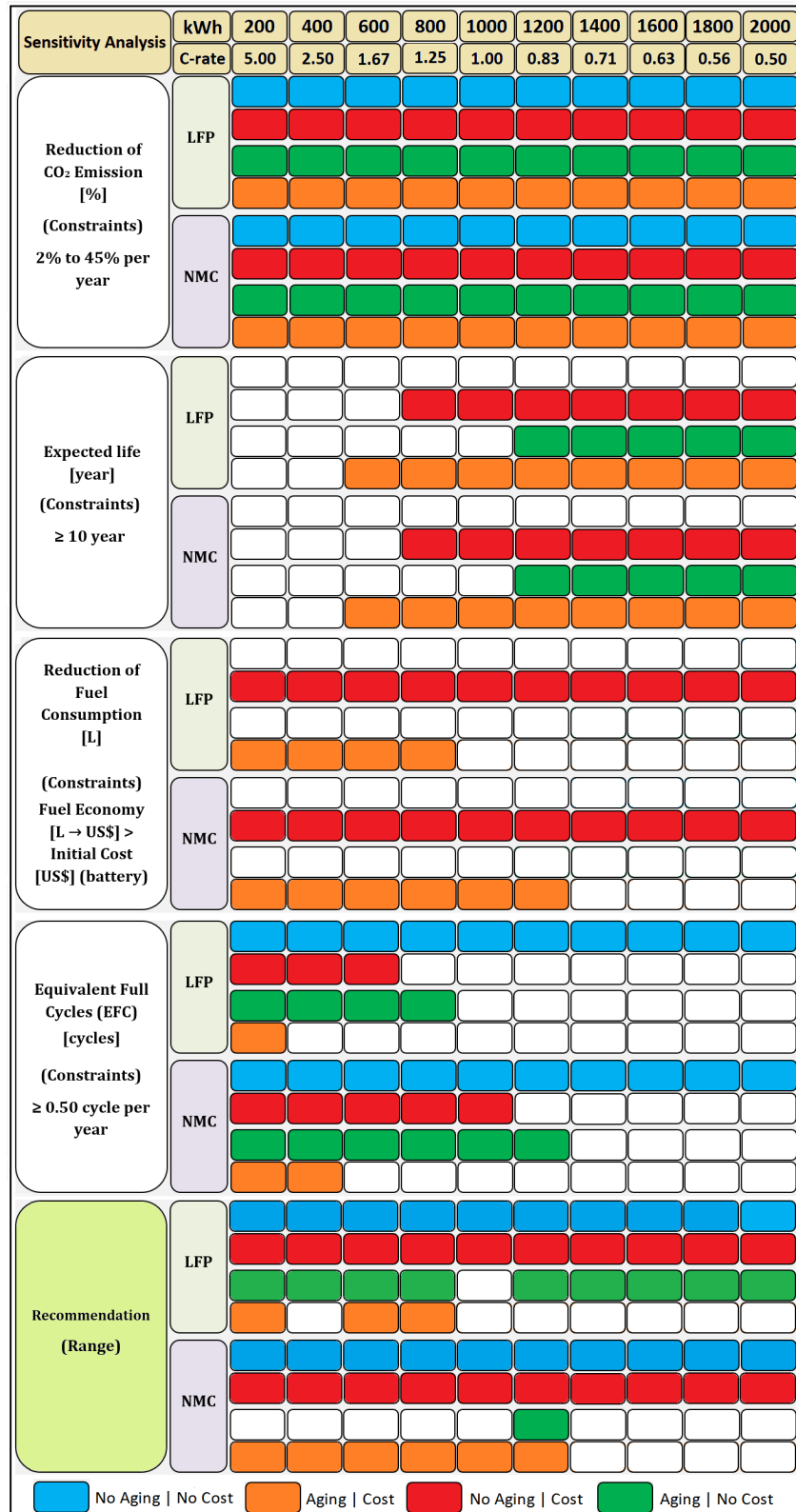
APPENDIX A

Recommendations for battery operation – performance of indicators

Figure 65 indicates the battery energy capacity range for *LFP* and *NMC* cells. For the *LFP* battery system, the all capacity range is adequate for the "No Aging | No Cost" and "No Aging | Cost" cases. The "Aging | No Cost" case also provides all range as adequate for operation, except energy capacity at 1000 kWh. The "Aging | Cost" suggests the range from 200 to 800 kWh, except 400 kWh in this interval. Moreover, for *NMC* battery technology, the "Aging | No Cost" recommends only the capacity of 1200 kWh. Besides, a similar performance of *NMC* compared to *LFP* cell recommends the all range capacity range is adequate for the "No Aging | No Cost" and "No Aging | Cost" cases. Finally, the "Aging | Cost" case provides an interval lower than 1200 kWh.

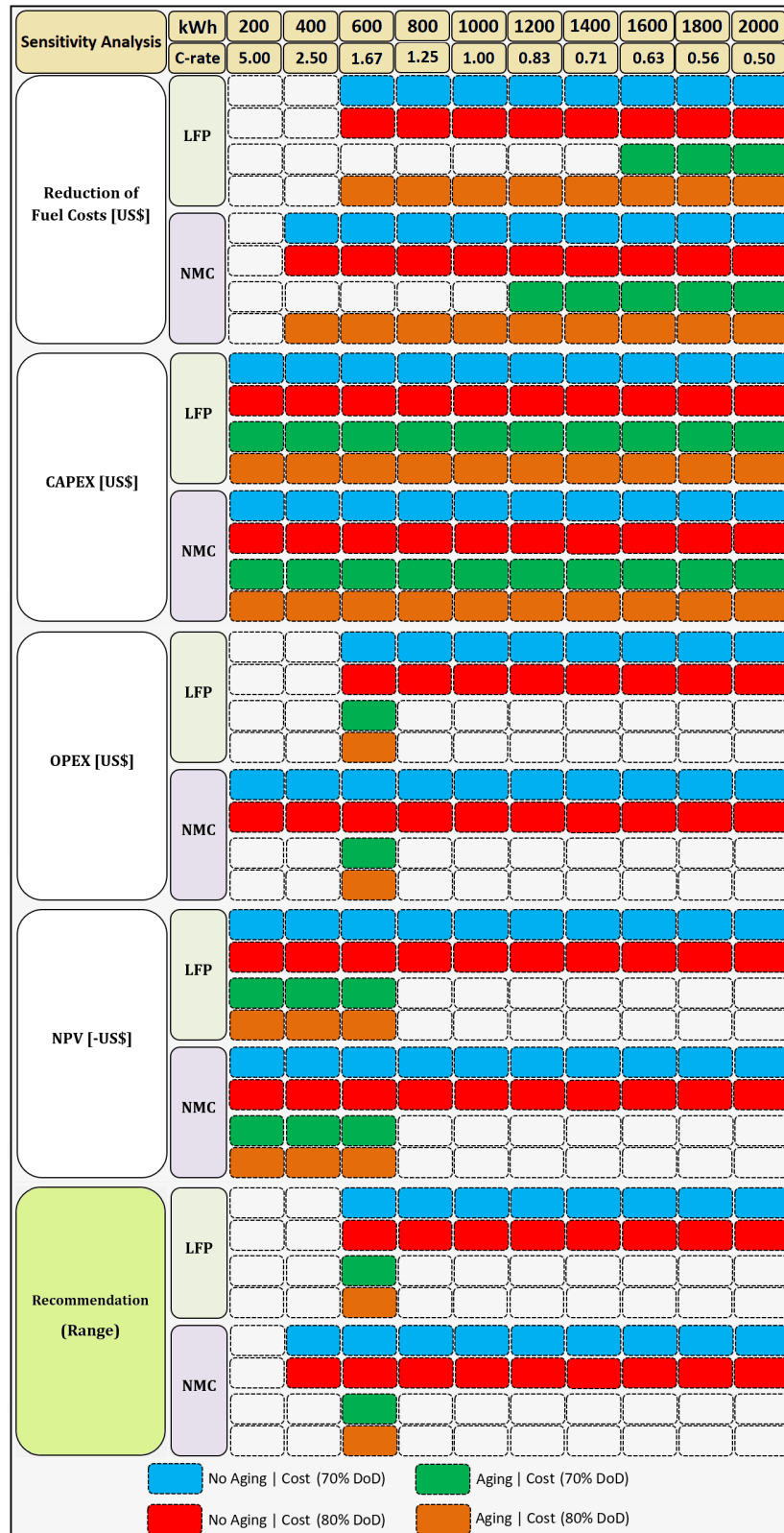
Similarly, the range recommended for power capacity variation and techno-economic performance can be seen from Figure 66 to Figure 68.

Figura 65 – Battery models performance – Range recommended for battery energy capacity variation from 200 to 2000 kWh (Sensitivity analysis). The Nominal C-rate represents the fixed battery power capacity of 1000 kW. Indicators evaluated for the battery models. Reduction of CO_2 emission, expected life, reduction of fuel consumption, and EFC.



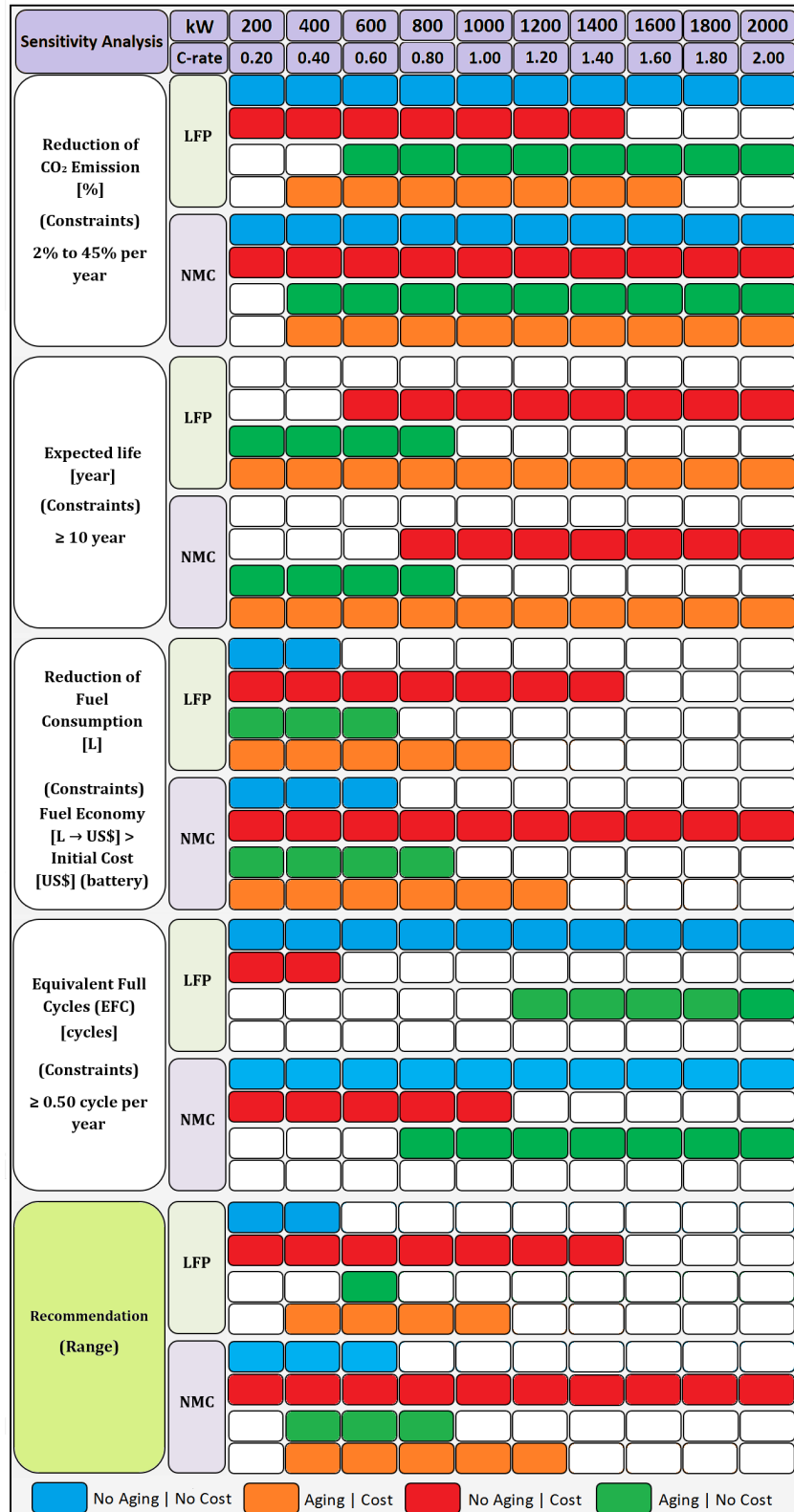
Fonte: Author.

Figura 66 – Economic performance – Range recommended for battery energy capacity variation from 200 to 2000 kWh (Sensitivity analysis). The Nominal C-rate represents the fixed battery power capacity of 1000 kW. Indicators evaluated for the battery operating at 70% and 80% DoD. Reduction of fuel costs, CAPEX, OPEX, and NPV.



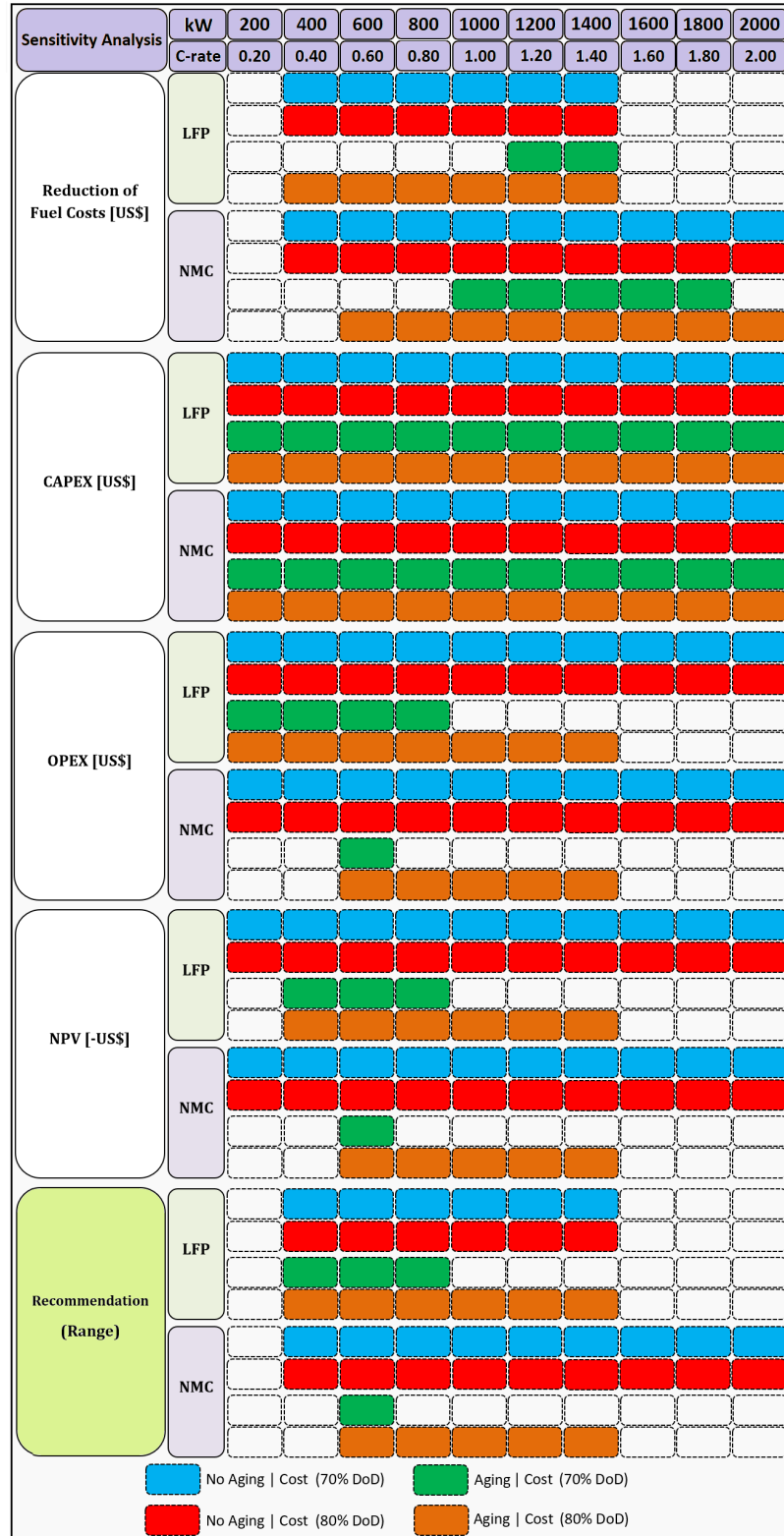
Fonte: Author.

Figura 67 – Battery models performance – Range recommended for battery power capacity variation from 200 to 2000 kW (Sensitivity analysis). The Nominal C-rate represents the fixed battery energy capacity of 1000 kWh. Indicators evaluated for the battery models. Reduction of CO_2 emission, expected life, reduction of fuel consumption, and EFC.



Fonte: Author.

Figura 68 – Economic performance – Range recommended for battery power capacity variation from 200 to 2000 kW (Sensitivity analysis). The Nominal C-rate represents the fixed battery energy capacity of 1000 kWh. Indicators evaluated for the battery operating at 70% and 80% DoD. Reduction of fuel costs, CAPEX, OPEX, and NPV.



Fonte: Author.

APPENDIX B

Glossary

The variables used as a parameter to size battery cells, modules, and packs can be classified as technical specifications and battery operation condition ones. The former can be obtained through the battery manufacturer data-sheet and the later is related to materials property of cells.

Cycle Life

The number of charge-discharge cycles the storage systems can supply before it fails to meet specific charge and discharge conditions [59, 60]. For instance, if a battery operates from 100% State-of-charge (SoC) to a minimum SoC at 20%, the number of charge-discharge will be different in comparison with a battery that operates to a minimum *SoC* at 10%. In the last case, the number of cycles will be low than the first case.

The number of cycles [63] can be calculated by Equation 40:

$$N_{cycles}^{NoAging} = \frac{E_{battery}}{2 \cdot (E_{SoC_{max}} - E_{SoC_{min}})} \quad (40)$$

where $N_{cycles}^{NoAging}$ is the number of cycles disregarding degradation process, $E_{battery}$ [kWh] is the total cycled energy through the battery, and $E_{SoC_{min}}$ and $E_{SoC_{max}}$ are Battery capacity defined a specific range *SoC*.

For the Advanced Battery Model the number of cycles ("cycle degradation") is estimated by following Equation 41 [25]:

$$\frac{1}{N_{cycles}^{Aging}} = \alpha \cdot DoD^{\beta} \quad (41)$$

where N_{cycles}^{Aging} is the number of cycles to failure given by cycle curve to the specific battery cell, $DoD[\%]$ is Depth-of-discharge (a fractional number between 0 and 1), α and β are fitted constants. These constants are fitted to the data you enter in the cycles versus DoD . The constant α is scaled so that the degradation variable goes from zero to capacity degradation limit defined by a user as is illustrated in Figure 11. The inverse of α presents a physical significance related to the nominal cycles to failure at 100% DoD times the capacity degradation limit chosen. However, β equal to 1.0 indicate a constant number of kWh-throughput to EoL . The constant β is 0 for a set number of cycles to failure, without dependence on DoD .

C-rate

The C-rate can be represented by the number of full charges or full discharges per hour relative to its maximum capacity, that is, an indirect measure of battery current during charging or discharge e a direct measure of the rate at which a battery can be recharged [31]. Besides, C-rate also can be considered as power capacity to energy capacity ratio; or as a measure of current to ampere-hour capacity ratio or the number of charges or discharges a one hour [39]. C-rate is used for providing the effect of current on aging for different current amplitudes. Consequently, the C-rate for a battery can be defined as nominal, charge and discharge C-rates. Depending on charge-discharge C-rates values, a battery can be classified as High Power (HP) or High Energy (HE) for the same Nominal C-rate. Current rate is defined by Equation 42 [56]:

$$C-rate = \frac{I}{C_{nom}} \quad (42)$$

where I is the current measured in ampere and C_{nom} is the nominal capacity in Ah. A similar way define C-rate by Equation 43:

$$C-rate = \frac{P}{E_{nom}} \quad (43)$$

where P is the power capacity measured in watts and E_{nom} is the nominal energy capacity in watts - hour. As a consequence, C-rate presents the dimension of $time^{-1}$, usually given in $hour^{-1}$.

End of Life - EoL

The battery End of life - EoL - is expressed as a function of performance parameters such as the current, power capacity, energy capacity, SoC , battery voltage and can be modeled over several parameterised models: electrochemical, equivalent circuit models, artificial neural networks, and analytical models with empirical data fitting [102]. In this work, the Homer

Energy software used in the simulation run the Rainflow Counting Algorithm [103] for an estimate the number of cycles to battery failure and also can estimate the total kWh throughput to *EoL*. Homer Energy use the analytical models with empirical data fitting for *DoD* curve data of the battery.

Internal Resistance and Internal Impedance

Internal resistance can be defined as the resistance to the flow of an electric current within a cell or battery and also dependent on the State-of-charge. Normally, the internal resistance is different for charging and discharging current and is considered as the sum of the ionic and electronic resistances of the battery cells. The internal impedance presents the resistance that depends on frequency denominated reactance [59, 60].

Maximum Continuous Discharge Current

Maximum continuous discharge current [59] or Maximum-power discharge current [60] is the discharge current at which maximum power is transferred to the load. For a discharge current purely ohmic, the discharge voltage is about equal to one-half of the open-circuit voltage.

Nominal Capacity or Ampere-hour Capacity

Defined as total ampere-hours available that can be withdrawn from a fully charged cell or battery under specified conditions of discharge (*C – rate*) from 100% to State-of-Charge (*SoC*) to the cut-off voltage [59, 60]. Ampere-hour capacity is generally measured in *Ah* and calculated to the integral of the current [55]:

$$C_{Ah} = \int_{t_0}^t I(t)dt \quad (44)$$

Nominal Energy or Energy Capacity

Nominal energy (or Energy capacity) is specified as total watt-hours available when a cell (or a battery) is discharged from 100% to State-of-Charge to the cut-off voltage, that also can be calculated by multiplying the discharge power by the discharge time (hours). This parameter decreases with increasing C-rate [59]. The energy capacity is generally measured in *Wh* and calculated to the integral of the power:

$$C_{Wh} = \int_{t_0}^t P(t)dt \quad (45)$$

Round-trip Energy Efficiency

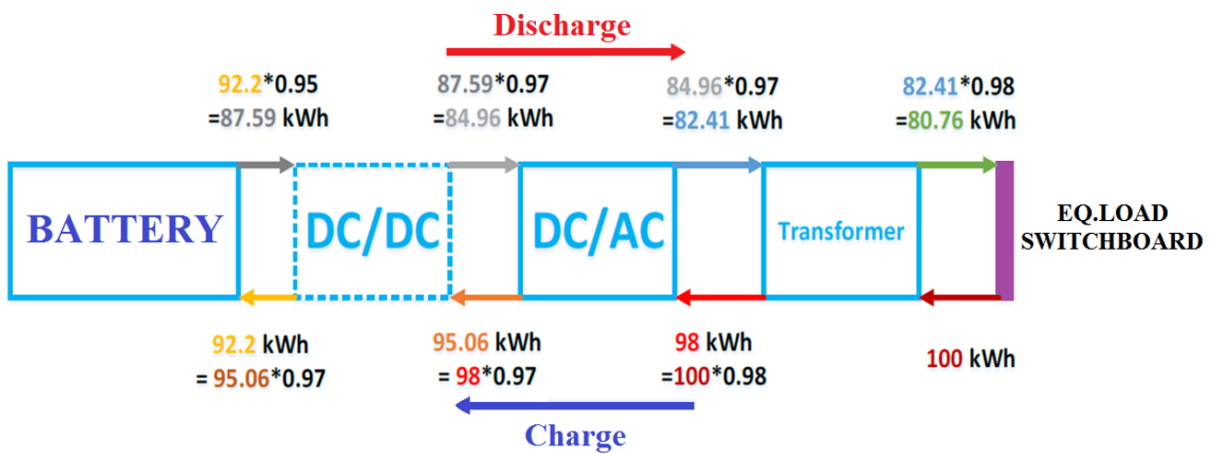
The Round-trip energy efficiency η_{RTEE} is defined by Equations 46 and 47 [74]:

$$\eta_{RTEE} = \frac{\text{Energy delivered to loads during discharge}}{\text{Energy injected to restore initial charge level}} \quad (46)$$

$$\eta_{RTEE} = \frac{\text{Average discharge voltage} \cdot \text{Ah capacity}}{\text{Average charge voltage} \cdot \frac{c}{d} \text{ ratio} \cdot \text{Ah capacity}} \quad (47)$$

where the charge efficiency η_{RTEE} is also known as the Coulombic-efficiency and can be determined as the inverse of the $\frac{c}{d}$ ratio. The round-trip efficiency values to several Li-ion battery cells are detailed in Table 9 (Annex C). The Figure 69 illustrates the example of *RTEE* calculated for a battery system connected to Vessel Switchboard. The *RTEE* is estimated in $80.76\% = 98\% \cdot 97\% \cdot 97\% \cdot 95\% \cdot 97\% \cdot 97\% \cdot 98\%$ [104].

Figura 69 – Example of Round-trip Energy Efficiency for a battery connected to Switchboard.



Fonte: Adapted from [104].

Specific Energy and Energy Density / Specific Power and Power Density

The ratio of the energy output of a cell to its weight (or the nominal battery energy per unit mass), sometimes referred to as the gravimetric energy density and usually measured in Wh/kg . However, energy density presents a similar definition measured in Wh/L and sometimes is called volumetric energy density. In addition, the ratio of the power delivered by a cell to its weight (or the maximum available power per unit mass) and usually measured in W/kg . However, Power Density is a similar definition measured in W/L [59, 60].

State-of-Charge - SoC

State-of-Charge (*SoC*) is an expression of the present battery capacity as a percentage of maximum capacity [59, 60]. *SoC* is calculated following [56]:

$$SoC(t) = SoC(t_0) - \frac{1}{C_{max}} \int_{t_0}^t I(t) dt \quad (48)$$

where $SoC(t_0)$ is the initial *SoC* expressed in percentage; C_{max} is the maximum battery capacity in *ampere – hour* and $SoC(t)$ express the present condition of battery. If *SoC* presents a percentage of 100%, it means that the battery is totally charged. Second term of expression (48) can be also defined by:

$$\frac{1}{E_{max}} \int_{t_0}^t P(t) dt \quad (49)$$

where P is the power capacity measured in *watts* and E_{max} is the maximum energy capacity in *watts – hour*. According to [58], different ranges of *SoC* can be applied to operational modes of the vessels. Consequently, a *PSV* can be operated with a battery by Strategic Loading mode [105] and the excess power engine charges the battery until it reaches SoC_{max} . After that, the engines stop (or operates at low loads) and the battery supplies the power demand until SoC_{min} , and the cycle is repeated. SoC_{max} and SoC_{min} are parameters that should be defined by marine operators (Marine Pilot). Additionally, a battery can be degraded faster if it operates a significant amount of time at a high *SoC* than a mid-level *SoC*. Equivalently, a battery operating at very low average *SoC*, it will be degraded faster [39].

State-of-Charge Swing - SOC Swing

The *SoC – Swing* (or windows) is an expression of the present battery capacity as a percentage of maximum capacity and is calculated by the same expression (48). However, *SoC – Windows* is a range of testing at different *SoC* to determine the battery performance best (and the worst). According to testing performed in DNV-GL's Labs [31] – the world's leading

classification society for the maritime industry – not only is the average *SoC* condition should be considered, but so is the amount of “swing” around that *SOC* condition. The testing has been indicating that shallow cycling within a narrow *SoC* range does not necessarily promote increase throughput depending on battery technology.

Throughput or Turnovers

The battery life is defined by Ah-throughput or Wh-throughput, that is the in and out charge from 0 to *EoL* one, considering which the battery is charge/discharge to cycle $I_{nom}(t)$. The nominal throughput in ampere-hour and in energy unit can be defined by Equations 50 and 51 [102]:

$$Ah - \text{throughput}_{nom} = \int_{I_0}^{I_{EoL}} I_{nom}(t) dt \quad (50)$$

or

$$Wh - \text{throughput}_{nom} = \int_{P_0}^{P_{EoL}} P_{nom}(t) dt \quad (51)$$

where *EoL* was defined in the previous item, I_{EoL} and P_{EoL} are current and power to *EoL*, respectively, $I_{nom}(t)$ is instant current of battery, and $P_{nom}(t)$ is instant power of battery. HOMER software define Wh-throughput using the Equation 52 [25]:

$$kWh - \text{throughput}_{lifetime} = N_{cycles} \cdot DoD \cdot \frac{Q_{max} \cdot V_{nom}}{1000W/kW} \quad (52)$$

where N_{cycles} is the number of cycles to failure given by cycle curve to specific battery cell, $DoD[\%]$ is Depth-of-discharge, $Q_{max}[\text{Ah}]$ is the maximum battery capacity, and $V_{nom}[\text{V}]$ is nominal voltage.

APPENDIX C

Types of battery cells and their characteristics

Tabela 8 – Types of battery cells, packing, manufacturers, historical, applications and their main chemical/constructive characteristics.

Type	Name Battery Cell	Packing (Typical)	Prominent manufacturers	Historical	Battery Chemistries			Applications
					Cathode	Anode	Electrolyte	
<i>LFP – LiFePO₄</i>	Lithium Iron Phosphate (Li-phosphate)	18650 Cylindrical, Prismatic and 26650	A12 Systems, BYD, Amperex, Lishen	1996	<i>LFP</i>	Graphite	Lithium Carbonate	Stationary with high currents and endurance
<i>NMC – LiNiMnCoO₂</i>	Lithium Nickel Manganese	18650 Cylindrical, Prismatic and pouch cell	Johnson Controls, Saft	2008	<i>NMC</i>	Graphite, Silicon	Lithium Carbonate	Medical, devices, EV's, industrial, E-bikes
<i>LTO – Li₂TiO₃ or Li₄Ti₅O₁₂</i>	Lithium Titanate (Li-titanate)	Prismatic	ATL, Toshiba, Leclanché, Microvast	2008	<i>LMO</i>	<i>LTO</i>	Lithium Carbonate	EV, solar street lighting
<i>LMO – LiMn₂O₄</i>	Lithium Manganese Oxide (Li-manganese)	Prismatic	LG Chem, AESC, Samsung SDI	1996	<i>LMO</i>	Graphite	Lithium Carbonate	Powertrains, devices, medical, power tools
<i>LCO – LiCoC₂</i>	Lithium Cobalt Oxide (Li-cobalt)	18650 Cylindrical, Prismatic and pouch cell	Samsung SDI, BYD, LG Chem, Panasonic, ATL, Lishen, Sony	1991	<i>LCO</i>	Graphite	Lithium Polymer	Cameras, laptops, tablets, Mobile phones
<i>NCA – LiNiCoAlO₂</i>	Lithium Nickel Cobalt Aluminum Oxide (Li-aluminum)	18650 Cylindrical	Panasonic, Samsung SDI	1999	<i>NCA</i>	Graphite	Lithium Carbonate	Industrial, EV (Tesla), Medical

Source: Adapted from [33, 93].

Tabela 9 – Parameters for main Li-ion batteries cells: Lifetime, *EFC*, Nominal/minimum voltage, Full dis(charge), C-rate(dis-charge), Cont. Power Cap. and round-trip efficiency.

Parameters		<i>LTO</i>	<i>NCA</i>	<i>LFP</i>	<i>NMC</i>	<i>LMO</i>	<i>LCO</i>
Degradation Processes	Calendar aging [years] - Lifetime	10 [39], 10 – 20 [36], 3000 – 7000 [33], 2000 – 25000 [93], 15000 [39] (100% <i>DoD</i> , 25°C, 1C)	5 – 20 [36] 1000 [106], 500 [33], 800 – 5000 [93]	5 [72]; 10 [39], 5 – 20 [36] 1000 – 2000 [33], 200 – 2000 [93], 2000 [39] (100% <i>DoD</i> , 25°C, 1C)	10 [39], 5 – 20 [36] 1000 – 2000 [33], 800 – 2000 [93], 3500 [39] (100% <i>DoD</i> , 25°C, 1C)	5 – 20 [36] 300 – 700 [33] 800 – 2000 [93]	- 500 – 1000 [33] 300 – 800 [93]
	Cycle aging [cycles] – <i>EFC</i>						
Nominal Voltage [V]	2.40 [33], 2.3 [66]	3.6 [33,66]	3.20, 3.30 [33], 3.2 [66]	3.60, 3.70 [33], 3.7 [66]	3.70, 3.80 [33]	3.60 [33], 2.50 [33]	2.50 [33]
Minimum Voltage [V]	1.50 [33]	2.50 [33]	2.00 [33]	2.50 [33]	2.50 [33]	2.50 [33]	2.50 [33]
Dis(charge) Voltage [V]	Full charge 2.85 [33]	4.20 [33]	3.65 [33]	4.20 [33]	4.20 [33]	4.20 [33]	4.20 [33]
	Full discharge 1.80 [33]	3.00 [33]	2.50 [33]	3.00 [33]	3.00 [33]	3.00 [33]	3.00 [33]
C-rate (charge)	1C (5C max) [33] 1C – 3C [39]	1C [33]	1C [33] 1C – 2C [39]	0.7 - 1C (3h) [33] 1C [39]	0.7 - 1C (3h) [33]	0.7 - 1C (3h) [33]	0.7 - 1C (3h) [33]
C-rate (discharge)	10C (possible) [33]	1C [33]	1C (25C pule) [33]	1 - 2C [33]	1C, 10C (possible) [33]	1C (1h) [33]	
Cont. Power Cap. (Discharge/Charge)	8C/>3C (>2.67) [66] NCR18650B – Panasonic (Cylindrical)	2C/0.5C (4) [66] NCR18650B – Panasonic (Cylindrical)	6C/1C (6) [66] NCR18650B – Murata (Cylindrical)	3C/1C (3) [66] SDI94Ah-	-	-	
Round-trip Efficiency [%]	95 [36], 93 [61]	94 [36], 91.6 [61]	91 [36], 93 [61]	94 [36], 93.8 [61]	94 [36], 93 [61], 91 [61]		

Tabela 10 – Parameters for main Li-ion batteries cells: maximum and minimum temperature, specific energy density, volumetric energy density, self-discharge efficiency, and comments.

Parameters	<i>LTO</i>	<i>NCA</i>	<i>LFP</i>	<i>NMC</i>	<i>LMO</i>	<i>LCO</i>
Temperature Min. Temperature operation [°C]	-	-20 (discharge), 0 (charge) [34]	-30 (discharge), 0 (charge) [34]	-20 (discharge), 0 (charge) [34]	-30 (discharge), 0 (charge) [34]	-20 (discharge), 0 (charge) [34]
	-	55 [106], 60 (discharge), 45 (charge) [34]	60 (discharge), 45 (charge) [34]	60 (discharge), 45 (charge) [34]	60 (discharge), 45 (charge) [34]	60 (discharge), 45 (charge) [34]
Specific Energy Density [Wh/kg]	42 [72], 80 – 95 [93]	680 – 760 [107], 120 – 160 [93], 175 – 240(cylindrical), 130 – 200 (polymer) [34]	518 – 587 [107], 85 – 105 [93], 60 – 110 [34]	610 – 650 [107], 120 – 140 [93], 100 – 240 [34]	410 – 492 [107], 80 – 95 [93], 100 – 150 [34]	546 [107], 140 – 200 [93] 175 – 240 (cylindrical), 130 – 200 (polymer) [34]
		462 [106], 211 – 620 [36], 400 – 640 (cylindrical), 250 – 450 (polymer) [34]	211 – 620 [36], 125 – 250 [34]	200 – 750 [36], 250 – 640 [34]	200 – 750 [36], 250 – 350 [34]	400 – 640 (cylindrical), 250 - 450 (polymer) [34]
Self-Discharge Efficiency [% per day]	5% in 24h, then 1 – 2% per month (plus 3% for safety circuit) [108]	5% in 24h, then 1 – 2% per month (plus 3% for safety circuit) [108]	5% in 24h, then 1 – 2% per month (plus 3% for safety circuit) [108], 2 – 10% [34]	5% in 24h, then 1 – 2% per month (plus 3% for safety circuit) [108]	5% in 24h, then 1 – 2% per month (plus 3% for safety circuit) [108]	5% in 24h, then 1 – 2% per month (plus 3% for safety circuit) [108], 2 – 10% [34]
		Long life, fast charge, wide temperature range and safe. Low capacity, expensive [33]	Highest capacity with moderate power. Similar to Li-cobalt [33]; Highest energy density per unit mass [109]	Flat discharge voltage, high power low capacity, very safe; elevated self-discharge [33]; Very safe, high power, but lower energy density. Best high-temperature stability [109]	High capacity and high power. Market share is increasing. Also called NCM, CMN, MNC, MCN [33]	High power, less capacity; safer than Li-cobalt; often mixed with <i>NMC</i> to improve performance [33]; Safer and less expensive than <i>LCO</i> , but poor high temperature stability [109]
Comments						High energy, limited power. Market share has stabilized [33]; Original commercial type; expensive raw materials [109]

APPENDIX D

Investment, replacement and O&M costs

According to DNV-GL, the energy storage equipment includes the full DC battery systems such as Li-ion battery cells, flow battery electrolyte, internal wiring and connections, battery pack, containers, and Battery Management System (BMS).

Tabela 11 – Cost of investment, installation, O&M and Total Cost Fixed for Li-ion battery cells.

Parameters	<i>LTO</i>	<i>NCA</i>	<i>LFP</i>	<i>NMC</i>	<i>LMO</i>	<i>LCO</i>
Cost of investment [\$/kWh]	900 – 2200 [93], 500 – 800 [39]	240 – 380 [93]	550 – 850 [93], 350 – 525 [39]	550 – 750 [93], 325 – 500 [39]	300 – 700 [93]	210 – 500 [93]
(1) Cost of investment [\$/kWh]						
Input HOMER (average max/min of the row above)	1350	310	600	537.5	500	355
(2) Cost of Installation [\$/kWh]	150 [39] 450 – 1200 [36] 675 (Average min/max)	150 – 800 [36] 475 (Average min/max)	150 [39] 150 – 800 [36] 475 (Average min/max)	150 [39] 150 – 800 [36] 475 (Average min/max)	150 [39] 150 – 800 [36] 475 (Average min/max)	-
(3) Total Cost Fixed = (1) + (2) [\$/kWh]	2025	785	1075	1012.5	975	-
O&M [\$/kW year]	5 [30] – generic battery 6 – 11 [39] 8 (Average min/max)	5 [30] – generic	5 [30] – generic battery 6 – 11 [39] 8 (Average min/max)	5 [30] – generic battery 6 – 11 [39] 8 (Average min/max)	5 [30] – generic battery 6 – 11 [39] 8 (Average min/max)	5 [30] – generic battery 5 [30] – generic battery

Tabela 12 – Investment, replacement, O&M costs and lifetime for Generator-sets, control system and converter.

Parameters	Main Generation-set	Auxiliary Generator-set	Power Control System (PCS) Controller CC – Cycle Charging Strategy	Power Conversion System Equipment (PCSEq) - Converter (1)	Balance of system (2)	Converter (3) = (1) + (2)
Power output Capacity [kW]	1700	425	–	–	–	–
Investment Cost [\$/kW]	236 – 315 (High Speed – MGO); 289 – 433 (Medium Speed – MDO/HFO) [12]; 200 [30]; 316.5 (Average min/max)	236 – 315 (High Speed – MGO); 289 – 433 (Medium Speed – MDO/HFO) [12]; 200 [30]; 316.5 (Average min/max)	80 – 120 [39] 100 (Average min/max)	200 [30] 350 – 500 [39] 350 (Average min/max)	80 – 100 [39] 90 (Average min/max)	440
Replacement Cost [\$/kW] (Adopted Costs)	236 – 315 (High Speed – MGO); 289 – 433 (Medium Speed – MDO/HFO) [12]; 200 [30]; 316.5 (Average min/max)	236 – 315 (High Speed – MGO); 289 – 433 (Medium Speed – MDO/HFO) [12]; 200 [30]; 316.5 (Average min/max)	80 – 120 [39] 100 (Average min/max)	200 [30] 350 – 500 [39] 350 (Average min/max)	80 – 100 [39] 90 (Average min/max)	440
O&M [\$/op.h]	0.5 (Operational Cost) [30]	0.5 (Operational Cost) [30]	–	–	–	–
O&M [\$/year]	–	–	–	–	–	10 [30]
Lifetime [hour]	15,000	15,000	–	–	–	–
Lifetime [year]	–	–	10	–	–	–

APPENDIX E

Theoretical *payback* calculation parameters.

Tabela 13 – Theoretical *payback* calculation parameters for PSV powered by battery.

Battery model	No aging Cost				Aging Cost			
	LFP		NMC		LFP		NMC	
Battery cells	80% DoD	70% DoD	80% DoD	70% DoD				
Depth-of-discharge	80% DoD	70% DoD	80% DoD	70% DoD				
A_{pb} (LFP) [US\$] = Capacity x Price	1075	1075	1075	1075	1075	1075	1075	1075
A_{pb} (NMC) [US\$] = Capacity x Price	1013	1013	1013	1013	1013	1013	1013	1013
B_{pb} [US\$/Liter] [92]	1.02	1.02	1.02	1.02	1.02	1.02	1.02	1.02
C_{pb} [Liter/hour] (for Battery Energy Variation)	24.6 - 24.7 (HOMER)	24.6 - 24.7 (HOMER)	24.2 - 24.3 (HOMER)	24.2 - 24.3 (HOMER)	26.1 - 25.7 (HOMER)	26.2 - 25.8 (HOMER)	26.0 - 25.6 (HOMER)	26.1 - 25.7 (HOMER)
C_{pb} [Liter/hour] (for Battery Power Variation)	24.9 - 26.9 (HOMER)	25 - 26.9 (HOMER)	25.0 - 26.0 (HOMER)	25.1 - 26.0 (HOMER)	26.6 - 26.8 (HOMER)	26.6 - 26.9 (HOMER)	26.6 - 26.2 (HOMER)	26.6 - 26.2 (HOMER)
D_{pb} [day/year] (operation PSV) [90]	230	230	230	230	230	230	230	230
E_{pb} [hour/day] (Stand-alone mode - PSV) [58]	17.112	17.112	17.112	17.112	17.112	17.112	17.112	17.112
F_{pb} [hour/day] (Stand-connected mode - PSV) [58, 101]	6.888	6.888	6.888	6.888	6.888	6.888	6.888	6.888
G_{pb} [US\$/kWh] Shore connection electricity cost) [110]	0.097	0.097	0.097	0.097	0.097	0.097	0.097	0.097
H_{pb} [kW] (Battery)	Sensitivity analysis (or fixed at 1000)	Sensitivity analysis (or fixed at 1000)	Sensitivity analysis (or fixed at 1000)	Sensitivity analysis (or fixed at 1000)	Sensitivity analysis (or fixed at 1000)	Sensitivity analysis (or fixed at 1000)	Sensitivity analysis (or fixed at 1000)	Sensitivity analysis (or fixed at 1000)
I_{pb} (LFP) [36]	0.91	0.91	0.91	0.91	0.91	0.91	0.91	0.91
I_{pb} (NMC) [36]	0.94	0.94	0.94	0.94	0.94	0.94	0.94	0.94
J_{pb} [US\$/ton] (Based on Current Policies [111])	23.56	23.56	23.56	23.56	23.56	23.56	23.56	23.56
K_{pb} [ton/year] (for Battery Energy Variation)	5665.79 - 5700.69 (HOMER)	5683.41 - 5700.49 (HOMER)	5581.59 - 5597.26 (HOMER)	5602.17 - 5595.79 (HOMER)	6027.86 - 5937.63 (HOMER)	6040.13 - 5947.25 (HOMER)	6007.95 - 5915.37 (HOMER)	6029.03 - 5926.37 (HOMER)
K_{pb} [ton/year] (for Battery Power Variation)	5747.41 - 6204.91 (HOMER)	5763.43 - 6204.91 (HOMER)	5772.42 - 5998.20 (HOMER)	5793.19 - 5998.20 (HOMER)	6137.10 - 6192.38 (HOMER)	6137.95 - 6204.44 (HOMER)	6136.00 - 6037.01 (HOMER)	6147.37 - 6037.01 (HOMER)

Index

- Advanced Battery Model, 32, 45, 48, 136
- Ampere-hour Capacity, 50, 138
- Automatic Identification System – AIS, 59
- Available energy, 51, 53
- Average or middle SoC, 42
- Balance of System Cost, 69
- Battery aging, 41
- Battery cell form factor, 34
- Battery cells, 30
- Battery costs, 72
- Battery electrode, 42, 46
- Battery electrolyte, 42, 46
- Battery Management System – BMS, 37
- Battery models, 48
- Battery Module, 36
- Battery Pack, 37
- Battery Space, 38
- Battery temperature, 42
- Bound energy, 51, 53
- C-rate, 36, 42, 137
- C/D Ratio life, 49
- Calendar Aging, 35, 42
- Capacity fade, 43
- Capacity ratio – c, 51
- CAPEX, 74
- Capital costs, 69
- Carbon credit, 75
- Charge C-rate, 42
- Charge voltage, 51
- Charging battery bank, 63
- CO2 emissions, 29
- Components costs, 69
- Conductance, 51
- Container, 37
- Cooling systems, 38, 50
- COVID-19 pandemic impact on seaborne trade, 26
- Cut-off voltage (or end voltage), 50
- Cycle Aging, 42
- Cycle curve to the specific battery cell, 45, 137
- Cycle Life, 35, 136
- Cycle-charging strategy, 63, 64, 72
- Cylindrical battery cell, 34
- Depth-of-discharge – DoD, 42, 43
- Diesel Gen-sets, 27

- Diesel generator-sets, 58, 60
Diesel-electric generation, 29
Diesel-electric propulsion, 27
Discharge current, 42
Discounted Payback, 75
Dispatch modeling, 63, 64
Dynamic positioning -- DP, 26, 29, 39, 56, 58, 59
Electric propulsion system, 27
Electrochemical kinetics, 51
Emissions Control Areas – *ECA*, 25
End of Life – *EoL*, 43, 137
Energy Capacity, 138
Energy Density, 140
Energy Efficiency Design Index – *EEDI*, 25, 26
Energy Efficiency Design Index for Existing Ships – *EEXI*, 26
Engineer-Procure-Construct – *EPC*, 70
Enhanced dynamic performance, 29
Equipment costs, 69
Equivalent Full Cycles – *EFC*, 43
Facilitate energy harvesting, 39
Financial criteria, 30
Fire Safety, 38
Fixed Operation and Maintenance - *O&M*, 69
Fuel consumption and emissions, 29
Fuel consumption curve, 60, 61, 77
Generator-set redundancy, 27
Greenhouse Gas, 25
Harbor mode, 39
High transit, 26
Historical development of the Marine Vessel, 28
Homer Energy software, 32, 48, 49
Hybrid Ship Power Systems, 25
Hybrid Vessel, 64
IEC 62620 (2014), 36
IMO Tier 2, 62
IMO Tier 3, 26
Installation Costs, 69
intercalation of Li-ions (Li+), 47
Internal Impedance, 42, 138
Internal Rate of Return – *IRR*, 75
Internal Resistance, 42, 138
International Convention for the Prevention of Pollution from Ships, 26
International Maritime Org. – IMO, 25
Investment cost, 72
kWh-throughput, 46, 137
Levelized Cost of Energy – *LCOE*, 76
Lifetime throughput, 42
Lithium Cobalt Oxide (*LCO* – LiCoC2), 35
Lithium Iron Phosphate (*LFP* - LiFePO4), 35, 36
Lithium Manganese Oxide Cell (*LMO* – LiMn2O4), 35
Lithium Nickel Cobalt Aluminum Oxide (*NCA* – LiNiCoAlO2), 35
Lithium Nickel Manganese Cobalt Oxide (*NMC* or *NCM* – LiNiMnCoO2), 35, 36

- Lithium Titanate (*LTO* – Li₂TiO₃ or Li₄Ti₅O₁₂), 35
Lithium-ion batteries, 30, 34
Lithium-ion cells, 36
Low transit, 26
Lower Explosive Limit – *LEL*, 38
Marginal cost, 72
Maximum Continuous Discharge Current, 138
Modified Kinetic Battery Model (*MKBM*), 48
Net Present Value, 73
Nominal Capacity, 138
Nominal Energy, 138
Nominal voltage, 50
Number of cycles - cycle degradation, 45, 136
Number of cycles to failure, 45, 137
Objective function, 76
Operational costs, 69, 76
Operational performance criteria, 30
Operational profile for PSV, 56–59, 61, 63
Operational profile of vessels, 26
OPEX, 74
Optimization software, 64, 73
Paris Protocol, 26
Peak-shaving, 29, 40
Platform Supply Vessel, 26, 37, 39, 56, 70
Positive-negative electrodes, 46
Pouch battery cell, 34
Power Control System Cost, 69
Power Conversion System Equipment Cost, 69
Power Density, 140
Power Management System – PMS, 37
Power redundancy, 39
Prismatic battery cell, 34
Rate constant – k, 51
Replacement cost, 72
Round-trip efficiency, 31, 138
Safety criteria, 30
Sensitivity analysis, 30, 73, 77, 78
Ship Energy Efficiency Management Plan – SEEMP, 25
Shipboard microgrids, 27
Shore connection electricity cost, 75
Simple Payback, 75
Simplified Battery Model, 32, 45, 51
Simplified Battery Model (*SBM*), 48
Solid Electrolyte Interphase Layer – SEI, 46–48
Space criteria, 30
Specific Energy, 140
Specific Fuel Oil Consumption – *SFOC*, 29, 61
Specific Power, 140
Spinning reserve, 29
Stand-by operation, 26
State-of-Charge – SoC, 140
State-of-charge range, 34
State-of-Charge Swing, 140
Storage SoC, 42
Storage temperature, 42

- Storage wear cost, 72
- Strategic loading, 29
- Strategic-loading, 41
- String in parallel, 50
- String in serie, 50
- Switchboard, 27

- Throughput or Turnovers, 141
- Thruster devices, 27
- Thrusters, 39
- Time step (simulation), 52

- Zero-emissions operation, 29